BIM-based Motion Planning of Mobile Crane Operation in Modular-based Heavy Construction Sites

by

Sang Hyeok Han

A thesis submitted in partial fulfillment of the requirements for the degree of

Doctor of Philosophy

in
Construction Engineering and Management

Department of Civil and Environmental Engineering
University of Alberta

Abstract

Modular-based construction is becoming increasingly a key role in oil sands development in Alberta, Canada. Modules are generally installed by large-capacity mobile cranes based on one of two lifting options: (1) pick from fixed positions, in which case the crane delivers the payloads from a single (fixed) position for the duration of the project; and (2) pick and carrying operation, in which, because of site congestion, the crane is required to walk with the payload until it reaches a location from where it can finally deliver it to its set resting position. Since the current manual-based crane lift planning is time-consuming, costly, tedious, error-prone, and unable to efficiently react to changes in lift schedule and/or site constraints, this research presents a methodology which allows motion planning of mobile cranes to be developed automatically. The series of computer program developed in this research are integrated with external databases and building information modelling (BIM)-based software in order to develop a system that reacts to changes in project site layout and schedule. The core of this work is a 3D visualization module which monitors the motions of the mobile crane body configurations during lifting and carrying operations. Although the 3D module is built upon numerous algorithms, three in particular are mentioned here since they have been specifically developed for crane operations: (1) the procedure which automatically builds the mobile crane operation, (2) the routine used to calculate lift angles, and, finally, (3) the function which tracks quasi-dynamically the movements of the payload and the body of the crane in order to identify and eliminate potential collision errors. The

developed system also provides collision and lift information for 3D visualization to ensure crane operations do not exceed allowable crane capacity, clearances, and working radii during crane operation. This research also assists practitioners in selecting the most appropriate crane location(s) associated with the module pick positions by evaluating the cycle time of mobile crane operations using simulation. A case study—a modular-based heavy industrial construction project by PCL Industrial Management Inc. in Alberta, Canada—is presented to demonstrate the effectiveness of the proposed methodology.

ACKNOWLEDGEMENTS

There have been a great number of exceptional people who have contributed to my research.

First and foremost, I wish to express my deepest gratitude to my supervisor, Dr. Mohamed Al-Hussein, for his continuous encouragement, support and valuable advice throughout all stages of this research. I would like to extend my gratitude to my co-supervisor, Dr. Ahmed Bouferguene, for his valuable advice and support and assistance in developing various mathematical equations.

I also appreciate the assistance from NCSG Crane & Heavy Haul Services (Edmonton, Canada) and Wilbert Kranservice GmbH (Germany).

I owe special thanks and appreciation to my parents, for their unconditional love and endless encouragement throughout my life. Their patience, support and sacrifice made all this work possible and they will remain my inspiration. I appreciate everything they have done for me. I would like to thank my wife, Mrs. Ji Eun Kim, my brother, Mr. Sang Jun Han, my friends, Mr. Romano Penheiro, and my colleagues at the University of Alberta.

Finally, I am grateful to the Natural Sciences and Engineering Research Council of Canada (NSERC) and Collaborative Research and Development (CRD) for their financial support throughout this research. I am also grateful to Mr. Jonathan Tomalty, and other staff in the Department of Civil and Environmental Engineering at the University of Alberta.

TABLE OF CONTENTS

LIST OF TABLES

LIST OF FIGURES

LIST OF NOTATIONS

α	boom angle
θ	swing angle
β	jib angle
L	boom length
R_S	radius from crane location to outside boundary of the superlift
R_L	lifting radius
R_{min}	minimum radius
R_{max}	maximum radius
P_G	center gravity position of the crane
P_C	position of each crane configuration
$\overrightarrow{V_C}$	current motion of the crane body configuration
$\overrightarrow{V_D}$	desired motion of the crane body configuration
V_{TO}^n	number of vertices on the target object
V_{TS}^m	number of vertices on the target obstacles
SF_j	number of surfaces on the target obstacles
Q_j	number of points on the SF_j
D_{actual}	distance from the target object to the target obstacle
r	collision risk range
C	clearance
S_{hoist}	speed of hoist up and down
$S_{rotation}$	rotation speed
GC	gross capacity
H	lifting height

H_{min}	minimum lifting height
H_A	obstacle height
H_B	load height
H_C	required clearance
RH	required lifting height to prevent potential conflicts
$Min\text{-}H_{rope}$	minimum rope height to maintain clearance
W_{total}	total weight
W_{lifted}	lift or object weight
W_{Hook}	hook weight
W_{sling}	weight of sling
$W_{spreaderbar}$	weight of spreader bar
W_{Hoist}	weight of hoist wire
TO	target object
TS	target existing obstacle

Chapter 1: Introduction

1.1 Motivation and Background

Canada, ranked third in the world in proven oil reserves, is becoming one of the most attractive industrial construction markets in the world as Alberta's oil sands continue to be the primary source of growth in Canada's oil and gas industry. As for the scale of development, based on the oil sands market analysis by Ernst and Young (2012), the impact of the oil sands on Canada's economy is forecasted to reach a total of nearly $4.93 trillion for the years 2010 to 2035, and over 90% of the economic impact will be felt in Alberta. Meanwhile, according to the Alberta oil sands supply chain opportunity analysis (Sierra Systems 2011), total capital expenditures on oil sands projects are forecasted to exceed $150 billion over the next 10 years. The range of estimated total expenditures on maintenance, repair, and operation between 2011 and 2022 is from $227 billion to $330 billion (Sierra System 2011). Based on the actual figures and projections, steel fabrication and machinery manufacturing are expected to play a critical role in oil sands projects, which increasingly utilize modular construction for structural components, boilers, pressure vessels, tanks, heat exchangers, and steel pipes and tubes, as well as services such as field installation of equipment, repair, and maintenance.

As oil sands development continues to mature, modules have evolved from 1st generation (simple and light) and 2nd generation (complex, large and heavy) to what have come to be known as 3rd generation (more compact, larger and heavier, with exterior walls installed). Given the properties of today's modules,

the successful completion of modular-based construction projects is contingent upon how efficiently construction equipment handles the modules during the process of on-site assembly. In the context of 2nd and 3rd generation modular construction, where modules are increasingly heavy, cranes are an indispensable component without which assembly cannot be carried. Cranes use requires careful planning to increase the safety and productivity of their utilization. In this respect, it is worth noting that 33% of construction accidents (including both injuries and fatalities) are linked to mis-operated cranes (Neitzel et al. 2001). According to an investigation of crane-related fatalities from 1992 to 2006 in the United States, the most common types of crane failure include electrocution, struck by loads, crane collapse, failure of boom/cable, and struck by cranes or crane parts. As shown in Figure 1.1, these failures represent approximately 85% of all crane-related fatalities and injuries. Although mobile cranes are in high demand in heavy industrial construction due to their high lifting capacity, mobile cranes are also the most high-risk equipment among material handling systems for construction projects (Beavers et al. 2006; Shapira et al. 2007). In this regard, designing efficient and safe mobile crane operation is integral to successful completion of modular-based construction projects. It reduces the risk of crane failure, which in turn improves project schedule control and quality of construction projects in terms of delivery and installation of modules in order to increase productivity. These improvements can allow construction companies working on oil sands projects to enhance their competitiveness by reducing construction time and cost.

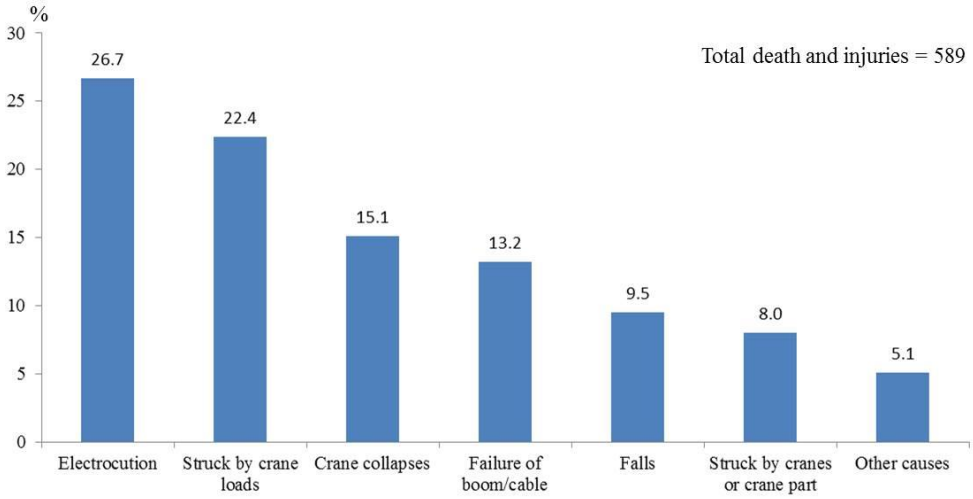

Figure 1.1: Failure types of associated crane types
(US Bureau of Labor Statistics from1992 to 2006)

Many researchers and practitioners have developed new methods to improve lift planning for safe and efficient mobile crane operation. However, current lift planning procedures suffer from several practical issues. (1) Lift planning is performed manually by lift engineers using computer tools (e.g., AutoCAD). This approach is time-consuming and error-prone for heavy industrial construction projects involving a large number of lifts since changes to the assembly schedule (sequence) or project scope necessitate re-planning of numerous crane lifts. (2) Lift planning primarily focuses on checking the feasibility of the lift at its pick and set points of lifted objects while overlooking lifting path planning, which may present conflicts between the crane body configurations and surrounding obstacles. (3) Lift engineers generally select a crane location from among a number of feasible crane locations based on first-hand experience. This experience-based decision making can lead to crane relocation and low efficiency of mobile crane operation, which in turn

compromises project productivity and safety. (4) Current lift planning in practice still uses static and tedious 2D analyses which focus on checking the feasibility of a crane operation at the object's pick and set points rather than considering the entire crane operation. This static method makes collaboration and communication among project participants challenging, and often leads to crane relocation and collision errors due to poor management and decision making. The combined effect of the above mentioned limitations is an increase in the risk of delays and cost overruns. To overcome these limitations, this research proposes to examine motion planning of mobile crane operations for heavy industrial projects based on functionalities of building information modelling (BIM). The proposed motion planning encompasses the following capabilities: (1) responding efficiently to dynamic changes of the site layout due to existing obstacles, especially when dealing with a large number of lifts and unexpected design changes; (2) utilizing 3D visualization to identify any design errors during dynamic crane operation; (3) evaluating cycle time of crane operations using discrete event simulation in order to understand the impact of crane location and path selection on the overall schedule of the assembly operation; (4) providing 3D visualization with engineering information such as lift angles, lifting heights, crane capacity and working radii in order to establish better collaboration and communication among upper project management personnel; and (5) developing an automated design system in order to reduce manual works and human errors in crane lift planning.

1.2 Research Objectives

This research is built upon the following hypothesis:

"Automated motion planning of mobile crane operations with efficient interoperability among applications of crane lift planning in heavy industrial projects will reduce lift planning time and cost, as well as improve project safety and productivity."

In order to explore and validate this hypothesis, this research focuses on the following objectives:

1. Apply existing functionalities of the building information modelling (BIM) paradigm, which revolves around sharing and integration of data in order to ensure consistent project-wide information allowing efficient communication among all participants. This part of the work is developed in two steps, which are described as follows.

   (a) Centralize relevant project information, (e.g., crane parameters, site layout, assembly schedule), in a central repository. Data exchange between the crane analysis tools and the 3D visualization module, developed in 3D Studio (3ds) Max, is carried out (through the central repository) by means of a two-way exchange procedure.

   (b) Develop an automated 3D model builder which uses relevant data stored in the central repository, (e.g., crane geometry and capacity, site layout), in order to generate 3D models of the construction site, including existing obstacles.

2. Develop 3D visualization-based motion planning which integrates 3D visualization with mathematical models based on various project constraints such as geometry of the crane body, site layout, and lift schedule. The 3D visualization module involves three procedures:

   (a) Calculate lift angles and directions of crane body configurations;
   (b) Design load (material) lifting paths; and
   (c) Conduct dynamic detection of collisions between the crane body, the load, and existing obstacles.

3. Build a decision support system which integrates 3D visualization with simulation in order to assist in selecting the appropriate crane operation.

4. Validate the BIM-based motion planning in an actual project.

1.3 Organization of the Thesis

This thesis comprises five chapters. **Chapter 1** describes the scale of modular-based construction markets, especially oil sands, and the need for BIM-based motion planning of mobile crane operations. **Chapter 2** (Literature Review) describes the current state of knowledge related to lift planning. The application of simulation and 3D visualization for crane planning in the construction field are described in this chapter. **Chapter 3** (Proposed Methodology) presents the methodology for BIM-based motion planning of mobile crane operations. **Chapter 4** (Case Study) describes the effectiveness of the proposed methodology in a modular-based heavy industrial project which has a large number of lifts. **Chapter 5** (Conclusion and Recommendations) summarizes the

research, outlining its contributions and limitations and offering recommendations for future work.

Chapter 2: Literature Review

2.1 Introduction

Based on the workflow of the lift planning and application tools needed to achieve the objectives of this research, a literature review is conducted. Although various systems have been introduced to establish efficient lift planning, the current lift planning in practice still has deficiencies because of inefficient information exchange leading to time-consuming and error-prone activities. In order to address these challenges, engineers and researchers have developed innovative crane management systems. This chapter presents a summary of the existing research related to crane lift planning, and an overview of building information modelling (BIM), a tool which helps to improve interoperability and communication among project participants. In this respect, this chapter provides the roadmap for the development of this research.

2.2 State-of-the-Art Research in Crane Location

In past decades, site layout and material handling systems as a means to improve production efficiency and safety in construction sites have received attention. The successful design of site layout and material handling systems depends on optimal locations of equipment on construction sites to ensure efficient construction equipment operations. In this respect, efficient selection of crane locations can improve project safety and productivity since cranes are the most readily utilized heavy equipment in construction sites, transporting heavy materials such as prefabricated elements, steel beams, and mixed concrete to

their set positions. However, selection of crane locations in practice tends to be time-consuming and costly since locations are often determined through a process of trial-and-error. In an effort to move beyond these rudimentary methods, practitioners and researchers initially focused on developing approaches to optimize crane locations associated with material supply. Rodriguez-Ramos and Francis (1984) have introduced design of optimal locations of a crane within a construction site based on a mathematical model to minimize the total transportation cost between the crane and construction supportive facilities serviced by the crane. Zhang et al. (1999) have developed a computerized model to optimize location of a group of tower cranes in complex construction projects requiring multiple cranes to provide coverage of all demand and supply points within the constraints of a tight construction schedule. This model consists of: (1) an initial location generation module, which classifies tasks into groups and identifies feasible locations of each crane; (2) a task assignment module, which adjust tasks into groups in order to yield smooth workloads and minimal conflicts with cranes; and (3) a single-crane optimization module, which searches for optimal crane locations based on minimized hook transportation time. However, the crane location may not be optimized when material supply locations are changed. Lin and Haas (1996) have proven that the material supply points must be considered when optimal crane locations are determined. Corresponding to this requirement, Tam et al. (2002) have used a genetic algorithm (GA) model to optimize supply locations and the tower crane location concurrently in high-rise building construction. Previous research to

optimize crane locations and material supply points for the purpose of enhancing safety of crane operations has been implemented in 2D work envelopes, which lack the ability to identify potential spatial conflicts between crane parts and existing obstacles. In order to address this challenge, Tantisevi and Akinci (2008) have presented an approach to crane planning which identifies collision-free crane locations in a 3D environment, accounting for dynamic crane behaviour and facilitating accurate interference checks. Although many researchers have developed algorithms by which to determine optimal crane locations, these locations still require the crane to relocate because of schedule delays, and costs increase due to inaccuracy of spatial conflict identification and failure to satisfy crane capacity constraints. To overcome these limitations, Huang et al. (2011) have proposed mixed-integer linear programming to optimize location selection for tower cranes and material supply points, and optimization results generated by their model are found to outperform those optimized by GA in terms of cost and time. However, Safouhi et al. (2011) have noted that previous methods are not adaptable to heavy industrial projects which include a large number of objects to be lifted according to designed lifting sequences for a variety of site layouts. They employed a GA in order to determine the workspace areas, which produced feasible mobile crane position areas on-site by calculating the crane body configuration for a given clearance distance. As a continuation of this work, Lei et al. (2013) have developed a binary (yes/no) checking methodology for mobile crane lifts which checks feasible fixed crane locations on the possible mobile crane position areas by calculating minimum and maximum crane lift

radii in a configuration space (C-Space) approach. This simple method is implemented by checking for the existence of paths linking pick points to set points of the object to be lifted. When the mobile crane lift binary checking does not provide any feasible crane paths on various fixed crane locations, crane walking path checking can be used as an alternative to successfully complete crane lifts (Lei et al. 2014). This walking path checking provides crane walking paths involving start and finish crane locations for each object. Depending on the level of congestion and complexity of the project, however, these approaches present two limitations: (1) there is an approximately 15% to 20% rate of failure to find feasible crane locations; and (2) pick areas provide uncertain material supply points where objects will be hooked by the feasible crane locations. To overcome these challenges, 3D-based motion planning is required to validate feasible crane locations with associated material supply points for heavy construction projects involving a large number of lifts. It is then necessary to evaluate the performance of crane operations designed by the proposed motion planning in order to assist in selecting the crane location and associated material supply points which ensure the most efficient crane operation. This research presents a methodology which accounts for these two requirements.

2.3 State-of-the-Art Research in Crane Type and Model Selection

Since the crane selection process is a central step and time-consuming task in crane lift planning, researchers and engineers have attempted to develop applications and methodologies using various algorithms in order to select cranes efficiently and effectively. Appropriate crane type and model selection

contributes to the efficiency, timeliness, and profitability of projects. Based on previous studies, crane selection algorithms are categorized as follows: (1) project factor-based algorithms; and (2) scenario-based algorithms. As a project-based algorithm, Hanna and Lotfallah (1999) have developed a fuzzy logic approach by which to select the best crane type in a construction project by converting the factors in projects to fuzzy sets, and then finding the highest expected overall efficiency aggregated with importance weightings for the following factors: (1) site conditions; (2) building design; (3) economy of the use of the crane; (4) capability of the crane (e.g., power supply); and (5) safety. Sawhney and Mund (2002) have introduced a neural network-based crane type and model selection system, called IntelliCranes, in order to support crane type selection (tower or mobile crane; crawler, terrain, or truck crane) and crane model selection based on historical data of project factors, type of work for which the crane is used, site layout spaciousness, and construction heights. Since the selection of crane type is affected by the heaviest lift and/or the largest lift radius (capacity) determined by the distances from crane locations to pick and set positions of lifted objects on site, some researchers have developed scenario-based algorithms for effective and efficient mobile crane type selection. The notion of a relational database management systems (DBMS), which is a tabulated system including crane type, geometric lifting configuration specifications, and lifting capacity, has been introduced by Al-Hussein et al. (2000). Al-Hussein et al. (2001) have proposed a methodology which is incorporated into an integrated computer system capable of advising users on the

selection of feasible cranes from a previously developed crane database. Moreover, Al-Hussein et al. (2005) presented an optimization algorithm for the selection and location of mobile cranes on construction sites in order to provide a powerful, accurate, and instant evaluation tool by assessing lift configurations retrieved from the crane's database. The algorithm has been developed in Microsoft Visual Basic programming language and its optimization module is implemented using Microsoft Solver. However, these procedures may be inadequate for heavy industrial construction projects involving a large number of lifts, which require the selection of multiple crane types, models and configurations to satisfy demands such as working radius and crane lifting capacity. In order to address this challenge, Taghaddos et al. (2010) has developed a simulation-based methodology for heavy lift planning of industrial projects which selects mobile cranes, locations, and configurations for different lifts, and then produces a lifting schedule in the design stage in place of on-site lifting sequences designed based on the experience of lift engineers. This method serves to reduce total cost and overall construction time. Furthermore, Wu et al. (2011) have suggested a newly developed algorithm for selecting mobile cranes on construction sites which takes into account the lifting capacity, the geometrical characteristics of the crane, the dimensions of equipment and riggings, and the ground bearing pressure. This algorithm has been integrated into a 3D computer-aided system that performs the following functions: (i) crane selection, (ii) crane modelling, (iii) 3D-simulation, (iv) 3D computer-aided design modelling, (v) rigging calculation, and (vi) data management. While for

most projects a single crane suffices to perform the required lifts, in some instances a lift may require two cranes. One such example is the lifting of heavy-pressure vessels which need to be rotated from a horizontal to a vertical position prior to being set at their final position. This type of operation requires planning and arranging adequate crane support, and preparing collision-free rotation of the vessel from a horizontal position to a vertical position. To satisfy these requirements, two mobile cranes are selected based on their respective lift capacities, and the lifts of each crane are analyzed individually for potential crane locations associated with pick positions determined based on expert knowledge. Since this method of crane selection is time-consuming in practice, Hermann et al. (2011) have proposed a crane selection methodology to lift long vessels in industrial projects. Since large-scale industrial construction projects generally require more than one single crane type selected by experienced lift engineers, Han et al. (2012) have developed a framework to optimize crane type (mobile crane versus tower crane) using more than 40 different project factors. 3D visualization of crane operation using the selected crane type and model is designed to validate collision-free and efficient crane operation. Although many researchers and practitioners have attempted to develop appropriate crane selection tools and frameworks, none of these studies provide validation of the selected crane type and model, such as crane working radius and crane capacity checks, in consideration of changes to the selected crane locations and material supply points due to site layout and/or lift schedule changes. In this regard, this research presents a method which monitors the status of crane working radius

and capacity, thereby assisting in identifying whether or not the crane lifting capacity is exceeded during crane operation. It allows lift engineers and project managers not only to validate selected crane types and models, but also to ensure safe crane operations when feasible crane locations and lifting sequences are changed.

2.4 State-of-the-Art Research in Crane Support System Design

Construction is generally recognized as one of the most hazardous industries, with relatively high fatality rates in most countries (Suraji et al. 2001). Behm (2005) has also reported that in North America construction is ranked as the most hazardous industry in terms of its share of total work-related fatalities from all industries. Since cranes are one of the most commonly used resources in construction projects, accidents on construction sites are often related to crane operation. According to the US Bureau of Labor and Statistics (2008), which cross-correlated the types of crane failures with their causes, the most common type of crane failure is crane collapse, which is caused by one or a combination of the following factors: (i) overload, (ii) loss of center of gravity control, (iii) outrigger failure, (iv) high wind and side pull. These in turn are the result of either inaccurate mobile crane design, lack of a proper support system, or a faulty decision to carry a load which exceeds the lifting capacity of the crane (Hasan et al. 2010). With regard to stability of crane operations, Tamate et al. (2005) have emphasized that crane support systems are an important factor to prevent outrigger failures, which are caused by instability as a result of rapid penetration of the outriggers into the ground during crane operation. In practice,

crane support systems are designed using rules of thumb, including outrigger reaction and support design calculations. However, these rules do not consider maximum reactions as the crane body elements and the payload are moving. This limitation leads to design of an inappropriate crane support system, which is a cause of outrigger failure. Therefore, dynamic loading of a slewing crane is a critical factor in calculating the exact reaction of each outrigger and designing efficient crane support systems in order to maintain stability of crane operation until a project is complete. Based on a mathematical model to investigate the dynamic loading of the slewing crane, the dynamic forces, which act on the crane's steel structure during crane lifts, have been analyzed by Jerman (2006). Sochacki (2007) has considered specific geometrical factors such as rope length and load conditions (without taking damping) in order to analyze the dynamic stability of a truck crane. Sun and Kleeberger (2003) have developed an integrated model which calculates dynamic stability of mobile cranes based on the structures of the crane, external loads, and the dynamic body motions of mobile cranes as input factors. As a continuation of the work of Sun and Kleeberger, Kłosiński (2005) has built a mathematical model of the control system to minimize the swing motions of mobile crane operations in order to reduce instability accidents. Based on these previous studies, Hasan et al. (2010) have developed an automated support design system for mobile cranes which calculates the outrigger's reaction values for truck and crawler cranes. This system represents a reaction influence chart that describes the dynamic relationship between a truck crane's outrigger reaction or a crawler crane's

pressure, the boom's horizontal swinging, and vertical boom angles to the ground. This chart assists practitioners to design the support system using steel plates or timbers. For the design of a tower crane support system, Kim et al. (2011) have developed an automatic optimal design algorithm for foundations of tower cranes. Moreover, as summarized in the existing body of research in this area, crane motions such as horizontal and vertical lift angles are critical inputs based upon which to identify the maximum reactions used to design an accurate crane support system. However, it is difficult to predict exact slewing operation in 2D-based crane lift planning for heavy construction projects, which typically involve numerous lifts on different site conditions. As an alternative, Han et al. (2014) suggested 3D visualization of crane operations, including expected lift angles as input factors, in order to design a crane support system. In this regard, the proposed motion planning in this research efficiently and automatically provides lift angles and loads for crane support system design. Corresponding to dynamic motions of the crane, various site conditions, and loads, this interactive system can facilitate accurate design of crane support systems. At this juncture, it should be noted that the present research does not encompass crane support system design.

2.5 State-of-the-Art Research in Crane Collision Detection

According to statistics from the U.S. Bureau of Labor Statistics (2008), collision errors between other components (e.g., existing building facilities and temporary structures) and crane equipment were the most common cause (61%) of crane-related occupational fatalities in 2006. These spatial conflicts also lead to

injuries, work interruptions, reduced productivity, cost overruns, and damages to existing structures. Investigations of these collisions underscore the need for potential spatial conflicts to be identified and eliminated by preventive actions prior to actual construction. To satisfy this demand, researchers have primarily used 3D-space, which assists in the development of collision detection methods for efficient and accurate identification and prevention of feasible collision errors. In this respect, previous research can be categorized into two groups of the collision detection methods: (1) detecting the collision status whether objects have collided or not; or (2) identifying the collision status and measuring the distance to the nearest possible collision in the case of a collision-free status. Based on Axis-Aligned Boundary Box (AABB) as a method from the first category, Bergen (1997) has presented a scheme for exact collision detection between complex models undergoing rigid motion and deformation. As a method representative of the second category, Lin and Canny (1991) have introduced a simple and efficient algorithm to provide feasible spatial conflicts and associated distances by identifying the closest points between two convex polyhedrons on models. However, both approaches pose critical limitations when applied to large and complex projects: slow running time and reduced accuracy of collision detection. To reduce the running time of the collision detection, Tantisevi and Akinci (2007) have developed an AABB-based approach which generates crane workspaces through translation of crane configurations (see Figure 2.1a). Although this approach is efficient for detecting collision errors, it does not provide distances between cranes and obstacles,

information which is essential for eliminating potential collisions in motion planning. In order to address this limitation, Lai and Kang (2009) have developed a simple algorithm, VC-COLLIDE (see Figure 2.1b), based on an outer boundary volume concept and built using either spheres or cylinders approximately corresponding to the crane configurations and structural elements of a construction site. This method uses approximate outer-boundary volumes of cranes, (which may be inaccurate in indicating collision status), as well as distances between the crane and obstacles on site. This method also requires the time-consuming task of accurately mapping boundary volumes to each crane configuration. This method thus may not be suitable in heavy industrial construction projects, which require high accuracy and efficiency of distance measurement and of collision detection between crane parts, objects to be lifted, and existing obstacles. In order to address these challenges, the motion planning method proposed in this research presents an approach which generates crane workspaces by translation of crane body configurations for not only collision detection, but also accurate distance measurement during crane operation.

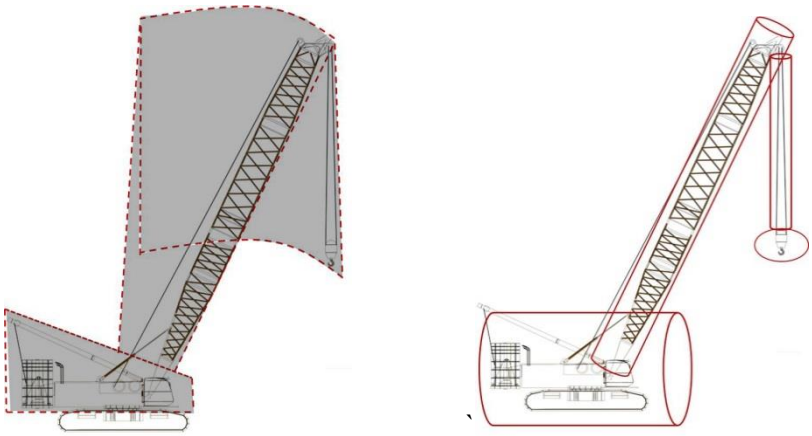

(a) Workspace using AABB (b) VC-COLLIDE

Figure 2.1: Concepts of collision detection methods

2.6 State-of-the-Art Research in Motion Planning of Crane Operation

In recent decades, industrial construction projects, including oil refineries, have increasingly involved heavy, large, and long objects such as vessels, modules, and reactors which are installed by single- or multi-cranes operations. Although cooperative lifts by two or more cranes carry a higher risk than single-crane lifts due to the interaction among the co-operative cranes, heavy industrial projects must adopt cooperative lifts to erect heavy and long loads or to install special equipment by means of a vertical lift Therefore, designing efficient, reliable, and safe crane operation prior to construction is essential, given its significant positive impact on the overall scheduling, cost, and safety of the project. To satisfy this demand, motion planning has garnered much attention as a means of efficiently designing reliable and safe crane operations based on the identification and elimination of potential risks such as collisions. Sivakumar et al. (2003) have presented heuristic search methods for automated path planning

of multiple cooperative cranes. Based on a concept described in existing research, Ali et al. (2005) have increased the efficiency of path planning based on cooperative crane manipulators developed using GA with an interference detection algorithm. Kang and Miranda (2008) have introduced an incremental coordination method for preplanning and coordinating the use of multiple tower cranes in relatively narrow construction sites based on consideration of the kinematics and geometrical constraints of cranes. This method is intended to design cooperated motions of multiple cranes in order to prevent collisions between multiple cranes, or between cranes and obstacles on the construction site. In spite of these efforts, previous methods have been developed as 2D-based systems, such that potential collision errors may not be accurately identified due to inefficient reactions to frequent design changes influencing the complexity of the project, such as changes to the site layout.

Successful motion planning involves efficiently searching for the shortest lifting path based on identification and elimination of potential spatial conflicts (Lai and Kang 2009; Tantisevi and Akinci 2007). In this regard, most researchers have attempted to integrate 2D-based algorithms used to optimize the lifting paths with 3D computer-aided systems used to validate the designed lifting paths. 2D-based algorithms such as customized applications and simulation engines have been used to analyze optimal lifting paths and site layout, with 3D visualization then implemented for validation (Al-Hussein et al. 2006; Kang and Miranda 2006). However, Tantisevi and Akinci (2009) have emphasized that detailed 3D site layouts that include existing obstacles are essential to detecting

and eliminating potential conflicts between crane configurations and obstructions. Given this, Kang et al. (2009) have presented a system which builds 3D simulation and animation of assembly processes in order to describe detailed planning of crane operation. A key feature of this system is to capability to increase safety of crane operations on job sites by preventing collisions and minimizing construction time. Chi and Kang (2010) have developed an integrated approach to simulate the detailed motions of cooperative crane operations in 3D visualization based on physical properties of the lifted object, kinematics, and constraint-based dynamics. The aim of this system is to provide real-time and physics-based visualization of cooperative crane operations based on computing the cable sway and other reactions to collisions, as well as analyzing input data such as boom angles and crane capacity. Chang et al. (2012) have proposed a method by which to design single- and dual-crane operations automatically. This method has two steps: (1) convert the scene of the crane operation into a 3D C-space which includes the crane's load capacity and obstacles; and (2) identify any collision-free paths within the C-space using the probabilistic road map method. To extend utilization of the motion planning, Albahnassi and Hammad (2012) have introduced a framework and system architecture for the motion planning of crane operations, including visualization and simulation of crane operations, based on the dynamic changes of construction sites. The purpose of their study is to provide assistance to crane operators to re-plan safe paths in near real time. Zhang and Hammad (2012) have developed a multiagent-based approach involving site agent, coordinator

agent, and crane agents for real-time support to construction planners. The purpose of their approach is to achieve collision avoidance by informing crane operators about potential collisions and providing motion re-planning for safe and efficient crane operations. Their process involves creating a 3D model of the static environment, and identifying and designing collision-free motion plans by means of agents which consider engineering constraints and crane operation rules. Similar motion planning methods, sensor-based motion planning, and monitoring systems for mobile and tower cranes have been developed using various technologies and algorithms such as radio-frequency identification (RFID) (Lee et al. 2011). (Since the focus in the present research is on developing an off-line motion planning system, on-line motion planning methods are not reviewed in great detail.) As the visualization trend has gained momentum it has impacted every aspect of the industry, including design of crane lifts, which now utilizes static 3D models to assist practitioners in identifying lift challenges such as potential conflicts (Park et al. 2009). Based on two types of crane operation—crane operation from fixed location and crane walking operation, Han et al. (2014) have utilized dynamic 3D visualization in 3D Studio (3ds) Max in order to design practical motions of mobile crane operation. Although their study validates the usefulness of 3D visualization for lift planning in principle, in practice the development of 3D visualization is time-consuming and costly due to the manual and repetitive tasks necessitated when site layouts and lifting schedules are changed.

Based on an exploration of motion planning in the available literature, a number of limitations and requirements are identified. First, previous studies assume that the crane (i.e., crawler crane) operates from a fixed position for the duration of a project, i.e., they do not consider the possibility of a crane walking between positions (start and finish positions) while carrying the payload. Since crane walking operation is associated with higher rates of collision errors compared to crane fixed operation, engineers prefer utilizing the fixed location for crane lifts. However, crane walking operation in some cases is the only possible solution for transporting objects to their set positions. Second, most previous studies have focused on only collision-free material-lifting path planning, not considering the collision-free motion of crane body configurations which is critical on congested sites. Third, previous research has used 3D visualization solely for validation and verification of the optimal lift paths designed by 2D-based motion planning methods, but not as a design tool for motion planning, since 3D visualization is known to be a computationally intensive and thus time-consuming process. Another limitation is that previous motion planning approaches may be implemented as stand-alone applications that necessitate manual work, which can easily lead to information exchange errors. These errors may decrease accuracy and responsiveness to frequent design changes such as lifting schedules and/or site layout. The combination of these limitations has led to additional costs while preventing lift engineers from fully leveraging the benefits of 3D visualization for motion planning. To develop reliable, safe and efficient motion planning, two requirements are identified: (1) practical sequences of mobile

crane operation with clearance maintenance; and (2) changeable properties of construction sites for numerous objects to be lifted. To overcome the limitations of previous research and satisfy the given requirements, this research proposes a 3D visualization-based motion planning approach involving the following features: (1) integration of 3D visualization with mathematical algorithms to design mobile crane motions for both fixed and walking operations; (2) application of various 3D site layouts in accordance to crane location, site layout, and lift schedule changes; (3) reliable and efficient information exchange between existing applications of the lift planning, such as crane location selection, and/or project participants; (4) collision-free motions of the crane, including material-lifting paths satisfied by practical motions of crane operation; and (5) automated simulation and visualization of crane operations for large numbers of lifts.

2.7 State-of-the-Art Research in Building Information Modelling

The most popular recent trend in the architecture, engineering, and construction (AEC) industry has been building information modelling (BIM), which fosters better collaboration and communication among project stakeholders. It also helps to detect and address design errors prior to actual construction. Although BIM is widely used, its definition has not yet been clearly specified. Based on investigations of uses of BIM in various projects, this section seeks to define and explore the functions of BIM. As a standard definition of BIM, the International Organization for Standardization (ISO) articulates the role of BIM as to describe and display information required in the design, construction, and operation of

construction facilities to assist with decision making (ISO 29484-1 2010). As another function, BIM facilitates information exchange among the project stakeholders in order to improve the following criteria: (1) safety, by identifying conflicts and interference; (2) design and schedule efficiency, by reducing the amount of rework arising from design or schedule changes; (3) cost, by estimating material lists, dimensional properties, productivity analysis, quantity take-off, and related information; and (4) decision making related to finding the best solution, by evaluating and representing solution alternatives (Eastman et al. 2011). The traditional document-based project delivery method is archaic, error-prone, litigation-prone, high-risk, and reliant upon inefficient, difficult to predict construction processes that result in owners taking over projects with little information on how to operate and maintain their building (Neeley 2010). Based on advanced computer technology, BIM is helpful in reducing or eliminating the need for the many paper documents currently in use. As Hasan et al. (2012) have summarized, BIM generally addresses laws and regulations, material information and specifications, procurement information, facility information, construction information, simulation results, 2D/3D drawings, and visualization/animation models. Given these definitions and functionalities of BIM, BIM can be adapted, represented, and applied based on user requirements.

To implement BIM, as shown in Figure 2.2, a BIM model is built by means of reliable information exchange from various fields, resulting in graphical 3D representation of the building. As additions to BIM, time (duration) for scheduling and cost for estimating figure as the fourth dimension (4D) and fifth

dimension (5D), respectively. Based on this information, the BIM model is used to efficiently generate automatically a number of effective solutions related to quantity take-off, material lists, shop drawing, and spatial analysis for the design process. Although many researchers and stakeholders are interested in utilizing BIM models, its use in the AEC industry is inhibited by a lack of interoperability between various tools and among project participants. To overcome this critical issue, not only is advanced technology needed, but also a cultural change in the industry. In this regard, BIM is identified as a sociotechnical system (Moghadam 2014).

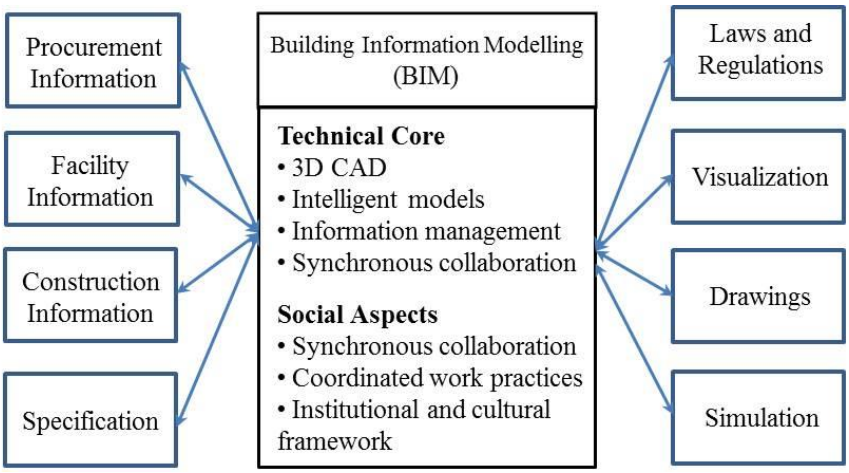

Figure 2.2: BIM system

Many research and development efforts have been made to extend the use of the BIM, addressing different application areas in AEC industry. Abudayyeh and Al-Battaineh (2003) have used BIM to manage information in order to support bridge maintenance. They have pointed out the need for inclusion of as-built data in the bridge management database, along with periodic inspection and maintenance data. Goedert and Meadati (2008) have extended the use of BIM

throughout the construction phase of the project life cycle by documenting 3D as-builts, producing a 4D as-constructed model, and capturing and storing construction documents for the owner. Russell et al. (2009) have applied 4D-CAD to represent a project's schedule and associated information combined with visual representations of the project in progress in order to identify shortening project duration, assess workability, and judging schedule quality. The 4D-CAD combined with linear schedules leads to the provision of clear, fast, and multi-dimensional feedback to the project team through rapid exploration of alternative construction methods and scheduling strategies for large-scale linear projects such as high-rise buildings. Yan et al. (2011) have integrated BIM and computer games which allow designers to play in their own designed environments with the capability for simulations of physical dynamics and user activities. This system provides a chance to connect diverse areas such as building modelling, equipment simulation and visualization, collision detection, navigation, and path planning. Porwal and Hewage (2012) have combined BIM with a one-dimensional cutting waste-optimization technique in order to analyze reinforced concrete structures in terms of the minimization of rebar waste. This integrated BIM plays a critical role in communicating project information among diverse design teams in order to simulate architectural and structural design requirements, and in comparing results quickly to make necessary changes in design. Kim and Anderson (2013) have proposed a new methodology to produce energy estimates and interoperability between the simulation engine and BIM tools. In their research, the information as an input file is extracted from a BIM

model and run in an energy simulation program on an hourly basis for a desired period so that users can easily understand the output of the simulation. In a view of the adoption of BIM, Giel and Issa (2013) presented a case study for the potential cost savings associated with implementing BIM based on analyzing the investment of paying additional fees in two projects: (1) a recently constructed BIM-assisted project and (2) an earlier project implemented without the use of BIM. As a result, the constructed BIM-assisted project has reduced change orders and schedule overruns as the qualitative benefits of using virtual construction during preconstruction. Bynum et al. (2013) have surveyed perceptions of the BIM utilization for sustainable design and construction among designers and constructors. As a result, sustainability was not a primary application of BIM since interoperability among the various BIM applications involving Autodesk Revit, Graphisoft ArchiCAD and Bentley Architecture and other sustainable tools such as Ecotect, eQUEST, IES Virtual Environment, and Green Building Studio in the industry has still not been achieved, but project coordination and visualization are of particular importance.

Although BIM is widely used in the AEC industry to obtain network-based environments for effective inter-organizational project collaboration, Kam and Fischer (2002) have identified some limitations, such as (1) the lack of information exchange between different software products; and (2) the near impossibility of achieving versioning and controlling user rights in file exchange. To overcome these limitations, a standardized BIM approach based on the industry foundation classes (IFC) model of BuildingSMART has been

developed for construction management purposes. A fundamental requirement of integrated project systems is to support the modelling and management of the design and construction information and to allow the exchange of such information among different project disciplines to improve the quality while reducing the time and cost of projects. Given this, the existing IFC data models have been extended to support the modelling of smart AEC objects as 3D parametric entities, combining the capability of these elements and integrating relevant information in order to represent various aspects of project information such as moisture and thermal performance (Halfawy and Froese 2007; Fazio et al. 2007). The purpose of this integration is to extract data pertaining to the geometric and material layers of a building from CAD drawings in the IFC data model, link it to the performance evaluation applications, and then compare the evaluation results. Gökçe et al. (2013) have introduced a type of product catalogue structure that is compatible with the data schema of the IFC standard, allowing for coherent integration of product and cost information for building maintenance.

Crane lift planning is implemented through one of two methods: (1) manual-based planning, which is tedious and error-prone, leading to cost increases and time consumption; and (2) customized programs, which provide automated and specialized analyses with less effort, time and cost. However, neither manual-based planning nor customized programs have yet fully leveraged the capabilities of BIM. Although many researchers have put effort toward investigating the application of BIM in the AEC industry, crane information has

not garnered much attention. Only 3D visualization—one of the BIM functions—is used to identify collision-free paths by detecting and eliminating design errors, mainly collisions, in crane lift planning prior to construction (Chi and Kang 2010; Tantisevi and Akinci 2007). In terms of efforts to integrate BIM functionalities, previous studies (Al-Hussein et al. 2006; Han et al. 2012) which have relied on 3D visualization in 3ds Max have suffered two limitations: (1) data exchange between external computer modules and 3ds Max has required ad hoc intermediate formats such as the American Standard Code for Information Interchange (ASCII), thereby failing to provide full automation; and (2) only one-way information exchange from the customized programs to 3ds Max has been implemented. These limitations cause miscommunication and misunderstanding, with low rates of collaboration reducing productivity and quality at the design stage of projects. They also make it impossible to establish an efficient and automated system, which is the objective of this research, in order to design reliable, safe, and efficient crane operations for a large number of lifts with less lift planning time and cost. To overcome the existing shortcomings, this research proposes to add the crane, (mobile crane, in the case of this research), as a sub-domain under construction domain in the BIM model by integrating relevant information, such as information about the object to be lifted; project information; and crane information, such as how much rotation is required for the crane configuration, as well as when, where, and to what height the rigging system or hook should be lifted up and down. As a result, the BIM-based motion planning proposed in this research has the following features: (1)

two-way information exchange between applications used in the lift planning; (2) automated motion planning of mobile crane operations for projects with a large number of lifts; (3) representation of 3D visualization and of lift information such as capacity check, lift angles, and lift heights; (4) improvement of communication and collaboration; and (5) a decision making support system by which to select the best crane operation.

2.8 State-of-the-Art Research in Crane Productivity

In terms of construction management, construction managers generally build a plan which directs the use of workers, equipment, and materials in a coordinated and timely fashion in order to deliver a project within the constraints of the limited funding and time available (Halpin and Riggs 1992). Cranes are typically selected among construction equipment in order to deliver building components to their set positions based on schedule demands. To ensure that the lifting schedule is met, selecting a reliable and efficient crane operation is essential. However, lift engineers in practice generally tend to select a crane operation among a number of options based on their experience. This experience-based decision making may lead to crane re-location and inefficient crane operations, thereby compromising project productivity and safety. Crane productivity analysis (cycle time of crane operation) is thus necessary to assist practitioners in selecting the best crane operation among a variety of crane operations. However, crane productivity analysis has not garnered much attention because of a lack of pertinent information, such as process times for each motion of crane operation. In practice, the expected cycle times of crane operations are determined by

perceptions of crane operators and/or lift engineers. These cycle times when used as input data at the design stage yield inaccurate lifting and project schedules. To address this deficiency, this research presents a framework to determine the cycle time of crane operations using a scientific approach based on the 3D visualization of mobile crane operation designed by means of motion planning. This framework can assist in improving project productivity and safety by selecting the best crane operation for each lift and designing accurate lifting and project schedules. To accomplish the objective of this research, this section investigates effective and efficient productivity analysis methods and/or tools from previous studies in various construction fields.

In recent decades, construction simulation has been recognized as the science of developing and experimenting with computer-based representation of construction systems in order to understand their underlying behaviour (AbouRizk 2010). Simulation models illustrate the overall logic of various activities required to construct a facility and the resources involved in carrying out the work, such as labour and equipment. Based on these representations in the simulation model, simulation has been utilized to develop better project plans and decision making, to optimize material handling system, to minimize costs or project duration, and to improve overall construction project management based on productivity analysis. Zayed and Halpin (2004) have used a simulation tool to assess productivity and cost for the installation process of pile foundations subject to variables such as soil type, drill type, weather conditions, and equipment driver efficiency. Song et al. (2006) have presented experimental

methods to support engineers in analyzing daily production performance for labour productivity and making informed decisions through the implementation of a virtual production environment. Wang et al. (2009) have developed a simulation-based approach which builds simulation models to experiment with the current production system and proposed production system in order to evaluate the performance of a complex and dynamic spool fabrication shop. Taghaddos et al. (2010b) have developed a simulation-based approach to produce a heavy lift planning system for mobile cranes in order to produce a lift schedule that reduces the total cost and enhances the schedule of the project. However, utilization of simulation requires the effort and knowledge to build and understand simulation models and experiment accurately and efficiently (Mohamed and AbouRizk 2005). As an alternative to overcome this limitation, simulation models have been integrated with 3D visualization. Al-Hussein et al. (2006), for instance, have used a simulation engine to design tower crane operations by analyzing productivity, and 3D visualization has been used to validate, verify and represent the expected tower crane operation. As an extension of this integration, Han et al. (2012) have developed an automated system which experiments with various scenarios in the simulation model of a modular building production assembly line, selects the scenario which has the highest productivity, and builds 3D visualization automatically to facilitate understanding and assessment of the proposed production line configuration. Thomas and Yiakoumis (1988) have forecasted future performance by

quantifying the environmental, site, management, and design factors affecting project productivity.

Another factor affecting project productivity is uncertainty related to the operation of equipment. When cranes are operated in congested areas, crane operators frequently lose vision of the load, so they generally rely on hand signals from personnel observing and monitoring the operation. To address the challenge of so-called "blind lifts", vision systems such as video and wireless and sensor-based navigation have been introduced to enhance productivity, safety, and cost savings by improving communication and coordination between crane operators and other personnel supporting the crane operation (Everett and Slocum 1993; Lee et al. 2012, 2006; Shapira et al. 2008).

Furthermore, since carbon emissions have emerged as an important issue facing the global community, the construction industry has been identified as one of the main sectors contributing to climate change. Hendrickson and Horvath (2000) have noted that the construction industry's energy use has a significant environmental impact. Cranes on construction sites consume large amounts of fuel and emit significant volumes of CO_2 (EPA 2005). In this respect, minimizing crane operations on construction sites will not only improve project productivity but also decrease energy consumption, thereby reducing CO_2 emissions. In this regard, Hasan et al. (2013) suggested a crane selection methodology for high-rise building construction projects based on crane productivity performance assessment, quantification of carbon footprint impact, and simulation. This method assessed the environmental footprint associated

with the tower crane swing operation. Moreover, based on a review of existing research, the simulation engine selected in the research presented here is the most effective and efficient tool by which to determine the cycle time of crane operation, and to support better decision making rooted in a scientific approach. The cycle times of crane operations can be used as key information by which to build more specific and detailed lifting schedules as well as a project schedule.

2.9 Crane Management System

This research contributes to the development of a new component of a crane management system for heavy industrial projects in PCL Industrial Management Inc. This component, virtual motion of crane operation (VMCO), illustrated in Figure 2.3, allows practitioners to achieve the entire system within the BIM paradigm. The identification of workflow and relevant information in the crane management system is helpful in understanding the concept of VMCO. The input in the crane management system consists of: (1) crane capacity charts; (2) module information, such as weights, dimension and set points; (3) selected crane configurations; and (4) site layout and boundaries. These inputs, extracted from AutoCAD drawings and provided by crane manufacturers, are stored into a central database in Microsoft Access 2010.

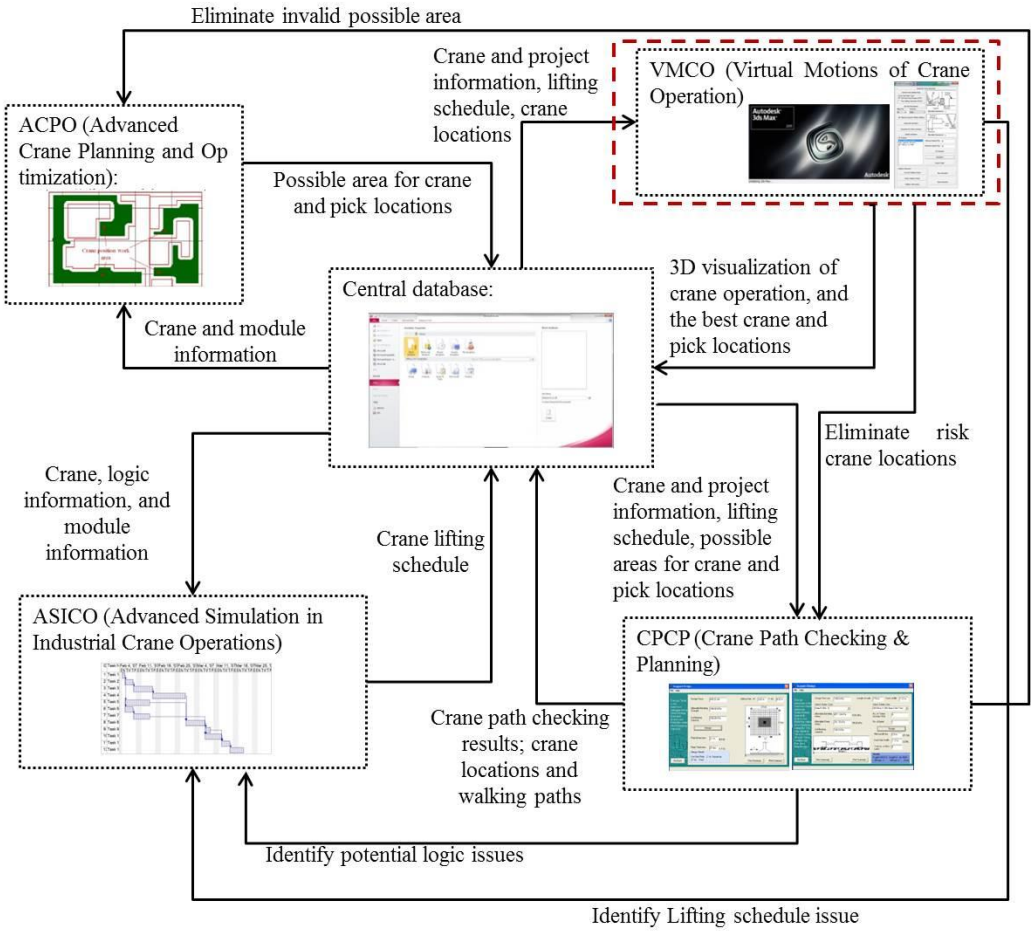

Figure 2.3: Crane management system in PCL Industrial Management Inc.

Since heavy industrial site layouts are complex and subject to frequent changes, crane location selection becomes difficult and time-consuming. To make this operation more efficient, an advanced crane planning and optimization system (ACPO) defines the potential crane location areas for each module, from where lifts can be performed without any conflicts, based on two site constraints (Hermann et al., 2010): (1) the inside boundary limit (ISBL), which defines a prohibited area for crane positioning inside the site plant; and (2) the outside site boundary limit (OSBL), which defines the outer limits of the project site. Meanwhile, a system for advanced simulation in industrial crane operations

(Taghaddos et al., 2012) plans lift sequences (schedule) based on the following logical considerations: (1) preventing a technical challenge which places a module between two adjacent modules; (2) identifying site constraints, which are the modules already installed before a given lifted module; (3) finding a mobile crane available to operate in predefined areas for a limited period of time; and (4) defining preceding activities, whereby the module at the bottom position should precede the above modules in the lift sequence. As a sequel to this previous work, Taghaddos et al. (2014) have proposed a simulation-based multi-agent approach to be used in arranging the field construction lift sequences and presented a case for the implementation of this system. There are two outputs of the system: (1) suitable mobile crane types and models for all lifts during the project; and (2) a lift schedule satisfying the availability and accessibility of the cranes, which considers crane mobilization and demobilization time, initial locations, crane configurations, and riggings.

Mobile crane operation consists mainly of two lifting methods: (1) pick from fixed position, in which the location of the crane is fixed during the lifting operation, and (2) pick and carrying operation, in which the mobile crane, unable to connect the pick point to the set point from a fixed location, is required to move while the load is lifted. In practice, the pick from fixed position method is generally the preferred approach of lift engineers and project managers since it has a lower rate of collision errors in comparison to its pick and carrying operation counterpart. Previous studies (Chang et al., 2012; Lai and Kang, 2009; Taghaddos et al., 2012) have evaluated path feasibility based on only the

framework of the pick from fixed position methodology. However, in some cases (usually in congested sites or when crane re-allocation is costly) the pick and carrying operation method is the only possible method for module assembly. Given this, a crane path checking and planning system is implemented in order to identify feasible crane locations for a large number of objects based on both crane pick from fixed position (Lei et al., 2013) and pick and carrying operation (Lei et al., 2014) methods. It selects a grid system to represent site layout, including ISBL, OSBL, and possible crane position work areas. Subsequently, the system creates the crane's tail-swing geometry on the grid points in the crane position areas and subtracts overlapping areas between the tail-swing geometry and the ISBLs in order to find points where the crane has sufficient capacity and boom clearance to load the modules. These positions are also swing-free crane locations. The output of this system results in feasible crane locations for each module. However, these possible crane locations may not permit successful crane operations, since the crane path checking and planning system mainly identifies potential crane locations by analyzing the feasibility of the lifting paths, while not taking into account motions of crane body configurations. Due to this limitation, the crane path checking and planning system has a 15% to 20% failure rate in terms of collision errors. Depending on the project size and type, the failure rate varies. To reduce this failure rate, designing the motions of crane operations in 3D visualization software is required in order to identify all feasible conflicts between cranes, lifted objects and surrounding site obstacles. In this respect, this research proposes 3D visualization-based motion planning to

validate the results of the crane path checking and planning system, whether or not there exist collision-free motions of crane operation. 3D visualization is paramount since it not only assists in designing motions of mobile crane operation and validating crane lifting plans by detecting potential errors and conflicts, but also allows practitioners to access crane operation data such as lifting angles and rigging (i.e., hook, sling, and spreader bar) heights. 3D visualization in this research can thus be used as a comprehensive design tool by which to plan various crane lifts.

Chapter 3: Methodology

3.1 Introduction

The aim of the research presented is to develop an integrated analysis and decision support system which will assist practitioners in (*i*) selecting the most appropriate crane associated with user-selected module pick positions or areas, and (*ii*) identifying the feasibility of crane operations satisfying static and dynamic spatial constraints. The constraints with respect to the second objective include (*a*) the site layout, (*b*) the geometry of the lifting equipment, (*c*) the potential crane location areas or points, (*d*) the module supply areas or points, and (e) the assembly schedules, which present new obstacles as the project progresses. Clearly, the integration mentioned above requires an information-centered paradigm, which allows the components of the system to maintain consistent data at each level of the decision process. From a practical perspective, this is achieved by adopting building information modelling (BIM) as the implementation paradigm, which requires the exchange of information among different models underlying the analysis/decision system. Stated simply, this work develops BIM-based motion planning for mobile cranes. It should be noted that although the methodology described in this work is applied to heavy industrial construction, the underlying algorithms are generic and can be applied in other fields of study. To support the understanding of the application described herein, the various types of mobile cranes are introduced in this section. Based on the type of boom (hydraulic/telescoping or lattice) and

undercarriage (wheeled or crawler-tracked), mobile cranes are categorized as follows: Boom Truck, Carry Deck, Crawler, Mobile Conventional, Mobile Hydraulic, Rough Terrain, Sky Horse, Tower Crawler, Transi-Lift, and Traveling Ringer. To simplify the analysis of lift planning, mobile cranes are divided into two types: truck cranes and crawler cranes. A crawler crane (see Figure 3.1a) , having both fixed and carrying positions for lifts, is mounted on a crawler carrier, while a truck crane, mounted on a wheel-base or outrigger-base (see Figure 3.1b) , has only fixed locations on site. Both crawler and truck cranes can mount a jib on the tip of the boom to extend the working radii, as well as a superlift (tail-swing) on the crane body to increase crane capacity in order to deliver all lifts to their set positions.

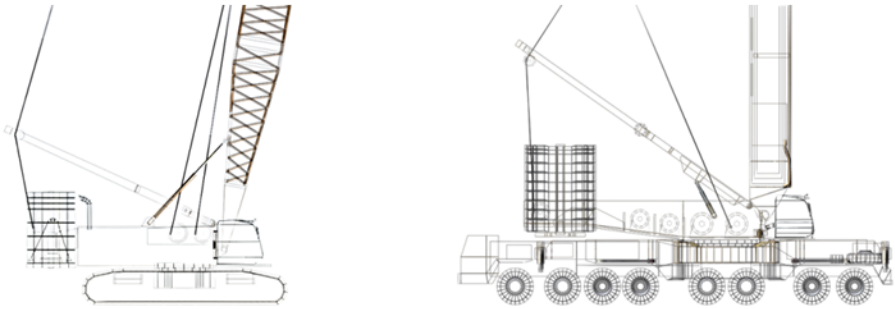

(a) Crawler crane (b) Truck crane

Figure 3.1: Different types of mobile cranes

The motion planning approach proposed in this research focuses on the crawler crane equipped with a superlift component (Figure 3.2), since modular-based heavy industrial construction projects often adopt this particular crane type to safely perform heavy lifts. Definitions of crane configurations and parameters vary depending on the particular crane owner, user, or installation designer. To bring together the information in these various definitions, the variables and

definitions of typical crawler crane configurations used in this research are listed in Table 3.1 and Table 3.2, respectively. Table 3.2 also describes the parameters occurring in the equations used for the calculations of the quantities required for motion planning.

Table 3.1: Definitions of crawler crane configuration components

Configuration	Description
Crawler carrier	The travelling base or carrier upon which the rotating superstructure is mounted: may be a car, truck, crawlers, or wheel platforms.
Superstructure	The rotating upper frame structure of the crane and the operating machinery mounted there upon.
Counterweight	A weight used to supplement the weight of the machine in providing stability for the lifting of working loads.
Superlift (tail-swing)	A device to increase lifting capacity.
Mast	A long, vertical pole used for supporting a structure.
Boom	A member hinged to the front of the rotating superstructure with the outer-end supported by ropes, leading to a gantry or A-frame used to support the hoisting tackle.
Jib	An extension attached to the boom point in order to provide added boom length for lifting specific loads. The jib may be in line with the boom, or may be offset to various angles.
Hook	A lifting device used to pick up loads. This is usually used with chains and slings.
Spreader bar	A device used to distribute weight while lifting wide frames.
Sling	A loop of material which connects the load to the lifting device. This can be made of chain, wire, or metal mesh.
Pick point	A position on the spreader bar which is connected to loads for lifts.

Table 3.2: Crawler crane parameters

Type	Notation	Description
Constant Parameter	t	Distance between boom pin and center of rotation.
	W_r	Weight of the suspended hoist ropes, hook block, and slings
	W_b, W_j	Weight of the boom and weight of the jib
	W_S	Weight of spreader bar
	L	Boom length
	V	Total weight of the crane and the lifted load
User defined parameter	W_{Lifted}	Weight of the lifted load
	R_L	Lifting radius
	R_S	Radius from center of the crane to outside site boundary of the superlift
Calculated parameter	θ	Boom horizontal swinging angle
	α	Boom angle to the ground
	C	Clearance, which is the distance between the crane configuration and any on-site obstacles
	H_{min}	Minimum lifting height, which is the distance from the ground to the top of the lifted object

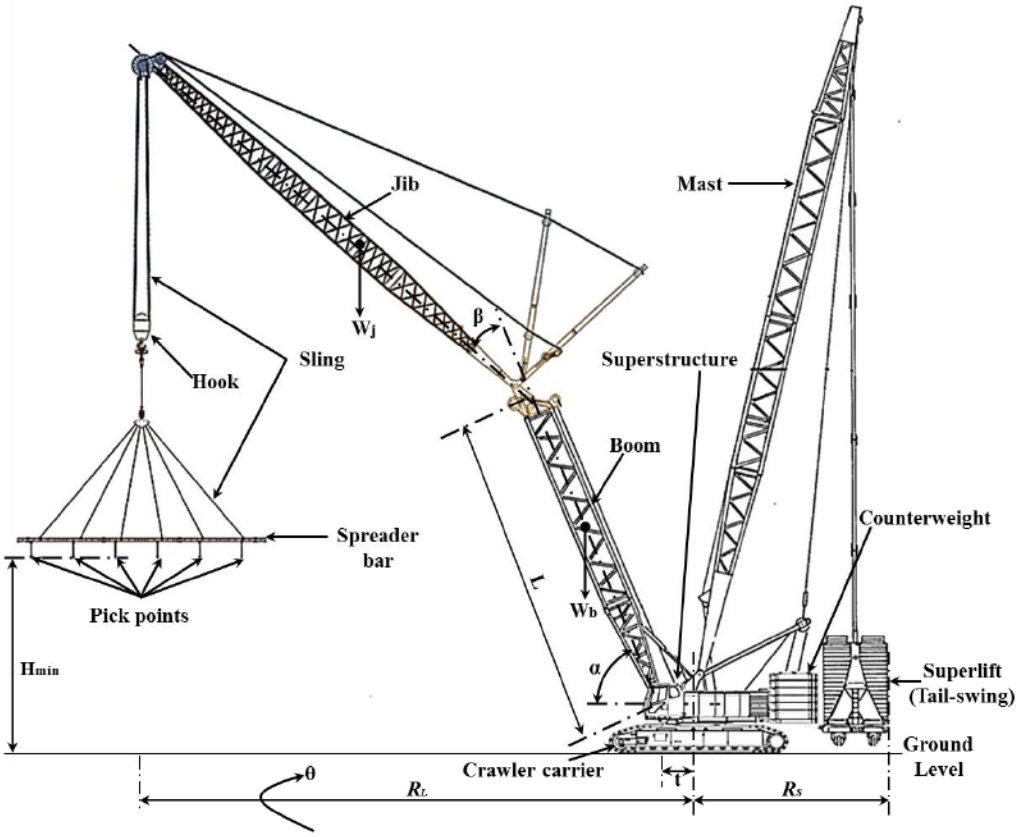

Figure 3.2: Crawler crane configuration and parameters

To achieve the research objectives, understanding definitions and workflow of crane lift planning is essential. As shown in Figure 3.3, lift planning mainly consists of four steps: (1) crane location; (2) crane selection; (3) motion planning of mobile crane operation; and (4) support system design. The initial step determines feasible crane locations associated with the pick and set points of the modules using an appropriate optimization technique in which the crane capacity, geometry are among the most important constraints. Based on these locations, a crane type and its configurations such as spreader bar, hook, counterweight and boom are selected satisfying the required crane capacity, lifting heights and clearances. The selected crane type and crane locations are used to design

motions of mobile crane operation in order to identify the shortest and/or optimized collision-free lift paths. At this juncture, it should be noted that the steps of crane location and crane selection are redesigned when any errors are identified in the motion planning since one of the objectives in the motion planning is to validate outputs of the previous steps. After planning the crane operation, the support design system is implemented for stable and balanced crane operations. To make the lift planning more (practically) accurate and efficient, engineers and researchers have analyzed more detail factors including productivity, wind speed and carbon factors.

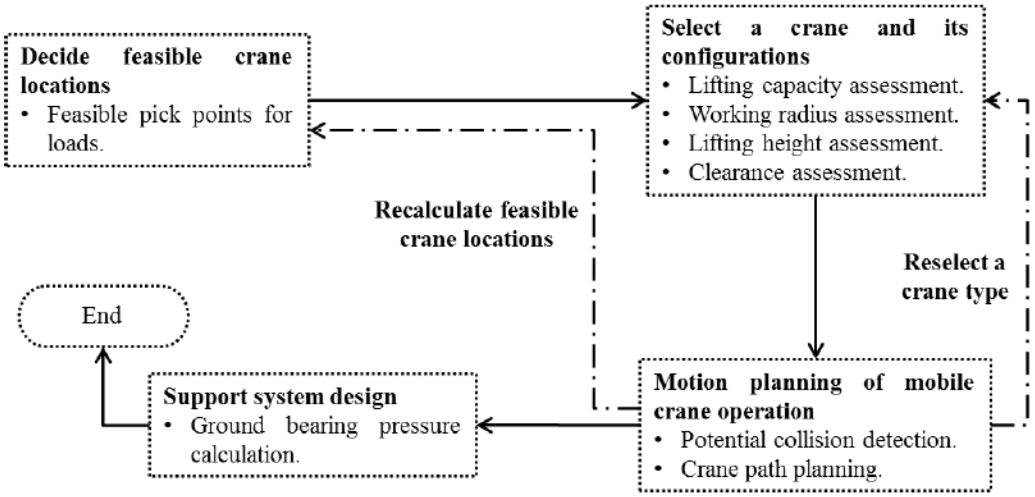

Figure 3.3: Process of the lift planning

3.2 System Architecture

As shown in Figure 3.4a, this research builds on a previous contribution, a crane path checking planning system developed by a binary algorithm (with yes/no outputs) using the configuration space (C-space) technique (Reddy and Varghese 2002) to check for the existence of feasible crane pick from fixed position (Lei et al., 2013) and pick and carrying operations (Lei et al., 2014). The crane path

checking planning system has been built in Microsoft Visual Studio 2010. At this juncture, it is important to note that, for quality assurance, every feasible path included in the final design of the crane motions is validated using 3D visualization in 3ds Max in order to eliminate potential design errors during the crane lift planning. To satisfy this requirement, this research proposes an implementation (in 3ds Max) of a BIM-based motion planning method, considering both feasible pick from fixed position and pick and carrying operation methods. The process flow of the proposed system is described by the pseudo code in Figure 3.4b. In order to satisfy the constraints of crane pick from fixed positions and pick and carrying operations, it is imperative to develop a mathematical algorithm allowing us the following: (1) to identify the locations of the mobile crane within a collision-free pick area that are sufficiently large to accommodate swinging of the tail-swing or super-lift counterweight; (2) to design motions of mobile crane operations without any collision errors during crane operation, including crane pick from fixed position and pick and carrying operation methods; and (3) to permit the mobile crane to lift the modules within the pick area only. Furthermore, given the objectives of this contribution in terms of software integration, the computer system must provide mechanisms to allow information in the user-defined database to be shared and/or exchanged between the crane binary pick from fixed position and pick and carrying operation checking procedures and 3ds Max.

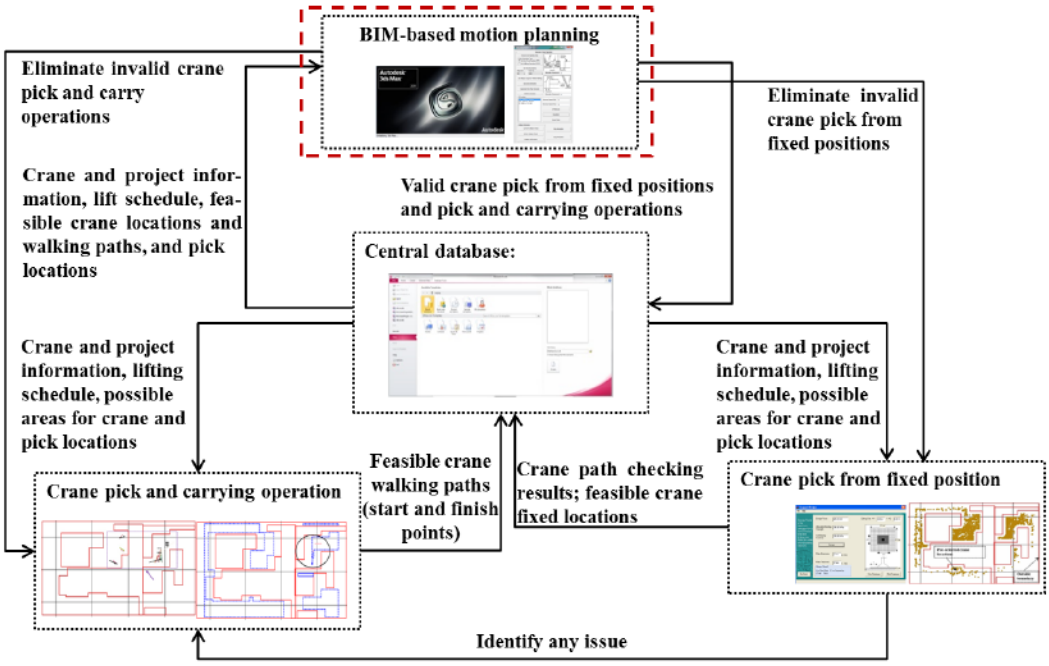

(a) The proposed system

```
S: set of all modules to be lifted
Q: List of validated paths (Motion plan)
O = [ ] /* Empty list */

For each module M in S do:
P ←Find all feasible lift checking for M using the pick from fixed position method (Lei et al. 2013)
If (P is empty) then:
P ←Find all feasible lift checking for M using the pick and carrying operation method (Lei et al. 2014)
End if

/* Design motion plan */
For each crane location p in P:
Design motions of crane operation to verify and validate pick from fixed position and pick and carrying operation paths in 3ds Max
If (p is 3ds Max-validated):
Append p to Q
Else:
Reject p
```

(b) Pseudo code of process flow

Figure 3.4: System Architecture

3.3 Methodology

The purpose of the methodology is to validate feasible crane locations, including crane pick from fixed position and pick and carrying operation methods, based on dynamic site layout and lift scheduling. The site layout and lift schedule in heavy construction projects are frequently changed for various reasons, such as delays in delivery of material, weather conditions, and other factors. These changes lead to repeated iterations of crane lift planning, a scenario which is time-consuming, costly, and fraught with design errors. The aim of the proposed methodology is thus to develop BIM-based motion planning of mobile crane operations in order to reduce the time-consuming repetition of lift planning tasks such as crane location selection and collision identification. The methodology comprises the following five modules, as shown in Figure 3.5: (1) an automated 3D model builder to develop 3D site layout and existing obstacles; (2) 3D visualization-based motion planning for the design of crane motions integrating 3D visualization with mathematical models; (3) a system for verification of 3D visualization through collision checking and lift analysis that encompasses crane capacity check and working radius; (4) post-visualization simulation, which evaluates 3D visualization of crane operation to determine cycle time of crane operation; and (5) a BIM-based crane information system for better collaboration and communication among project participants. To implement these modules, the input data consists of: (1) site layout data, which refers to the dimensions (length, width, and height) of site boundaries allowing a 3D representation of the site boundary model to be automatically constructed by means of the automated

3D model builder; (2) sequences of crane operation, which assist with build 3D crane motions using 3D visualization-based motion planning; (3) module information, which involves module supply and set positions, and dimensions of modules, all of which are needed to create 3D representations of existing obstacles and to design crane motions using the automated 3D model builder and 3D visualization-based motion planning; (4) crane location, which is required to determine the feasibility of crane operation using 3D visualization-based motion planning; and (5) crane geometry data, which assists in verifying 3D visualization of crane operation, particularly the 3D crane model.

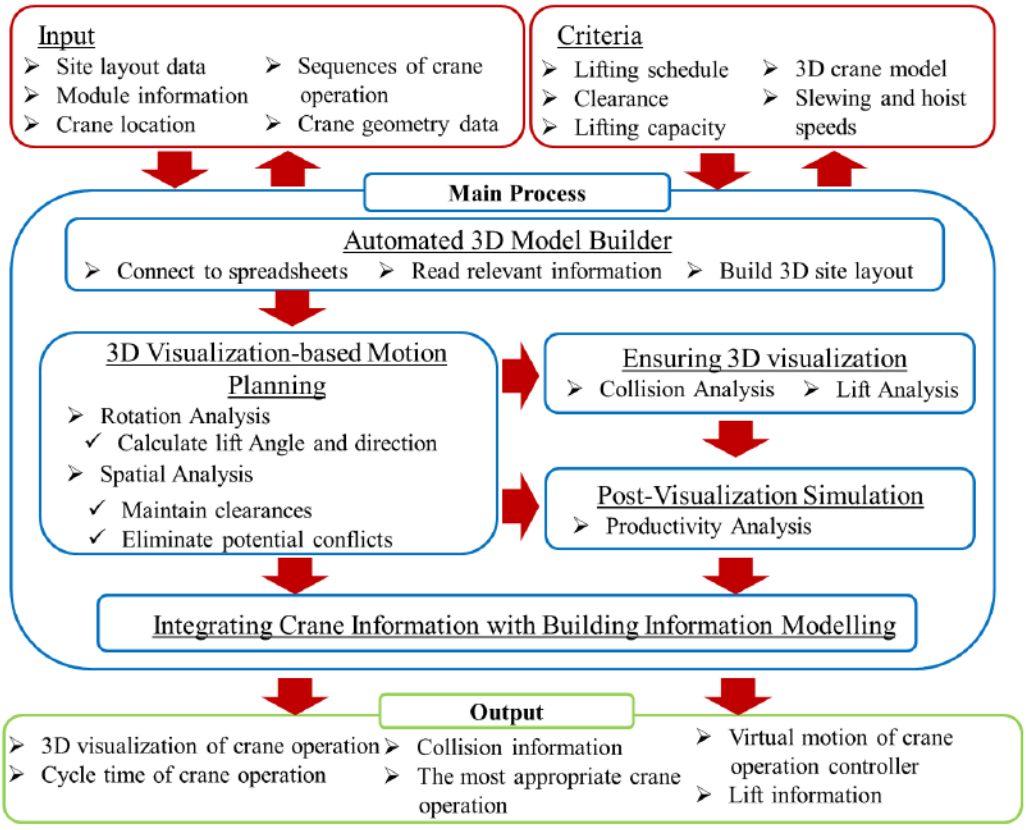

Figure 3.5: Methodology

The criteria required in order to implement the aforementioned motion planning system include the following: (1) lifting schedule, which assists in identifying existing obstacles already installed before an object to be lifted; (2) clearances, which are used to prevent potential conflicts during crane operation; (3) site boundaries, represented as the OSBL and ISBLs, (which are the inaccessible areas representing obstructions or ongoing construction activities); (4) lifting capacity, to facilitate 3D visualization of crane operation; and (5) slewing and hoist speeds, to determine the cycle time of crane operation. Since a crane pick and carrying operation is a straight line, it needs only the walking paths, which are defined by the start points from where the objects are loaded and the finish points where the modules are unloaded. Clearly, the process of the pick from fixed position method is more straightforward since the crane location is the only information needed in order to set up the operation. To be consistent with the input of previously developed routines, the information described, as input data in the methodology underlying the present research, is stored as 3D Cartesian coordinates in the central database. The outputs are: (1) 3D visualization of crane operations; (2) collision information, such as which, when, and where crane configurations collide with existing obstacles and/or lifted objects; (3) VMCO controller, which is an implementation application in 3ds Max; (4) cycle time of crane operation, which can assist to select the most appropriate crane operation among various crane operations; (5) lift information, which provides how much rotation is required for crane body configurations, and when, where, and to what height the rigging system should be lifted up and down; and (6) the most

appropriate crane operation, as determined by comparing the cycle times of crane operation.

3.3.1 Automated 3D Model Builder

The purpose of the automated 3D model builder is to build 3D models automatically in 3ds Max based on digital numeric information, such as site and module information, in a database. As shown in Figure 3.6, the automated 3D model builder consists of the following three procedures: (1) developing an interfacing system, which connects a central database in Microsoft Access 2010 to 3ds Max; (2) importing and mapping 3D crane models from computer-aided design (CAD) programs, which captures real-world transformation of a mobile crane; and (3) building 3D models automatically in 3ds Max. The outputs of this system are 3D site layout, 3D existing obstacles, and a 3D crane model.

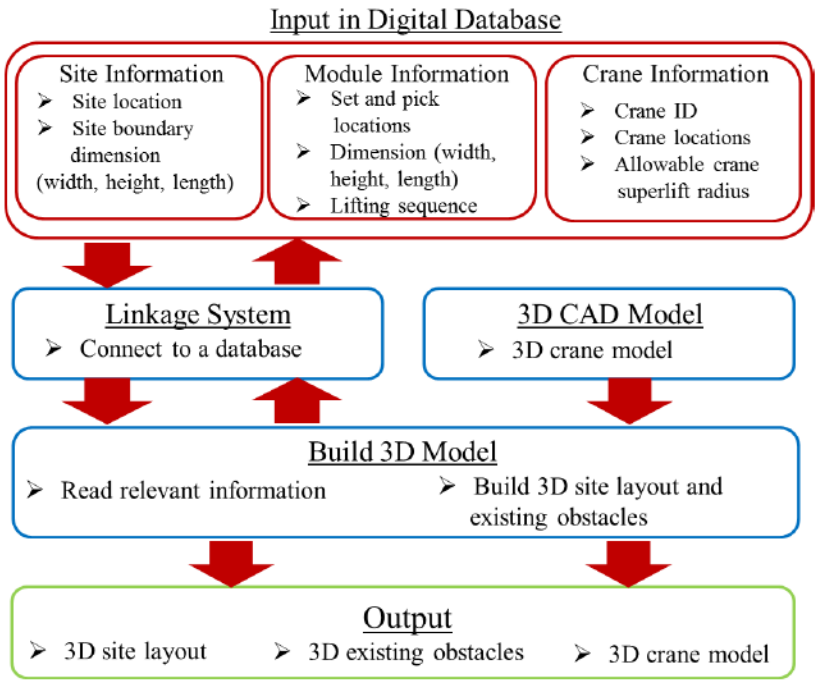

Figure 3.6: Automated 3D model builder module

The automated 3D model builder is developed using MAXScript, a built-in scripting language in 3ds Max. The interfacing system connects directly to external systems, (e.g., Microsoft Access 2010), and two-way information exchange (read, write, and update) between customized programs and 3ds Max is successfully established. 3D models are then built based on relevant information such as module dimensions (width, height, length) and site boundaries, which are represented by digital numeric information. The automated 3D model builder reduces the repetitive task of building 3D site layout and existing obstacle models for a large number of objects. It also allows project participants to react efficiently to design changes with less time and cost incurred. At this juncture it should be noted that a 3D crane model is imported from AutoCAD and modified to achieve the movements of 3D mobile crane configurations in 3ds Max, which effectively represent real-world crane motions.

3D Crane Model

To successfully develop motion planning in a 3D environment, one of the most critical factors is the transformation of a 3D mobile crane model, which must mimic *exactly* the movements of a real mobile crane. The motion planning must also provide positions of each crane configuration across the animation time in order to analyze slewing angles and lifting heights, as well as, to monitor clearances between the crane and obstacles. Corresponding to these requirements, three functionalities in 3ds Max are adopted: (1) a world coordinate system by which to identify the positions of crane configurations and to visualize movements of the 3D mobile crane; (2) a bones system; and (3) a

link constraint. The movements of 3D mobile crane configurations illustrated in Figure 3.7 should meet the following requirements: (1) all mobile crane configurations should be moved when the crane-base (carrier) is moved in the *x*, *y*, and *z* axes; (2) when a superstructure is rotated in the *z*-axis, the boom, superlift, and rigging are also rotated by the same angle as the superstructure; (3) the boom has an independent vertical rotation in the *x*-axis; and (4) the rigging is moved up and down in the *x*, *y*, and *z* axes independently. To satisfy these requirements, a bones system—jointed and hierarchical linkage of objects—is used in this research based on an inverse kinematics (IK) solver. In a linkage, the IK solver governs the transformations of the child objects, such as rotation and position, as well as its own behaviour and workflow (Figure 3.7). As a result, superstructure, boom, superlift, and rigging systems have their own rotations and positions, even though they inherit the crane-base movement. Since the virtual movements of the lifted objects by the mobile crane are followed by the movement of the rigging system corresponding to the real movements of the lifted objects, the objects being lifted are moved by a link constraint which inherits the position and rotation of its target object, i.e., the rigging system.

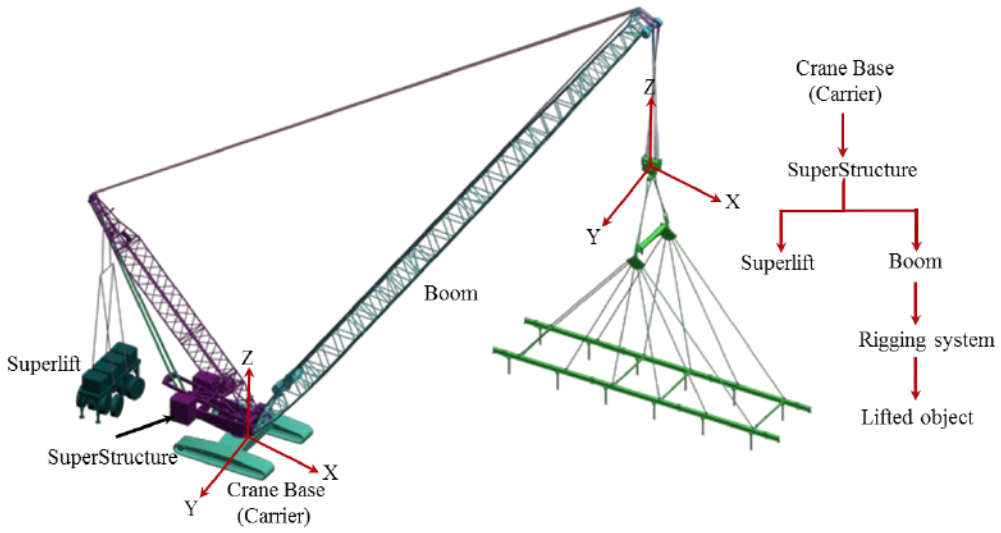

Figure 3.7: Linkage of mobile crane configurations

3.3.2 3D Visualization-based Motion Planning

The methodology for 3D visualization-based motion planning for mobile crane is illustrated in Figure 3.8. Based on the mobile crane pick from fixed position and pick and carrying operation methods, the input data consists of: (1) site layout, given in the form of site boundary limits, (which are the inaccessible areas representing obstructions or ongoing construction activities); (2) existing obstacles, which are modules already installed before the module to be lifted; (3) crane geometry; and (4) module information, such as identification number, module supply and set positions, weight and dimensions (length, width, and height). At this point it should be noted that the crane management system does not provide specific supply positions for modules, but rather pick areas in which modules should be located for loading. This research thus defines module supply positions based on the pick areas supplied by the user. Based on outputs of the

automated 3D model builder, the motion planning presented in this research has two analyses: rotation analysis and spatial analysis (Figure 3.8).

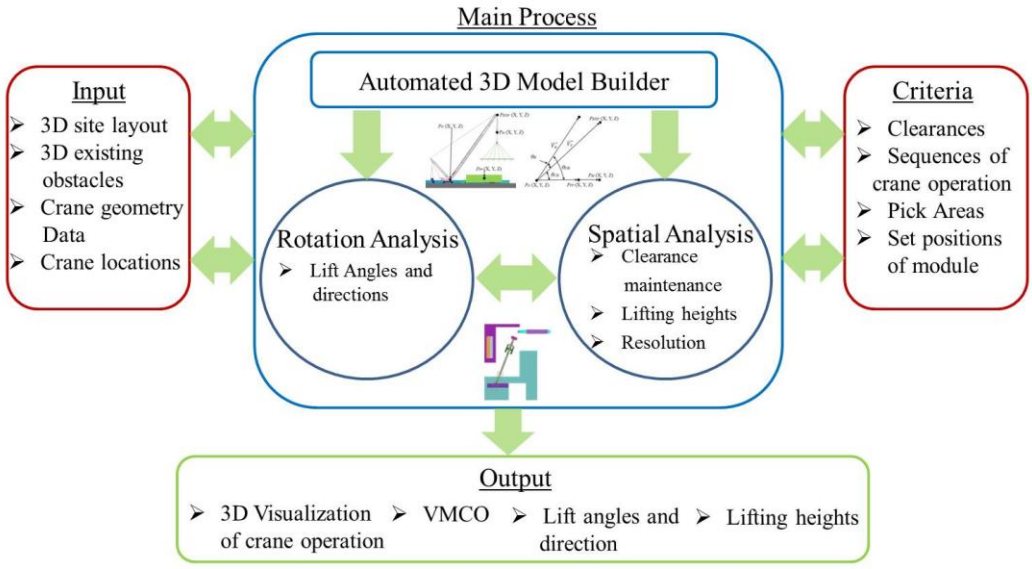

Figure 3.8: 3D visualization-based motion planning module

Based on sequences of crane operation, rotation analysis computes lifting angles and directions for the transformation of crane body configurations, i.e., the superstructure, boom, and rigging system, which establishes the crane in an orientation to pick and set the load. The spatial analysis has two functions: (1) monitoring and maintaining sufficient clearance between the lifted object, crane body configurations, and existing obstacles during the crane operation; and (2) calculating lifting heights, where the lifted object is vertically manoeuvred to avoid any conflicts while it is oriented horizontally in relation to the motion of the crane body configuration. At this juncture, it should be noted that crane operation can generally be categorized in terms of two types of motions: (1) motion of the crane body configuration using rotation analysis and the first

function of the spatial analysis; and (2) motion of the lifted object using the other function of the spatial analysis. In this regard, the rotation and spatial analyses are implemented interactively to design successful motions of mobile crane operation based on time-dependent positions (current and desired positions) of each 3D crane configuration in the animation. As shown in Figure 3.9, the time-dependent positions are defined by reading the pivot and center points of the 3D models in the coordinate system across animation time. The center points of each crane configuration are determined based on the following considerations: (1) the center points of the crane-base (carrier), superstructure, and boom are located in the center of gravity of the mobile crane; (2) the rigging system is located in the center of the hook, since it is linked to the hook; and (3) the lifted objects are defined by the positions of their centers.

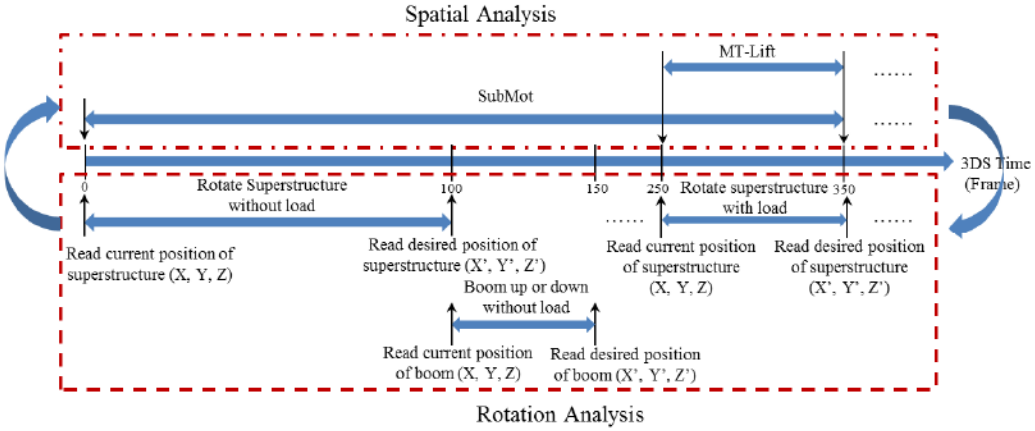

Figure 3.9: Animation time-dependent positions of 3D crane models

Rotation Analysis

To design the motions of mobile crane operations for numerous objects, the sequences of mobile crane operation are defined by "*What if*" scenarios developed by practical sequences of mobile crane operation. Based on these

scenarios, the proposed motion planning efficiently develops motions of mobile crane operation for both pick from fixed position and pick and carrying operation methods, even though factors affecting the site layout and lifting schedule, such as objects' pick positions and existing obstacles (congestion level), are changed in practice. The sequences of operation that need to be performed by a crane can generally be described using the flowchart in Figure 3.10. Regardless of the lifting method, i.e., pick from fixed position or pick and carrying operation, a series of rotations and translations, referred to as "common scenarios" in Figure 3.10, often need to be applied. These are applied to in order to bring the mobile crane into a favourable spatial orientation that permits it to pick and deliver the load from the module supply position to the final location. These rotations and translations are outlined as follows: (1) appropriately align the crane carrier based on the chosen lifting method, such that the alignment is completed at the start point in the case of the pick and carrying method or the fixed position in the case of the pick from fixed position method; (2) rotate the superstructure to load an object (lifted object) at a certain module supply position; (3) rotate the boom vertically to coincide with the geometric center of the lifted object; (4) rotate the rigging system to be aligned with the lifted object; (5) adjust the height of the rigging system (up or down) to allow the lifted object to be hooked; and (6) rotate the superstructure to bring the load to its set position in the case of pick from fixed position, or to the finish point of the walking path if the crane requires walking. It should be noted that the spatial analysis, SubMot and MT-Lift, is implemented in a quasi-continuous manner while the rotation

analysis is being executed. In some instances, the rotation angle and direction calculated by rotation analysis may be incorrect because they lead the crane configuration to enter an inaccessible area (within the ISBLs) or collide with an existing obstacle. As a proactive measure, the spatial analysis identifies and prevents potential conflicts between the crane and surrounding obstructions, and searches for material-lifting paths during crane operation.

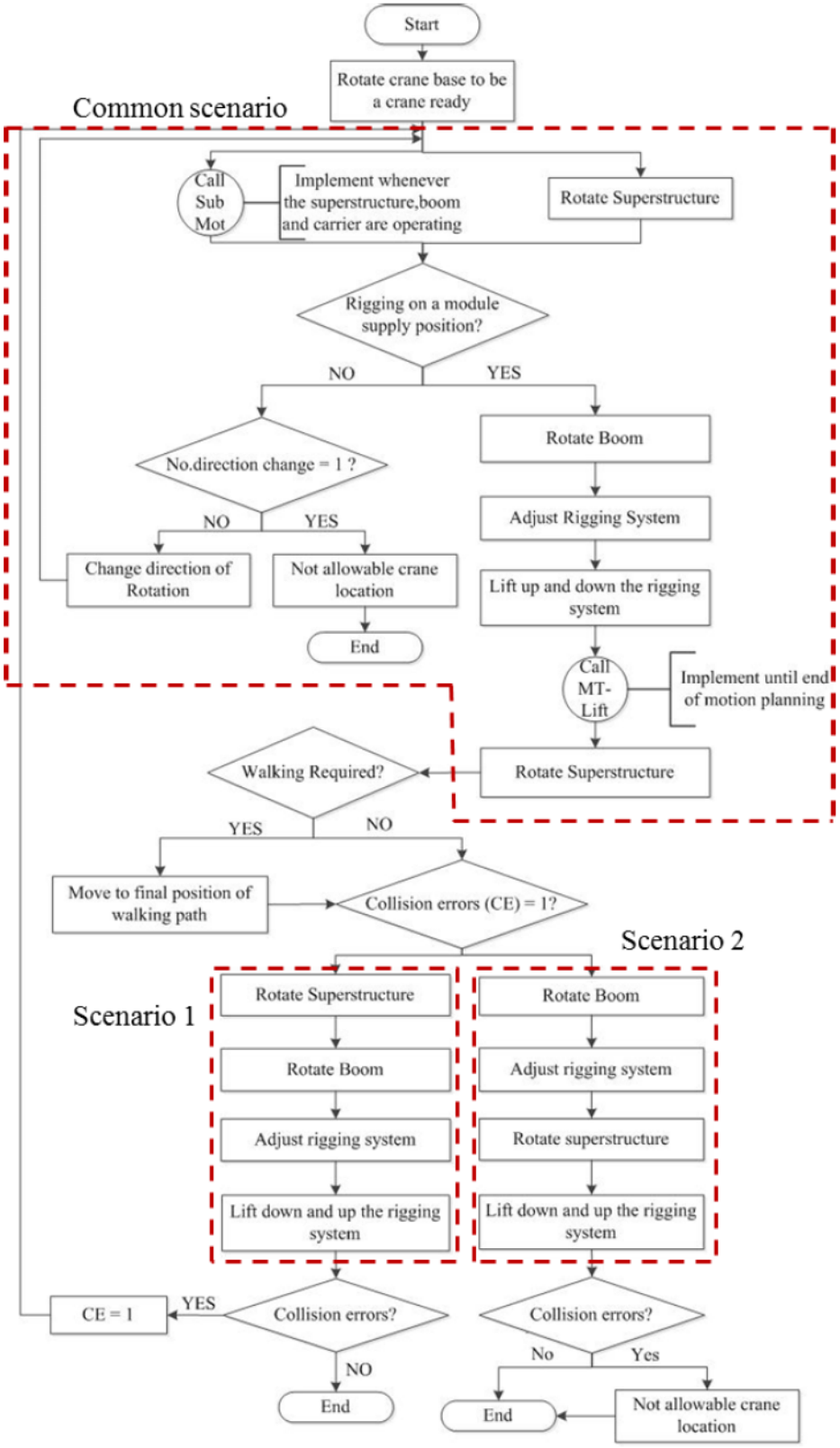

Figure 3.10: Flowchart of rotation analysis

After completing motions in the common scenario, the path planning algorithm branches into one of two scenarios, namely, pick from fixed position or pick and carrying operation (lifting modes). Possible lifts then undergo a collision check, and the algorithm branches to either scenario 1 (if there are no collision errors, i.e., CE = 0) or scenario 2 (CE=1). Based on the common scenario and scenario 1, motions of mobile crane operation are initially represented in the 3D environment to enable users to visually check for any collisions. If collisions are identified in the scenario 1-based crane operation, the lift is re-planned automatically according to the steps in the common scenario and scenario 2. If the mobile crane operation built using scenario 2 still contains collision errors, the current crane location and/or the supply position of the lifted object is rejected for the given lift. Of course, the crane location may still be permissible with a different module supply position (MSP) for the lifted object, since module supply positions in the pick areas may lead to a different sequence of crane motions. Based on the sequence of operations—i.e., rotations, translations, and walking (if applicable)—required by the common scenario and the selected lifting scenario, the lifting angles and directions associated with the crane body configurations are calculated by means of the rotation analysis procedure at any point on the planned path, or, equivalently, any time during the animation. In order to set up the equations underlying the calculation of the angles needed for the rotation analysis, four variables are required: (1) the crane-base (carrier) angle, $\theta^{Carrier}$; (2) the superstructure angle, θ^{SP}; (3) the boom angle, θ^{B}; and (4) the rigging angles, θ^{RI} (see Figure 3.11).

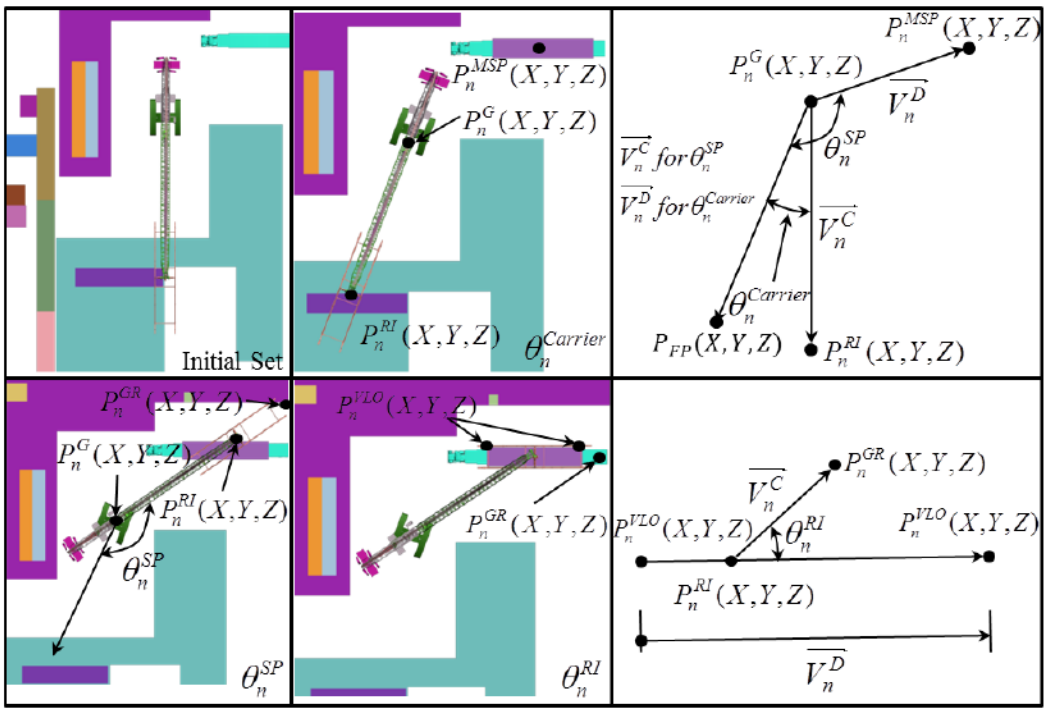

Figure 3.11: Calculation of $\theta^{Carrier}$, θ^{SP}, and θ^{RI}

According to Figure 3.11, all the angles of interest, with the exception of the rigging angle, have their vertices on the center of gravity, P_G, of the mobile crane, which is assumed to be the point at which the crane body configurations, namely, the boom, crane-base and superstructure, are connected. In addition, with the exception of the rigging system, P_G also represents the center of all of the rotations needed for crane operations and crane walking, including rotation of the crane carrier. At a given instant, t_n, of the animation time, the calculation of the lifting angles ($\theta_n^{Carrier}$, θ_n^{SP} and θ_n^{RI}) of each crane body configuration is calculated within the rotation analysis procedure, which considers the vectors, $\overrightarrow{V_n^C}$ and $\overrightarrow{V_n^D}$. These vectors represent the current and desired positions of the crane body configuration, i.e., crane-base (Carrier), superstructure (SP), boom

(B), or rigging (RI). To calculate θ_n^{SP}, for example, three points are used to calculate the vectors: (1) the center of gravity, P_G; (2) the geometric center position of the rigging system, P_{RI}; and (3) the module supply position (MSP) of the lifted object, P_{MSP}. As a result of this, two vectors are defined satisfying Equation (1):

$$\overrightarrow{V_n^C} = \overrightarrow{P_n^{RI} P_n^G} = \overrightarrow{\Omega P_n^{RI}} - \overrightarrow{\Omega P_n^G} \text{ and } \overrightarrow{V_n^D} = \overrightarrow{P_n^{MSP} P_n^G} = \overrightarrow{\Omega P_n^{MSP}} - \overrightarrow{\Omega P_n^G} \quad (1)$$

Where Ω is the origin of the coordinate system. In order to determine unambiguously the lifting angle, it is necessary to assess its sine and cosine. These values can easily be determined from the dot and cross products of the vectors defined above and satisfying Equation (2):

$$\cos\left(\theta_n^X\right) = \frac{\overrightarrow{V_n^C} \bullet \overrightarrow{V_n^D}}{\left\|\overrightarrow{V_n^C}\right\| \left\|\overrightarrow{V_n^D}\right\|} \text{ and } \sin\left(\theta_n^X\right) = \frac{\overrightarrow{V_n^C} \times \overrightarrow{V_n^D}}{\left\|\overrightarrow{V_n^C}\right\| \left\|\overrightarrow{V_n^D}\right\|}$$

$$\text{where } X \in \{Carrier, SP, B, RI\} \quad (2)$$

At this point, the lift θ_n^{X} can finally be determined satisfying Equation (3):

$$\theta_n^{\mathrm{X}} = \arctan\left[\frac{\sin\left(\theta_n^{\mathrm{X}}\right)}{\cos\left(\theta_n^{\mathrm{X}}\right)}\right] + \left[1 - \mathrm{sgn}\left(\cos\left(\theta_n^{\mathrm{X}}\right)\right)\right]\left(\frac{\pi}{2}\right) \quad (3)$$

Where the function $\mathrm{sgn}(z)$ is the sign function that returns (-1) when its argument, z, is negative and otherwise returns $(+1)$. For example, a rotation of the rigging system, (θ_n^{RI}), shown in Figure 3.11, requires the vectors, $\overrightarrow{V_C} = \overrightarrow{P_{GR} P_{RI}}$, in which $\overrightarrow{P_{GR}}$ is a global point belonging to $\overrightarrow{P_{RI}}$, and $\overrightarrow{V_D} = \overrightarrow{P_{VLO}}$,

where $\overrightarrow{P_{VLO}}$ is defined by two consecutive vertices of the object (assumed to be a rectangular prism) in the direction of highest inertia. Based on these two vectors, the lifting angle θ_n^{RI} is determined by Equations. (2) and (3).

The lifting angle α_n^B, illustrated in Figure 3.12, which indicates whether the boom needs to be raised or lowered, is only required when the point, P_n^{RI}, is not located right above the center of gravity of the payload, i.e., the module supply position. In this case, α_n^B is calculated as the difference between the current and the desired boom angles, i.e., α_n^{CB} and α_n^{DB}, shown in Figure 3.12. These angles are obtained by means of Equation (2) and Equation (3), in which the vectors, $\overrightarrow{V_n^{\mathrm{C}}}$ and $\overrightarrow{V_n^{\mathrm{D}}}$, represent the current and desired location vectors of the boom. The required parameters for these vectors consist of P_n^G, P_n^{MSP}, P_n^{RI}, as well as the boom length, which extends from the P_n^G to the boom tip (P_n^{BTIP}). To calculate these vectors accurately, the *z*-coordinates of the parameters, such as P_n^{MSP} and P_n^{RI}, must be the same as those of the P_n^G, with the exception of the boom length. It should be noted that the range of the boom rotation is determined by maximum (R_{max}) and minimum (R_{min}) radii analyzed by the crane capacity checking, based on the load weights and crane capacity chart in the central database. When the boom is up or down, there are two alternative methods for determining the hoist height: (1) to maintain the same height as that of the previous motion, which is the method adopted in this paper; and (2) to

change the height (up or down) according to existing obstacles. As well, cases in which the lifted object's longest side coincides with the crane boom plane should always be avoided in order to maximize clearances between the boom and the lifted object by minimizing the hoist height after the lifted object is loaded by the crane.

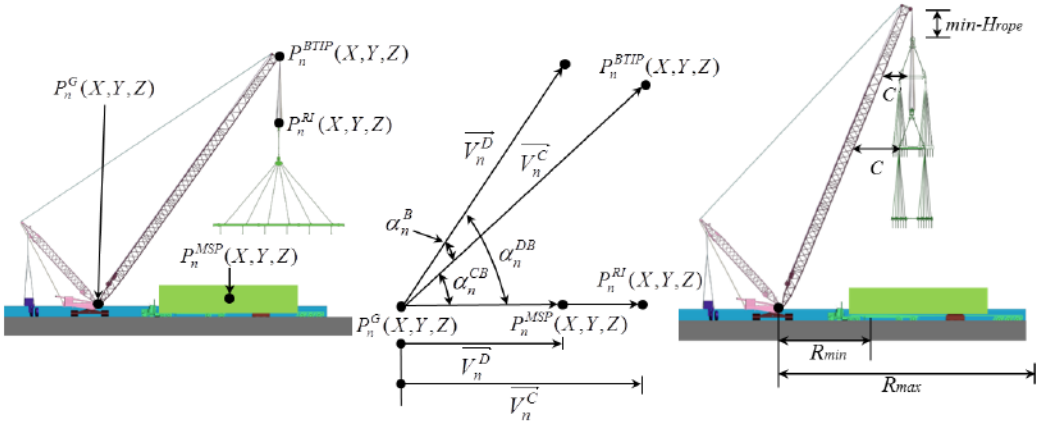

Figure 3.12: Calculation of α_n^B

Although the rotation analysis determines the lifting angles and directions for motions of crane body configurations based on readings of current and desired positions, two types of design errors, represented in Figure 3.13, can be encountered. With regard to rotation analysis characteristics, which are calculations of over lifting angles and incorrect lift directions, the rotation analysis does not consider clearance between crane body configurations and surrounding obstacles on site. In this regard, collision errors (see Figure 3.13a) can be encountered. To prevent these collisions, the current motion of crane operation is stopped any time when the minimum clearance is violated. However, the location of the rigging system may not be above the module supply positions

of the lifted objects for loading. This design error is known as direction error (see Figure 3.13b). To eliminate potential design errors in the rotation analysis, spatial analysis is implemented.

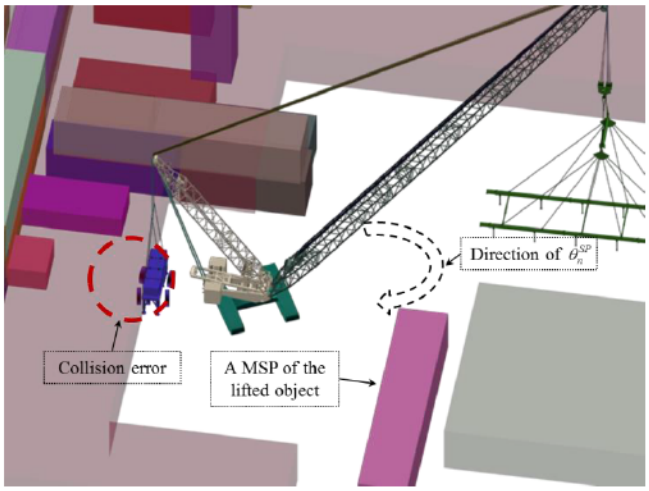

(a) Collision error

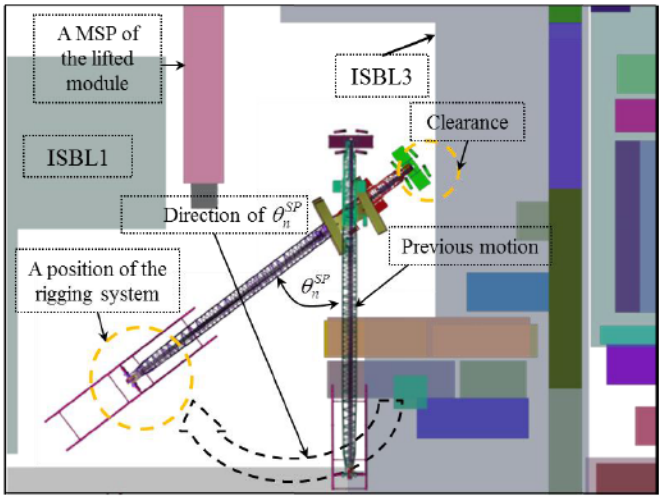

(b) Direction error

Figure 3.13: Design errors in rotation analysis

Spatial Analysis

The spatial analysis consists of two functions (see Figure 3.14), which in combination constitute the core of the spatial analysis process. The "SubMot" function checks clearances in a quasi-continuous mode between the crane, the

loads, and the surrounding site elements. The "MT-Lift" function provides a simple algorithm for designing material-lifting paths. One of SubMot's functions is to eliminate design errors in the rotation analysis. In this regard, the interferences between the crane (mainly superlift in this research), and the existing obstacles and/or ISBLs, which by design are areas prohibited for crane components, may be encountered to prevent design errors of the rotation analysis, which are over lifting angles or incorrect lift directions, during crane operation. When the crane is operating and the distance is equal to or less than the pre-defined clearance, the current motion is immediately stopped to avoid potential collision errors, and then the next motion is carried out. However, this effort may lead to a direction error in which the rigging in its current position cannot reach the module supply position for loading, or the set position of the lifted object for unloading. To resolve this error, the rotation analysis has a trigger to re-design motions of mobile crane operation by changing the direction of the rotation automatically after identifying the position of the rigging system (see Figure 3.10). If the rigging system still is unable to load and/or unload the lifted object, the given crane location and/or the module supply position is not allowable. In terms of computer implementation of the spatial analysis, the MT-Lift function applies a practical motion plan as follows: (1) lift the load and keep it as close as possible to the ground (which is the most widely adopted rule in practice); (2) move the load along, stopping the current motion of crane operation immediately when the pre-defined minimum clearance between the lifted object and any existing obstacles is reached; (3) raise the load above the obstacle (including the

appropriate clearance) and re-start the current motion from step (2). It is integral to note that, given a crane location, even though a material-lifting path is known to exist between the pick and set points of the lifted object based on implementation of the crane path checking planning system in crane management system, clearances between the crane components and the surrounding structures need to be constantly monitored since the movements of the crane body configurations are not analyzed. In essence, the MT-Lift function returns a path that can be expressed as a sequence of rotations and elevations, which can be formalized as follows:

$$\mathrm{P}(\mathrm{P}_n^{MSP} \rightarrow S) = \sum_{i=1}^{n} (\Re(\beta_i) \oplus \mathrm{E}_i) \tag{4}$$

Where $\mathrm{P}(\mathrm{P}_n^{MSP} \rightarrow S)$ represents the path of the load which starts at the module supply position (MSP), P_n^{MSP}, and ends at the set point, S, which is represented as n consecutive rotations, $\Re(\beta_i)$, occurring at elevation, E_i. As a result, the rotation and spatial analyses are implemented interactively in order to modify lifting angles and their directions by identifying and eliminating potential collision errors using SubMot, as well as to design material-lifting paths during crane operation across animation time using MT-Lift. In this respect, accurate distance measurement between crane body configurations, existing obstacles, and lifted objects is critical for the successful development of spatial analysis. That is, the distances provide essential information regarding which objects (crane parts, lifted objects, and existing obstacles) have potential collision errors

at a specific time. The sequences of SubMot and MT-Lift functions are as follows: (1) identify target obstacles that may collide with the lifted object and/or crane configurations; (2) monitor when and where clearances between the target obstacles, the lifted object, and the crane body configurations are not satisfied; and (3) determine which operations the crane must follow in order to prevent or resolve potential collision errors. The SubMot is implemented when the crane is operating, and the MT-Lift is executed after the crane loads the lifted object.

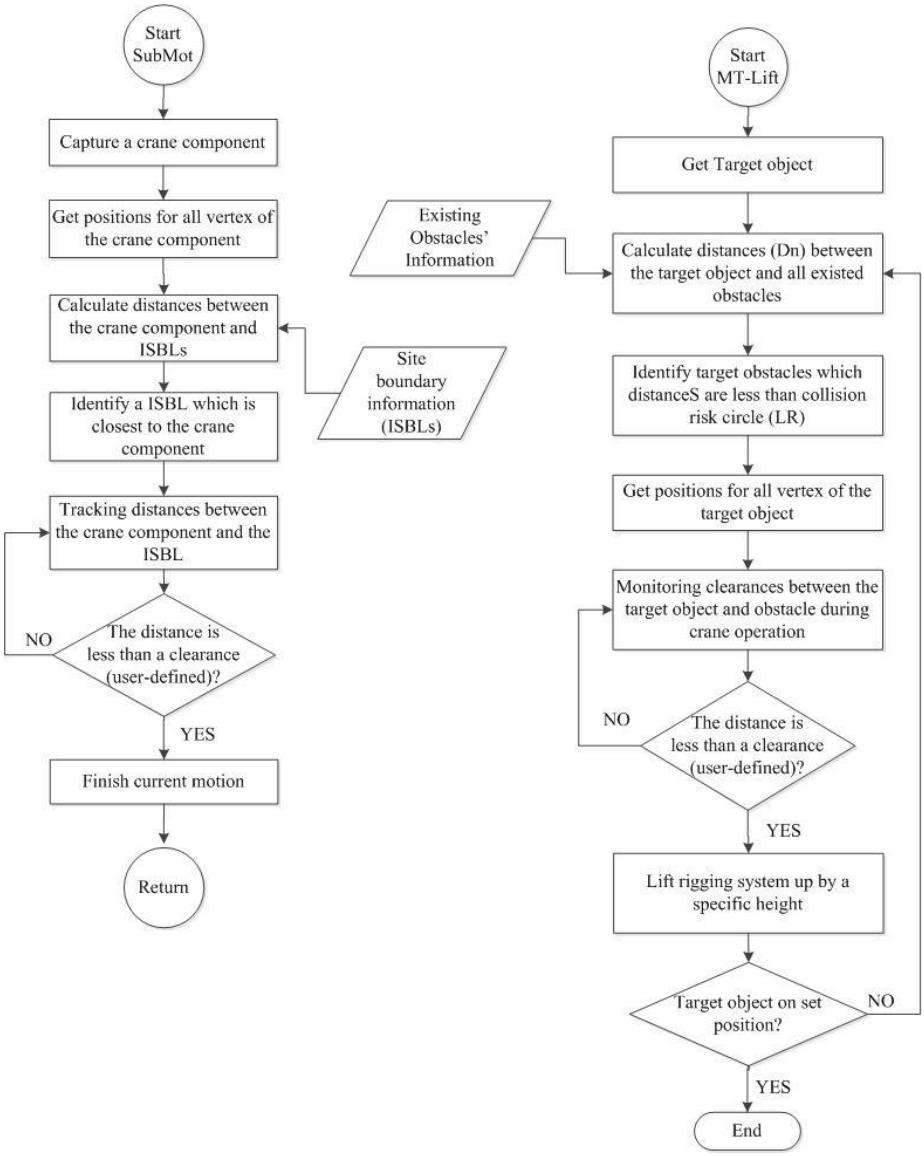

Figure 3.14: Flow of Spatial Analysis

Step 1. Identify target obstacles

To clearly illustrate the concepts underlying each function in the spatial analysis, the superlift for SubMot and a lifted object for MT-Lift are selected as target objects. The target objects are the principal objects to be considered in seeking to prevent conflicts. This is achieved by maintaining sufficient clearances from any obstacles during crane operation across animation time. Heavy industrial

construction projects generally involve congested areas with numerous existing obstacles. This feature can lead to inefficient and time consuming computation of the spatial analysis. To improve computational efficiency, clearances are only calculated between the target objects and the obstacles located in close proximity to the target objects. Obstacles that may interfere with the current target objects are defined as the structures located within a circle (referred to as the collision risk circle) centered on the geometric center of the target object (P_{TO}), and the radii of which are either user-defined (set by default to 15.25 m) or made object-specific according to the relationship $r = (1.5 \times \text{the target object (TO) length})$. As shown in Figure 3.15, the center of the collision risk circle (LR) is changed, as are the target obstacles (TSs) when the target object moves along the crane path, also known as the superstructure rotation. Given an LR, the set, $\Im$, containing all target obstacles, including ISBLs that may collide with the target object, is determined according to Equation (5).

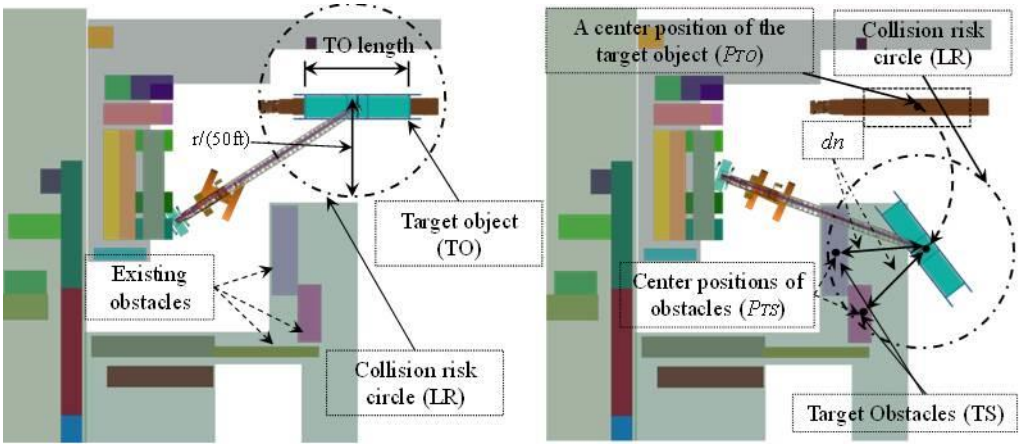

(a) Superstructure rotation at time 0 and time 120

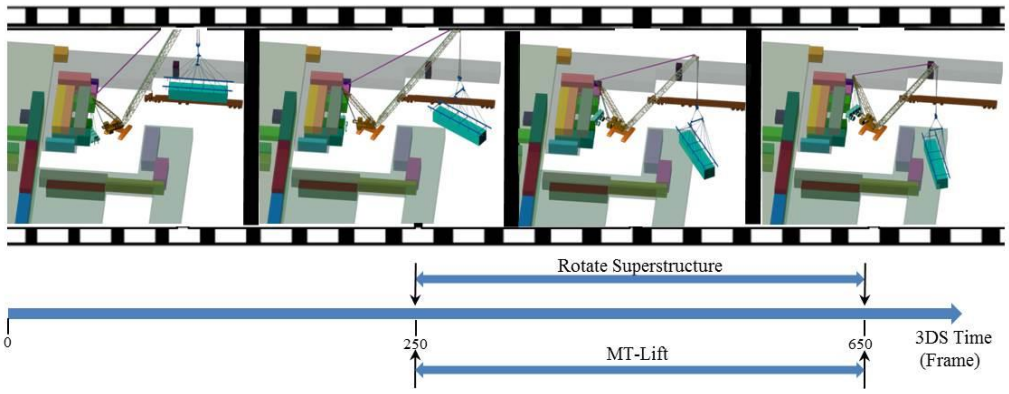

(b) Perspective view with 3ds Max timeline

Figure 3.15: Identification of the target obstacles in MT-Lift

$$TS_m \in \Im \Leftrightarrow d_n = dist(P_n^{TO}, P_n^{Obstacle}) = \left\| \overrightarrow{P_n^{TO} P_n^{Obstacle}} \right\| < LR \qquad (5)$$

Where P_n^{TO} and $P_n^{Obstacle}$ are, respectively, the geometric centers of the target object at a given instant, t_n, of the animation time and the m^{th} target obstacle. Of course, by limiting the number of target obstacles to only those located within the LR, the computational efficiency of the spatial analysis algorithm is improved since the number of target object—target obstacle pairs requiring clearance calculations, which is the most numerically intensive step, is kept within reasonable bounds.

Step 2. Monitoring clearances

After determining the target obstacles, distances (clearances) between the target object and target obstacles are monitored quasi-continuously during crane operation across animation time in order to identify when and where collision errors may be encountered. Since the clearance algorithms developed in this contribution use a ray tracing method in 3ds Max (Autodesk 2011), this research adopts the terminology of this software and refers to the points selected on target

objects and target obstacles for clearance calculation as vertices. The accuracy of the clearance calculation is thus determined by the number of vertices on the target objects and target obstacles defined by users based on the geometry and volumes of the target objects and target obstacles. In the MT-Lift, this research defines 15 vertices on each segment consisting of surfaces on the target object and target obstacle, which are assumed to be rectangular prisms. As shown in Figure 3.16, the function for monitoring clearances, MT-Lift, consists of three steps: (1) read the (x, y, z) coordinates of the vertices on the target object represented as $\left\{V_p^{\mathrm{TO}}\right\}_{p=1,2,\cdots,P}$ and the positions of the vertices of all the target obstacles within the set, represented as $\left\{V_q^{\mathrm{TS}}\right\}_{q=1,2,\cdots,Q}$; (2) identify the nearest vertex of the target object (N^{TO}) and of the target obstacle (N^{TS}) satisfied in Equation (6); and (3) calculate an actual distance (D_{Actual}), satisfied by Equation (7), between the N^{TO} and surfaces of the target obstacle (SF_k) which contains the vertex, N^{TS}.

$$\left[N^{\mathrm{TO}}, N^{\mathrm{TS}}\right] = \min \begin{bmatrix} \left\|\overrightarrow{V_1^{\mathrm{TO}} V_1^{\mathrm{TS}}}\right\| & \cdots & \left\|\overrightarrow{V_1^{\mathrm{TO}} V_Q^{\mathrm{TS}}}\right\| \\ \vdots & \ddots & \vdots \\ \left\|\overrightarrow{V_P^{\mathrm{TO}} V_1^{\mathrm{TS}}}\right\| & \cdots & \left\|\overrightarrow{V_P^{\mathrm{TO}} V_Q^{\mathrm{TS}}}\right\| \end{bmatrix} \tag{6}$$

$$D_{Actual} = \min\left[\left\|\mathrm{proj}_{\vec{L}}\left(\overrightarrow{N^{\mathrm{TO}} S_{k,r}}\right)\right\|\right] = \min\left[\frac{\left|\overrightarrow{N^{\mathrm{TO}} S_{k,r}} \bullet \overrightarrow{L_k}\right|}{\left\|\overrightarrow{L_k}\right\|}\right], \quad r = 1, 2, \cdots \tag{7}$$

Where $\mathrm{proj}_{\vec{v}}\left(\vec{u}\right)$ represents the projection of vector $\vec{u}$ on $\vec{v}$. The point, $S_{k,r}$, is the r^{th} vertex on the surface, SF_k, and $\overrightarrow{L_k}$ is its normal vector. As shown in Figure

3.16, one of the vertices on the target object and obstacle is identified as the nearest vertex on the target object and the target obstacle described as N^{TO} and N^{TS}, respectively, while the superstructure is rotating to a set position of the lifted object. The surfaces containing the point, N^{TS}, are identified as SF_3, SF_4 and SF_6, and are used to calculate the minimum distance, D_{Actual}, between N^{TO} and the obstacle surfaces referred to collectively as SF_k. When the D_{Actual} is less than and/or the same as the clearance defined by users, potential collision errors are encountered. To avoid these collision errors, the crane lifts the load up until sufficient clearance is reached. According to the sequences of the MT-Lift in Figure 3.14, the D_{Actual} is continuously monitored until the lifted object is delivered to its set position.

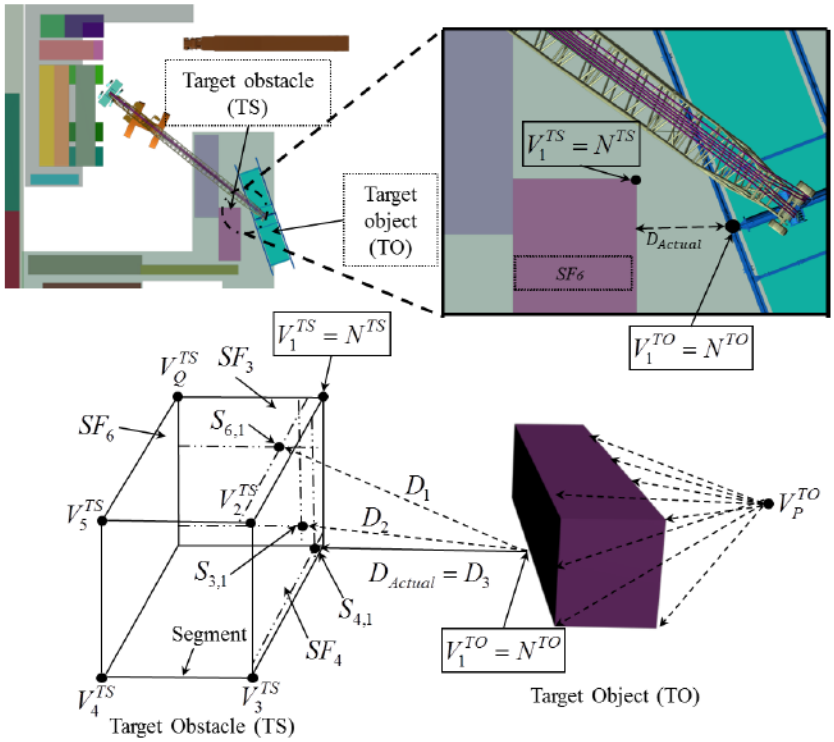

Figure 3.16: Illustration of the concept of monitoring clearances in MT-Lift

Step 3. Resolving collision errors

According to the functions of the spatial analysis, e.g., SubMot and MT-Lift, sufficient clearances to prevent collision errors are maintained by means of two reactions: (1) In SubMot, the current motion of the mobile crane operation is immediately terminated when the distance (D_{Actual}) between the target obstacles (ISBLs) and the target object, (e.g., crane-base, superstructure, superlift, etc.), is below the clearance defined by the user; and (2) in the MT-Lift, the current motion of mobile crane operation stops temporarily when the D_{Actual} between the target object (lifted objects) and the target obstacles (installed modules) is less than or equal to the pre-defined clearance, and the rigging system is lifted up to maintain a minimum height. As a reaction of the MT-Lift function, the minimum height is manually calculated under different boom and jib combinations. This research considers only the primary boom configurations shown in Figure 3.17, where the lifting height (H) must be greater than the minimum lifting height (H_{min}), satisfying Equation (8).

$$H > H_{min} = H_A + H_B + H_C \tag{8}$$

Where H_A, H_B, and H_C are the obstacle height, load height, and clearance defined by users, respectively.

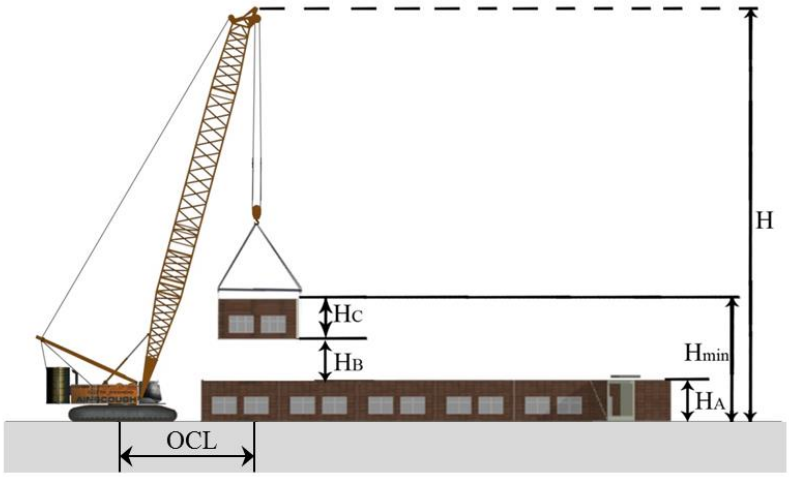

Figure 3.17: Crawler/mobile crane with main boom (Han et al., 2014)

Based on the principle of the lifting height calculation, the MT-Lift computes the minimum height, referred to as the required height (RH), satisfying Equation (9). After the crane lifts the target object up by the RH in order to maintain a sufficient clearance, the next motions are designed according to the scenario developed in the rotation analysis (see Figure 3.10). As the superlift moves as a result of the superstructure rotation and crane walking, the center of the collision risk circle changes, as do the target obstacles. Step 1 and 2 are thus simultaneously implemented in order to support recognition of when and where the target object must be lifted in order to ensure successful transportation to its set position. Step 3 is executed to avoid any conflicts when the D_{Actual} is the same as or slightly less than the clearance.

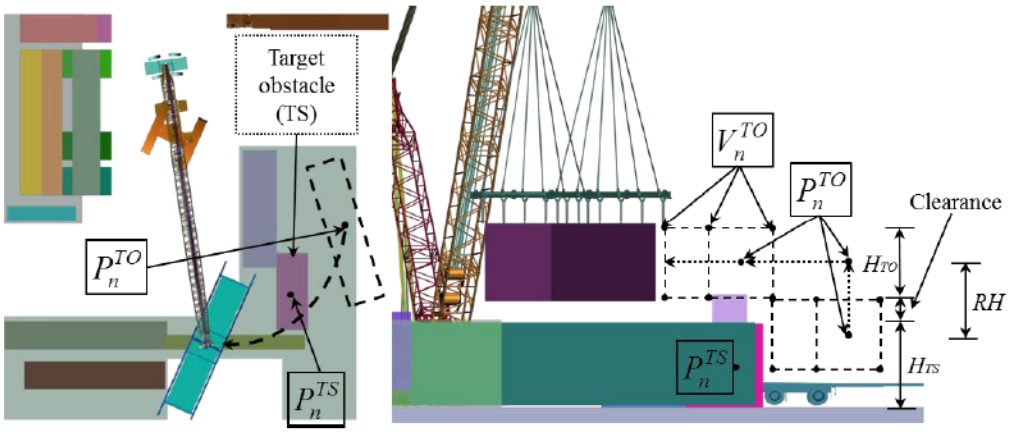

(a) Plan and elevation views

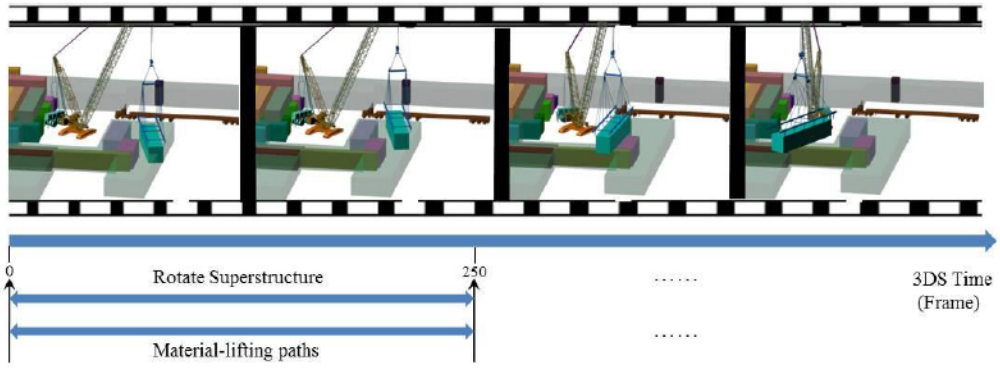

(b) Perspective view with 3ds Max timeline

Figure 3.18: Collision-free material-lifting path

$$RH = \left(P_n^{TS} + \frac{H_{TS}}{2} + \frac{H_{TO}}{2} + Clearance \right) - P_n^{TO} \tag{9}$$

Where P_n^{TO} and P_n^{TS} are geometric center positions of the target obstacle and the target object at a given instant, t_n, of the animation time, and H_{TO} and H_{TS} are the heights of the target object and the target obstacle, respectively. It should be noted that, as a solution to the case in which a collision error between the target object and the boom is identified due to violation of the *min-*H_{rope} (see Figure 3.12), there are two alternatives: (1) utilizing the same scenario, the crane

operation is redesigned with a direction change in crane rotation (i.e., superstructure rotation) in order to avoid the congested areas with many existing obstacles; and (2) a different scenario is used to re-plan the mobile crane operation.

SubMot is implemented following rules similar to those used for MT-Lift. The movement of the target object (superlift) is along the crane-base or superstructure due to the linkage of the crane configuration (see Figure 3.7). Depending on the respective volumes of the obstacles, the accuracy of the clearances, and the targeted computational speed, the number of vertices will vary from as low as one vertex on each object to a few hundred if the user needs to mimic a continuous representation of the target object and the surrounding obstacles. For this research, trial-and-error experimentation leads to the conclusion that 15 to 30 vertices on each segment (edge) of the obstacle (or ISBL) is a good compromise between accuracy and computational speed. As shown in Figure 3.19a, the center of the LR changes while the superstructure is rotating. It should be noted that the SubMot determines target obstacles by calculating distances (d_n) from P_n^{TO} to vertices of the ISBLs (V^{ISBL}). Given a collision risk circle, LR, the set, $\Im$, containing all target obstacles that may collide with the target object is determined according to Equation (10).

$$TS_m \in \Im \Leftrightarrow d_m = \min\left[dist\left(P^{\mathrm{TO}}, V_{m,i}^{\mathrm{Obstacle}}\right)\right] = \min\left(\left\|\overrightarrow{P^{\mathrm{TO}} V_{m,i}^{\mathrm{Obstacle}}}\right\|\right) < LR, \quad i = 1,2,\cdots \quad (10)$$

Where P^{TO} and $V_{m,i}^{Obstacle}$ are, respectively, the geometric centers of the target object and the i^{th} vertex of the m^{th} target obstacle. After identifying the target obstacles, clearances between the target object and target obstacles are tracked by calculating the D_{Actual} satisfied by Equation (7) and (8) in Figure 3.19b. When the D_{Actual} is slightly less than and/or the same as the user-defined clearance, collision errors may be encountered. Based on the procedures of the SubMot described in Figure 3.14, the superstructure rotation is terminated immediately in order to prevent potential conflicts. As a result of this effort, the rigging position may not be located on the module supply position for loading. At this point in the rotation analysis, the direction of superstructure rotation must be changed. Following this task, the motion of mobile crane operation is redesigned in order to transport the rigging system to the top of the module supply position. Figure 3.19c represents the successful superstructure rotation with direction change in which the rigging system is located above the module supply position of the lifted object. If the crane again fails to load the lifted object, the current crane location and/or the module supply position is deemed to be unacceptable. To accurately validate the feasible crane location, the current crane location with different module supply positions is used to build successful motions of mobile crane operation using rotation and spatial analyses. If this effort is not successful in developing collision-free motion of crane operation, the current crane location is invalidated. All sequences of the spatial and rotation analyses described above are implemented automatically to improve the efficiency of crane operation design for projects involving numerous lifts.

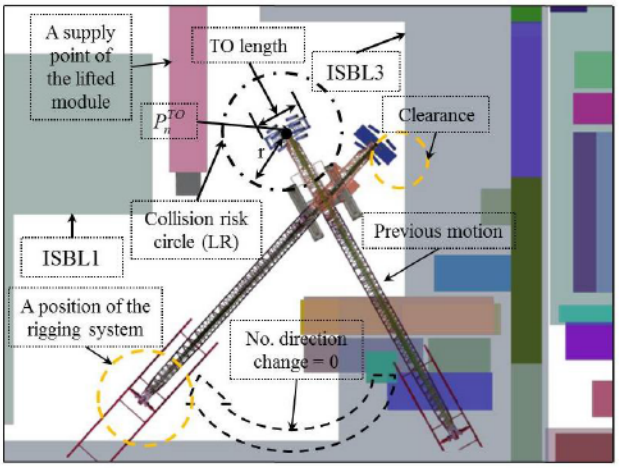

(a) Superstructure rotation without direction change

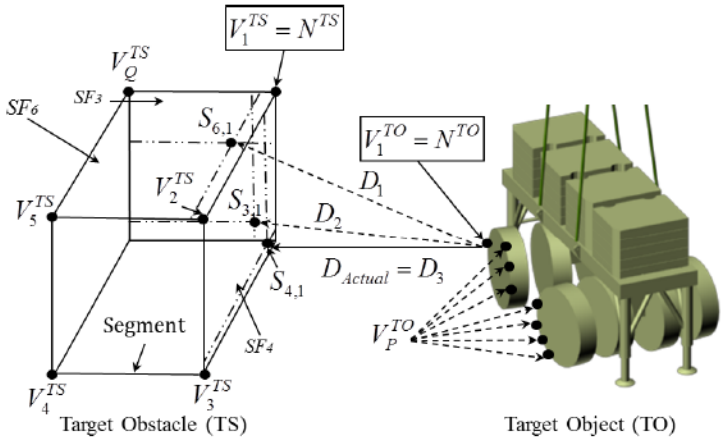

(b) Calculation of distances (clearances)

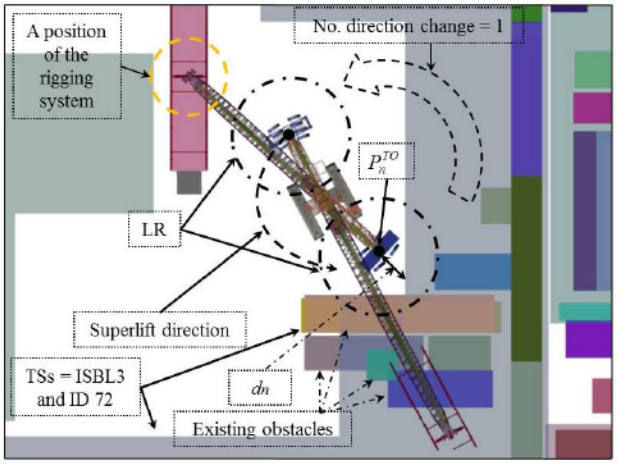

(c) Superstructure rotation with direction change

Figure 3.19: Illustration of the concept of SubMot

3.3.3 Ensuring 3D Visualization of Crane Operation

Although 3D visualization of crane operations is built based on motion planning, it is also dependent on the following factors: (1) whether or not the required crane capacities and working radii during 3D visualization of crane operation exceed the permissible crane capacity and working radius, which are designed based on the selected crane type and model; and (2) whether or not the 3D visualization of crane operation is reliable in terms of collision errors. As a result, 3D visualization of crane operations comprises collision and lift analyses. Collision analysis is used for collision detection either at a specific status of crane operation or during the entire crane operation. The lift analysis provides lift information such as lifting angles, lift heights, crane capacity, and crane working radius during 3D visualization.

Collision Analysis

3D visualization is defined as a process of computational methods to model and simulate construction scenarios on computers (Lai and Kang, 2009). 3D visualization has become an important management tool since it assists in identifying and solving many construction problems, such as spatial conflicts, schedule errors, and operation inefficiencies, prior to actual construction. Since these problems are identified by checking for collisions, this particular process is essential to ensuring reliable 3D visualization for crane lift planning (Han et al., 2014). This research designs 3D visualization of crane operations using rotation and spatial analyses. Lift engineers and project managers may request (as part of a quality assurance protocol) to ensure effective 3D visualization of crane

operations in consideration of the following factors: (1) potential computational errors in motion planning; and (2) a limitation of 3D visualization that may cause a visual illusion in various perspective views on a computer screen, especially for congested areas, as shown in Figure 3.20. Such a visual illusion may necessitate a closer investigation by the user to determine whether or not a collision in fact exists between the crane and a given obstacle. This may require the user to manipulate display by zooming-in and rotating the perspective view in order to identify a certain workspace in a closer view so that the 3D visualization of crane operation designed can be confirmed. This manipulation is repetitive and time-consuming when a large number of crane lifts are performed, and must be eliminated to satisfy the objectives of this research, (i.e., reduction of lift planning time and cost). To eliminate these unnecessary control measures and improve the viewing-angle ambiguities of 3D visualization, collision analysis is developed for the purpose of spatial conflict detection.

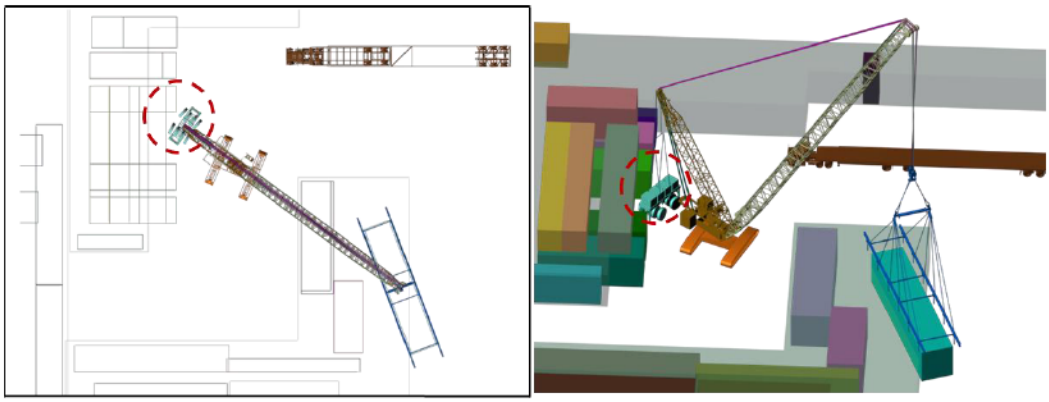

(a) Plan view (b) 3D perspective view

Figure 3.20: Visual illusion in 3D visualization

The collision analysis can be regarded as a clearance check, which is one of crane lift planning measures performed manually in the 2D environment. The

implementation of clearance checks consists of two steps: (1) calculate the minimum distance between the crane boom/jib and the building (C_1); and (2) calculate the distance between the crane boom/jib and the lifted load (C_2). Depending upon the given crane configuration, whether main boom or main boom with luffing jib, the process of calculating clearances varies. As shown in Figure 3.21, for lifts utilizing a main boom configuration, the minimum clearances can be calculated using Equation (11) and Equation (12).

$$C_1 = R_1 \times \sin\ \alpha \geq \text{default values defined by users} \quad (11)$$

$$C_2 = R_2 \times \sin\ \alpha \geq \text{default values defined by users} \quad (12)$$

$$\text{and } \alpha = \tan^{-1} \frac{(H - Z_1)}{R_L}$$

Where α is the boom angle, R_1 is the distance between Points B and C, R_2 is the distance between Points D and E, and Z_1 is the height of the boom rotation point.

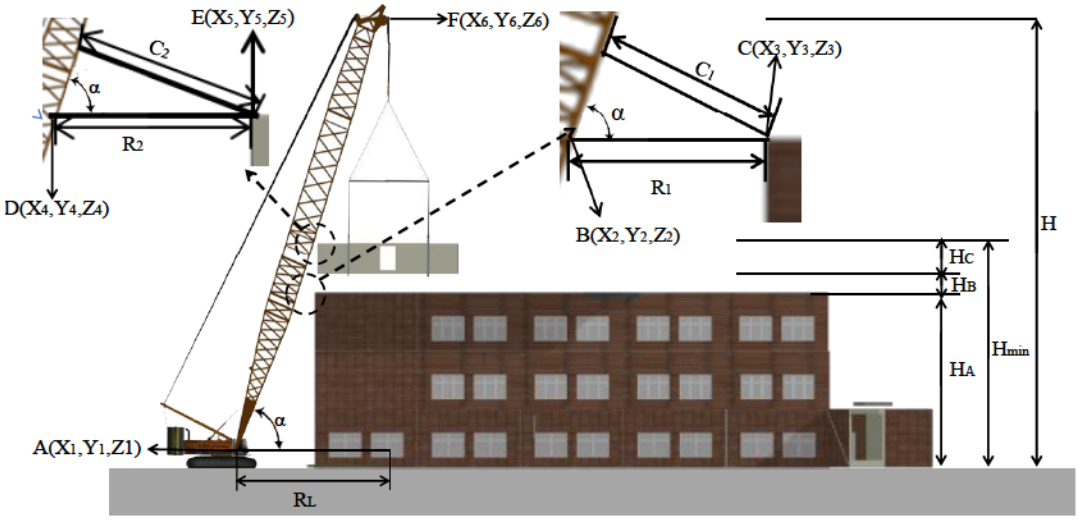

Figure 3.21: Calculation of minimum clearance for main boom (Han et al., 2014)

In terms of computing the clearance check, collision detection in previous research can be categorized as follows: (1) the approximation method, which identifies collision status; and (2) the workspace method, which provides collision status and distance between objects. Both have limitations: (1) as an approximation method, the outer boundary volume type is time-consuming in accurately mapping boundary volumes (boxes or spheres) to crane body configurations accurately; (2) the workspace method may not suitable for dynamic behaviours of crane operation. In order to overcome these challenges, the collision analysis in this research adopts full-scale 3D crane configurations as natural geometry 3D models in order to accurately identify undesirable intersections based on dynamic motions of crane operation across animation time.

As a computation technique, in consideration of the two collision detection methods, CAD-based programs generally use the ray tracing technique for visibility determination and collision detection between 3D objects. The objective of the ray tracing technique is to trace the beams of light from a particular object to other objects. As shown in Figure 3.22, based on the geometry of the 3D objects, the ray tracing technique is categorized into four types: (1) ray sphere intersect, which traces beams from a known point and direction to a center position and radius of a sphere; (2) ray plane intersect, which observes beams from a position and direction of the point to a plane; (3) ray intersection with a box, which traces beams from the point to a box described

by minimum and maximum points; and (4) ray intersection with segment, which monitors beams using two points (vertices) on a segment.

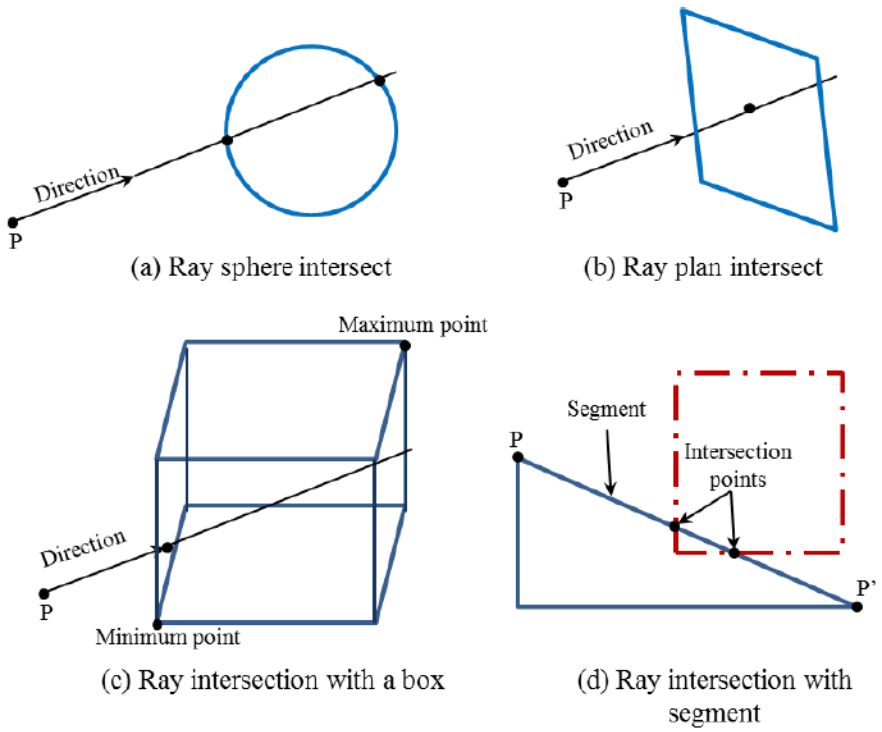

Figure 3.22: Types of ray tracing techniques

Since the collision analysis uses the geometry of crane configurations, which are composed of faces generated by segments, the ray intersection with segment is adopted for the collision analysis. The concept of the ray intersection with segment is illustrated in Figure 3.23. To provide a clear concept of the ray intersection with segment, the grid on the crane-base is generated and the parts of the grid representing intersection areas where segments of the ISBLs have been overlapped are indicated.

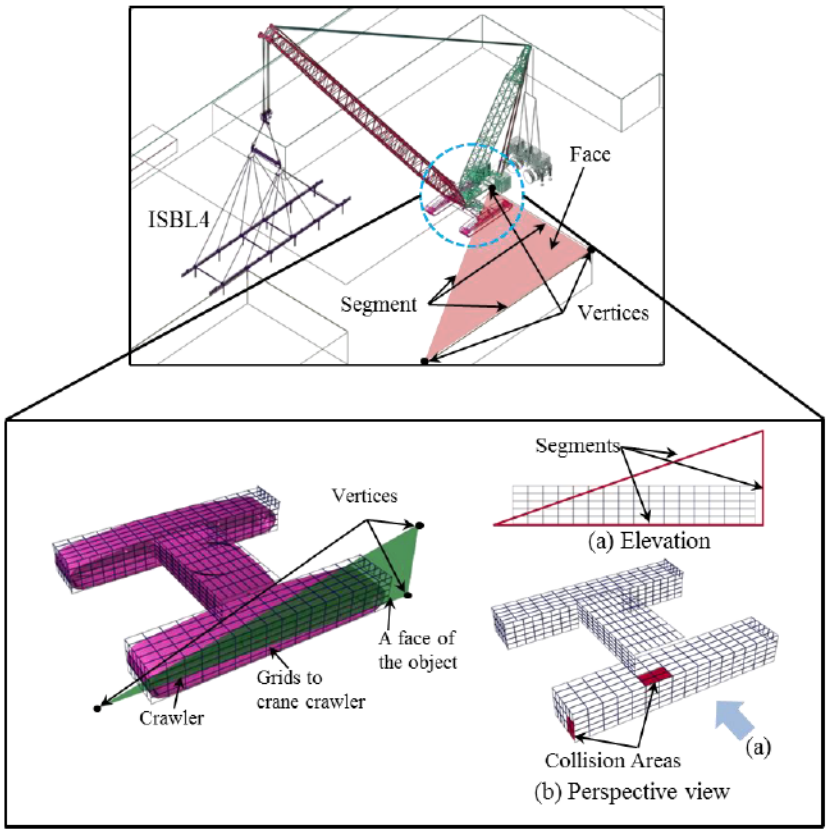

Figure 3.23: Concept of the ray intersection with segments

Rather than identifying all parts of the crane, specific components of the crane configuration are selected in order to accelerate the computation of the collision analysis based on the crane lift method, i.e., pick from fixed position or pick and carrying operation. When the pick from fixed position method is operating, the collision analysis detects interferences between the lifted object, superstructure, ISBLs, existing obstacles, and superlift (counterweight). Meanwhile, collisions are identified between the lifted object, superstructure, ISBLs, existing obstacles, crane-base (crawler), and superlift (counterweight) when the crane pick and carrying operation method is operating. Based on the ray intersection with segment technique and different parts of crane configuration, the process flow in the computation of collision analysis is described in Figure 3.24. To allow users

to check collisions automatically and efficiently for a large number of lifts, the collision analysis is established in VMCO.

```
objA: set of crane parts according to lift methods, crane pick from fixed position and crane
pick and carry operation methods
objB: existing obstacles at a particular animation time
objBfaces = [ ] ←list of faces on the objB which has collisions with the objA

Fn getFaceIntersection objA objB = ←Create a collision detection function
(
C = RayMeshIntersect() ← Create an instance of the ray tracing technique
C.initialize gridsize ← Generate a grid
C.addNode objA ←Add the grid on the objA
C.buildGrid() ←Attach faces of objA into the grid
intersectsegfn=C.intersectSegment ←Define ray intersection with segment method
numfaces=objB.numfaces ← collect a number of faces on the objB

 For i = 1 to numfaces do ← Loop to identify collisions between segments on the objB
and the faces on the objA.
(
  verts = get face objB i ← Return three vertices consisted of the face index i of objB
 n = get vertex objB verts.x ← Get a x position of each vertex on face index i
 m = get vertex objB verts.y ← Get a y position of each vertex on face index i
 L = get vertex objB verts.z ← Get a z position of each vertex on face index i
 If intersectsegfn n m false > 0 then objBfaces[i] = true ←
 If intersectsegfn m L false > 0 then objBfaces[i] = true ←
 If intersectsegfn L n false > 0 then objBfaces[i] = true ←

 If objBfaces[i] = false then:
 Append { } to objBfaces
 )
)
```

Find collisions between the grid on the objA and three segments on each face of the objB. If collision is identified, the face index is false.

Figure 3.24: Computation of the collision analysis in MAXScript

To provide a user-friendly collision detection system, the collision analysis offers two options: (1) specific collision detection, which identifies collision errors between parts of the crane configuration and existing obstacles at a specific moment in the 3D visualization; and (2) continuous collision detection, whether or not the selected crane configuration violates the inaccessible areas, such as existing obstacles and the ISBLs, across animation time. When conflicts are detected, the collision analysis provides a collision information table (see

Table 3.3). This table describes which crane parts, existing obstacles, and/or ISBLs clash at particular animation times. Based on these options, the collision analysis provides an automatic and reliable 3D visualization of crane operation that decreases the amount of time-consuming and costly manual work. It also provides clash places and animation times in order to assist users in identifying design errors, such as crane locations, module supply positions, lifting schedule, and motion of crane operation.

Table 3.3: Collision Information

Module ID	Tracking ID	Object conflicted	Crane configuration	Animation time
85	10163	ISBL3	Superlift	422f
85	10163	ISBL3	Crawler_CC2800 (Carrier)	431f

Lift Analysis

Based on the description of crane lift planning in Chapter 1, lift planning has four main steps: (1) crane location selection; (2) crane type and model selection; (3) motion planning of mobile crane operation; and (4) crane support design. According to these sequences, the motion planning in this research must satisfy the following requirements for crane location selection and crane type and model selection in order to design reliable and safe 3D visualization of crane operations: (1) confirm collision-free rotation on feasible crane locations for loading and unloading of lifted objects; (2) calculation of required crane lifting capacity; (3) measurement of required working radius; (4) assessment of lifting height; and (5) clearance check. This research thus implements lift analysis to check all requirements during 3D visualization of crane operations. At this juncture it

should be noted that the clearance check and lifting height assessment, having already been addressed in the spatial and collision analyses, are not considered in the lift analysis. Therefore, the lift analysis carries out only the calculation of the required crane capacity and the working radius checks. The purpose of calculating the required lifting capacity is to identify whether or not the lifting capacity setting identified from the lifting capacity chart meets the given constraints, such as lifting weight, reach height, and working radius. The lifting capacity chart is typically provided by the manufacturer, where the crane capacity associated with any given configuration should be greater than or equal to the total lift weight, which is the required lifting capacity. The crane's lifting capacity thus must satisfy Equation (13).

$$GC \geq W_{Total} = W_{Lifted} + W_{Hook} + W_{Sling} + W_{Spreadbar} + W_{Hoist} \quad (13)$$

Where GC = gross capacity, also called the lifting capacity setting; W_{Total} = total weight; W_{Lifted} = lift or object weight; W_{Hook} = hook weight; W_{Sling} = sling weight; $W_{Spreadbar}$ = spreader bar weight; and W_{Hoist} = weight of hoist wire. Figure 3.25 illustrates a typical rigging system. It should be noted that the weights of the spreader bar and the number of slings are not constant since they are adjusted based on the number of pick points on modules.

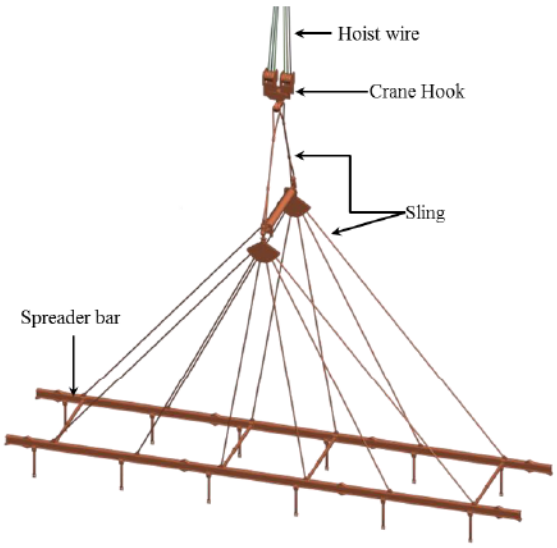

Figure 3.25: Rigging system

The crane working radius must be greater than or equal to the distance from the feasible crane locations to set positions of the objects (see Figure 3.17), satisfying Equation (14).

$$R_L \geq OCL \tag{14}$$

Where R_L = crane working radius and OCL = lifting radius distance from a center position of a crane to the center position of the lifted object. Based on the working radius of each motion and the given boom length, the crane capacity setting is identified from the lifting capacity chart provided by the manufacturer. The crane capacity assessment is then implemented using the safety factor calculated by means of Equation (15). To design safe crane operation, the safety factor must be $\leq 85\%$ or $\leq 90\%$, depending on the given company's regulations. When the safety factor is greater than 90% but equal to or less than 95%, the crane is operated under the supervision of lift engineers on site. If the safety factor exceeds 95%, the designed crane operation is not acceptable.

$$Safety\ factor(\%) = \frac{W_{Total}}{GC} \times 100 \quad (15)$$

The 2D-based lift analysis in practice is generally performed based only on distances from the feasible crane locations to module supply and set positions. This checking method may not be sufficient to determine with certainty whether or not the required lifting capacity is exceeded during the crane operation. In order to address this challenge, the lift analysis is implemented whenever crane motions in 3D visualization are changed in order to validate crane selection, feasible crane locations associated with module supply positions, and motions of crane operations. As shown in Table 3.4, the lift analysis takes into account lifted object ID, tracking No., total weight, working radius, crane capacity setting, safety factor, start and finish animation times, lift angles, and lift heights. This information can assist project participants in identifying where and when design errors in the lift planning exist. For example, the table indicates that the safety factors for animation times 150 to 540 exceed 100%. It can thus be determined that the required crane lifting capacity exceeds the crane lifting capacity settings while the crane is operating with the load. The reason for this failure is that the lifting radii are greater than the maximum working radius (110 ft) defined by the crane selection. That is, the crane operation designed by the motion planning procedure is not acceptable. To solve this design error, lift engineers and project managers have three alternatives: (1) to select a higher-capacity crane type and configurations; (2) to find other feasible crane locations; and (3) to change module supply positions. At this point it should be noted that

module supply positions on the pick areas are defined by users, since the crane path checking planning system (Lei et al., 2013) does not analyze optimal module supply positions for lifts. These uncertain module supply positions can influence the 3D visualization of crane operation whether or not it exceeds the acceptable crane lifting capacity and working radius. In this respect, this research considers the procedure of first changing the module supply positions, then the feasible crane locations if the required lifting capacity still does not meet the crane lifting capacity setting. Since the crane type and its configurations may be fixed by lift engineers, this option is not considered in this research. Based on these alternatives, the motion of crane operation is re-designed and the lift analysis is automatically implemented once more. Once all safety factors are within the acceptable range, the 3D-visualized crane operation associated with the feasible crane locations is deemed to be reliable and safe. Accordingly, the lift analysis assists not only to ensure the reliability of the 3D visualization of crane operation, but also to detect and solve design errors (e.g., required crane capacity and working radius) by changing module supply positions and feasible crane locations.

Table 3.4: Lift information

ObjID	TrackingNo	Weight	Radius	Capacity	Safety factor	S_AniTIme	F_AniTIme	LiftAngle	LiftHeight	Speed(°,ft/min)	MotionID
101	11858	54762	144.1075	286600	19.10747	0	5	-71.99176	0	131.9396655	1
101	11858	54762	144.1075	286600	19.10747	5	70	81.1828537	0	131.9396655	2
101	11858	54762	144.1075	286600	19.10747	70	100	6.89539483	0	131.9396655	3
101	11858	54762	144.1075	286600	19.10747	100	120	98.8213425	0	131.9396655	4
101	11858	54762	144.0997	286600	19.10747	120	150	0	53.67519	206.2866199	5
101	11858	314952	144.0997	286600	109.8925	150	180	0	7	63.20936399	6
101	11858	314952	141.6589	286600	109.8925	180	350	-143.86046	0	40.42832418	7
101	11858	314952	141.6589	286600	109.8925	180	295	-108.42973	0	40.42832418	7
101	11858	314952	141.6589	286600	109.8925	295	308	0	0	40.42832418	7
101	11858	314952	141.6589	286600	109.8925	308	350	0	0	40.42832418	7
101	11858	314952	141.6589	286600	109.8925	350	350	0	0	40.42832418	7
101	11858	314952	141.6589	286600	109.8925	350	350	0	0	40.42832418	7
101	11858	314952	141.6589	286600	109.8925	350	350	0	0	40.42832418	7
101	11858	314952	141.5164	286600	109.8925	350	480	78.2823805	0	40.42832418	8
101	11858	314952	141.6589	286600	109.8925	350	396	22.4676228	0	40.42832418	8
101	11858	314952	141.6589	286600	109.8925	180	396	0	0	63.20936399	15
101	11858	314952	141.6589	286600	109.8925	396	408	0	0	40.42832418	8
101	11858	314952	141.6589	286600	109.8925	396	408	0	9.78955078	63.20936399	15
101	11858	314952	141.6658	286600	109.8925	408	409	0.03221176	0	40.42832418	8
101	11858	314952	141.6658	286600	109.8925	408	409	0	0	63.20936399	15
101	11858	314952	141.6658	286600	109.8925	409	421	0	0	40.42832418	8
101	11858	314952	141.6658	286600	109.8925	409	421	0	12.4042969	63.20936399	15
101	11858	314952	141.5164	286600	109.8925	421	480	55.7885513	0	40.42832418	8
101	11858	314952	141.302	286600	109.8925	480	540	-25.294449	0	40.42832418	9
101	11858	314952	141.5164	286600	109.8925	480	502	-7.708252	0	40.42832418	9
101	11858	314952	141.5164	286600	109.8925	421	502	0	0	63.20936399	15
101	11858	314952	141.5164	286600	109.8925	502	514	0	0	40.42832418	9
101	11858	314952	141.5164	286600	109.8925	502	514	0	10.979126	63.20936399	15
101	11858	314952	141.302	286600	109.8925	514	540	-17.586197	0	40.42832418	9
101	11858	314952	141.302	286600	109.8925	514	540	0	0.00012207	63.20936399	15
101	11858	314952	82.41676	546700	57.60966	540	570	13.2989379	0	93.12945924	10
101	11858	314952	82.43532	546700	57.60966	570	590	-46.276764	0	93.12945924	11
101	11858	314952	82.43532	546700	57.60966	590	620	0	52.5922852	145.6071704	12
101	11858	54762	82.43532	546700	10.01683	620	650	0	-52.592285	220.6134655	13

Violation of crane capacity setting

3.3.4 Post-Visualization Simulation

The successful completion of modular-based industrial construction projects relies heavily on the operation of construction equipment. Among this construction equipment, mobile cranes are the principal equipment utilized in order to transport modules to their set positions. To design reliable and safe crane operation, the crane path checking and planning component of a crane management system (Figure 3.4) may identify more than one single crane location for each lift, such that the best crane location among the presented

options is chosen based on the lift engineer's experience. This experience-based decision making can lead to low efficiency crane operations and, consequently, reduced project productivity. In this respect, crane productivity analysis stands as a powerful tool to improve project productivity by selecting the most appropriate crane operation among a variety of crane operations for a given lift. However, crane productivity analysis has not received much attention by previous researchers and practitioners, due to insufficient information such as process times of crane motions as well as a lack of implementation tools. This research proposes post-visualization simulation framework which integrates 3D visualization with simulation in order to implement crane productivity analysis. Figure 3.26 the process flow of the proposed system. The aims of the post-visualization simulation are as follows: (1) to determine the value of the cycle time of crane operation in simulation based on 3D visualization of crane operation; and (2) to assist project participants in selecting the most appropriate crane operation and associated module supply positions. This framework can improve project productivity and decision making by supporting the selection of the best scenario for each lift. Crane productivity is influenced by various constraints, including crane locations, site layout, module supply positions, and proficiency of crane operators, but the proposed productivity analysis considers only site layout, module supply positions, and feasible crane locations, since these are the factors which most strongly affect the design of crane operations. The input data consists of: (1) crane lifting capacity, which assists with determining the slewing and hoist speeds for each crane motion; (2) motion

sequences, which are used to build a simulation model; (3) module weights, which are factored in in calculating the total weight of the rigging-object system; and (4) lift angles and lifting heights, which are used to calculate the process times of crane motions. Based on inputs and outputs of previous modules in this research, the procedures of the post-visualization simulation are: (1) to define ranges of slewing and hoist speeds based on user-defined percentages; (2) to calculate the process time of each motion based on safety factor and the range of crane speeds; and (3) to define additional times when crane motions are changed vertically and horizontally, in order to determine cycle time of crane operation, with the exception of assembly time based on time penalty.

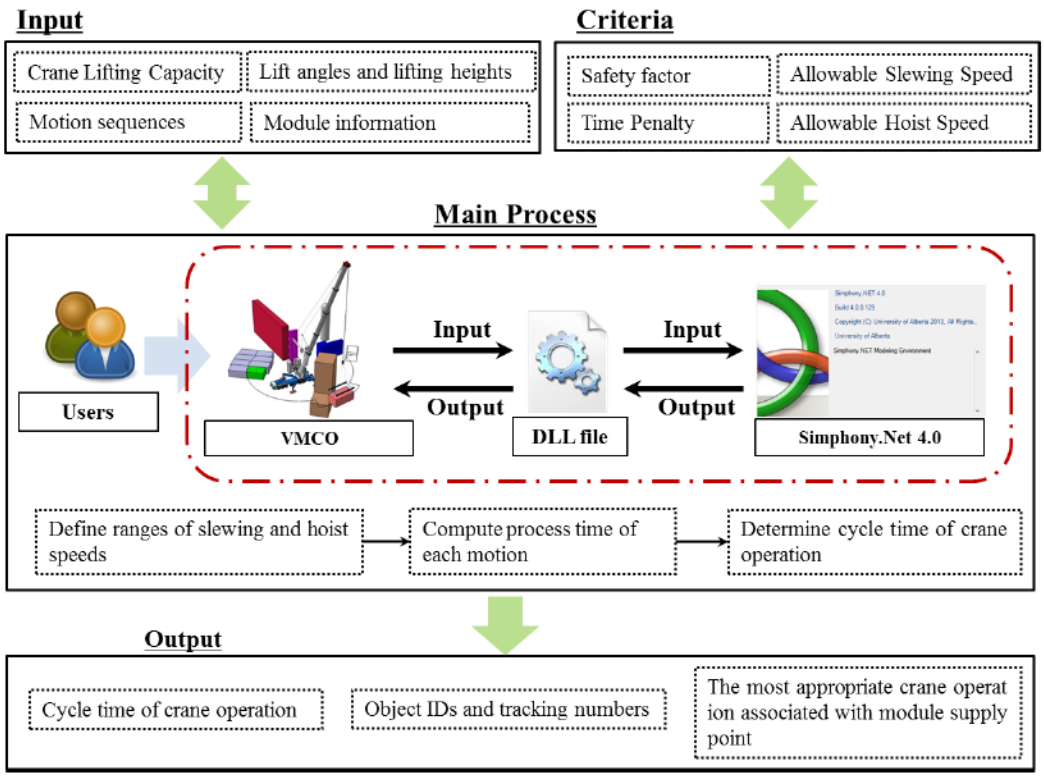

Figure 3.26: Post-visualization simulation module

The post-visualization simulation, also called crane productivity analysis, is developed by integrating 3ds Max as a visualization tool with Simphony.NET (Hajjar and AbouRizk 1999) as a simulation tool. The key to successful development of this integrated system is to establish an automated and efficient information exchange between the simulation and 3ds Max. However, systems developed in previous studies (Al-Hussein et al., 2006; Han et al., 2012) lack interoperability, leading to inefficient automation when the initial design and schedule changes. This limitation is usually circumvented using ad hoc solutions which use appropriately formatted ASCII files to exchange input and output between the different applications, including 3ds Max. However, this approach is error prone because it requires a considerable amount of manual work. In order to address this challenge and increase the integration of the system, the crane productivity analysis uses a Dynamic Link Library (DLL) file type, which provides a library of executable functions and/or data that can be adopted using windows applications. VMCO contains the DLL file developed in Visual Studio.Net. This file type allows users to develop an efficient and automated integrated system by eliminating time-consuming manual tasks involved in opening a simulation model, to insert any input data from 3ds Max to simulation, to execute functionalities of Simphony.NET in 3ds Max, and to return a simulation result—the cycle time of crane operation—to 3ds Max. To facilitate computation of the productivity analysis, each motion of crane operation is defined according to the motion IDs represented in Table 3.5.

Table 3.5: Motion IDs of crane operation

Motion ID	Description	Type of crane operation	
		PCO	PFP
1	Crane-Base rotation	Start point	Single location
2	Superstructure rotation		
3	Boom up or down without load		
4	Rigging rotation		
5	Hoist down for load		
6	Hoist up with load		
7	Superstructure rotation with load		
8	Crane walking with load	Finish point	
9	Superstructure rotation with load		
10	Boom up or down with load		
11	Rigging rotation with load		
12	Hoist down with load		
13	Hoist up without load		
15	Hoist up	To prevent collisions	

PCO: Pick and carrying operation, PFP: Pick from fixed position

Although the simulation is mainly executed with probabilistic data in order to predict the expected productivity of the proposed construction operation, this data type is not available for crane operation due to insufficient time data. As an alternative, the crane productivity analysis in this research uses hoist and slewing speeds (S) provided by manufacturers to calculate the process time of each motion of crane operation. Since these maximum speeds are not adopted in practice, the acceptable minimum ($P_{\min}$) and maximum percentages ($P_{\max}$) of slewing and hoist speeds are either defined by users or determined based on company regulations. Moreover, the allowable maximum ($V_{\max}$) and minimum speeds ($V_{\min}$) of slewing and hoisting are calculated using Equation (16) and Equation (17), respectively. As shown in Figure 3.27, the $V_{\min}$ and $V_{\max}$ are

represented as interval ranges of the speeds between a minimum safety factor ($F_{\min}$) and maximum safety factor ($F_{\max}$), which are 0% and 100%, respectively. Based on these speeds and safety factors, the gradient and its values satisfied by Equation (18) provide a diversity of hoist and slewing speeds based on safety factors at each motion of crane operation.

The safety factors are percentages of the crane capacity setting occupied by the required crane capacity during each motion of crane operation. This entails that the speed of crane operation is slow when the safety factor is high for a given motion, which may suggest a high total weight and/or long working radius. For example, slewing speed is 0.7 rpm and acceptable minimum and maximum percentages of slewing speed are 40% and 60%, respectively. The safety factor is 70% when the superstructure is rotated by 40° at a particular animation time. Based on the minimum and maximum slewing speeds, the associated speed is 80° per minute. The process time of this motion is thus 30 seconds.

$$V_{\max}(^\circ/\min) = (P_{\max} \times 0.01) \times S \times 360^\circ \text{ and } V_{\max}(ft/\min) = (P_{\max} \times 0.01) \times S \quad (16)$$

$$V_{\min}(^\circ/\min) = (P_{\min} \times 0.01) \times S \times 360^\circ \text{ and } V_{\min}(ft/\min) = (P_{\min} \times 0.01) \times S \quad (17)$$

$$y = \frac{V_{\min} - V_{\max}}{F_{\min} - F_{\max}} x + V_{\max}(^\circ/\min, ft/\min) \qquad (\frac{V_{\min} - V_{\max}}{F_{\min} - F_{\max}} < 0) \quad (18)$$

Where y is the speed associated with a safety factor, x, for the current motion of crane operation; x is a safety factor in a specific motion; S is rotation speed in (rpm) or hoist speed (ft/min) provided by manufacturers; $P_{\min}$ is the minimum

percentage of hoist and slewing speeds; and P_{max} is the maximum percentage of hoist and slewing speeds.

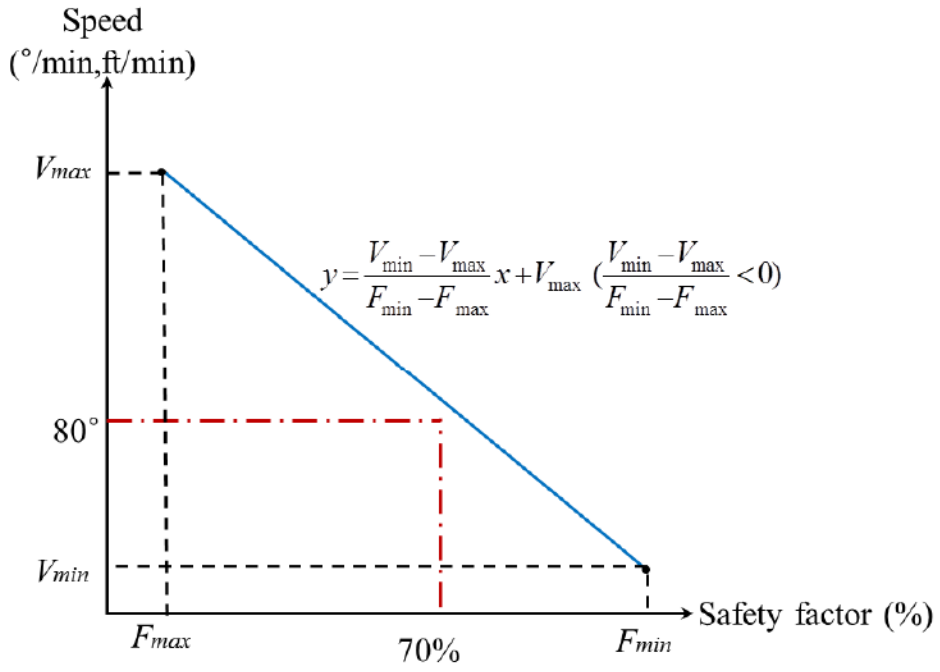

Figure 3.27: Interval ranges of speeds

Although the speed interval assists during the calculation of the process times of motions, these process times still are not realistic since other aspects of crane operation, such as preparation times when crane movements are changed, are not considered. To estimate the realistic process times, the productivity analysis modifies and adds the time penalty matrix developed by Olearczyk (2010). Table 3.6 describes the time penalties for crane movement changes. As a result, the process times for each motion of crane operation are calculated using Equation (19).

Table 3.6: Time penalty of crane movement changes

	Boom up or down	Rotate (Arc)	Hoist-up	Hoist-down
Boom up or down	0	0.75	1	0.5
Rotate (Arc)	0.75	0	0.5	0.75
Hoist-up	0.75	1	0	0
Hoist-down	0.5	0.75	0	0
Walking		2		

unit = minute

$$T_{motion} = \frac{L_{angle}, L_{height}}{y} + T_{Penalty} \tag{19}$$

Where L_{angle} is a lifting angle for a motion; L_{height} is a lifting height for a motion; and $T_{Penalty}$ is a time penalty for a crane movement change from a precedent motion to a subsequent motion. After calculating process times of crane operation motions in 3ds Max, VMCO using the DLL files delivers all information, such as object IDs, tracking IDs, and process times with the associated motion IDs to Simphony.NET, and requests Simphony.NET to run the simulation model illustrated in Figure 3.28. The simulation model is built based on sequences of crane operation in scenarios (Figure 3.10). Finally, VMCO represents the cycle times of crane operations described in Table 3.7 in 3ds Max after simulation. It should be noted that the simulation model in this research is used as a deterministic model to evaluate the cycle time of crane operations based on lifting angles, lifting heights, and interval ranges of speeds. It is also possible to use this as a probabilistic simulation model when probabilistic data for process times of crane operation is available. The productivity analysis can improve decision making in order to assist lift

engineers and project managers to select the best crane operation by comparing the cycle times of various alternatives for each lift. The analysis can also be actively used to design more accurate lift and project schedules.

Table 3.7: Cycle time of each lift

Motion ID	Tracking No	Cycle Time (min)
1	10	21.9551
2	56	24.2163
101	11858	20.3451
102	11877	18.1466
103	12068	11.8079
103	12049	11.8253
111	12972	11.2938
111	12981	11.3038
111	12987	12.6084

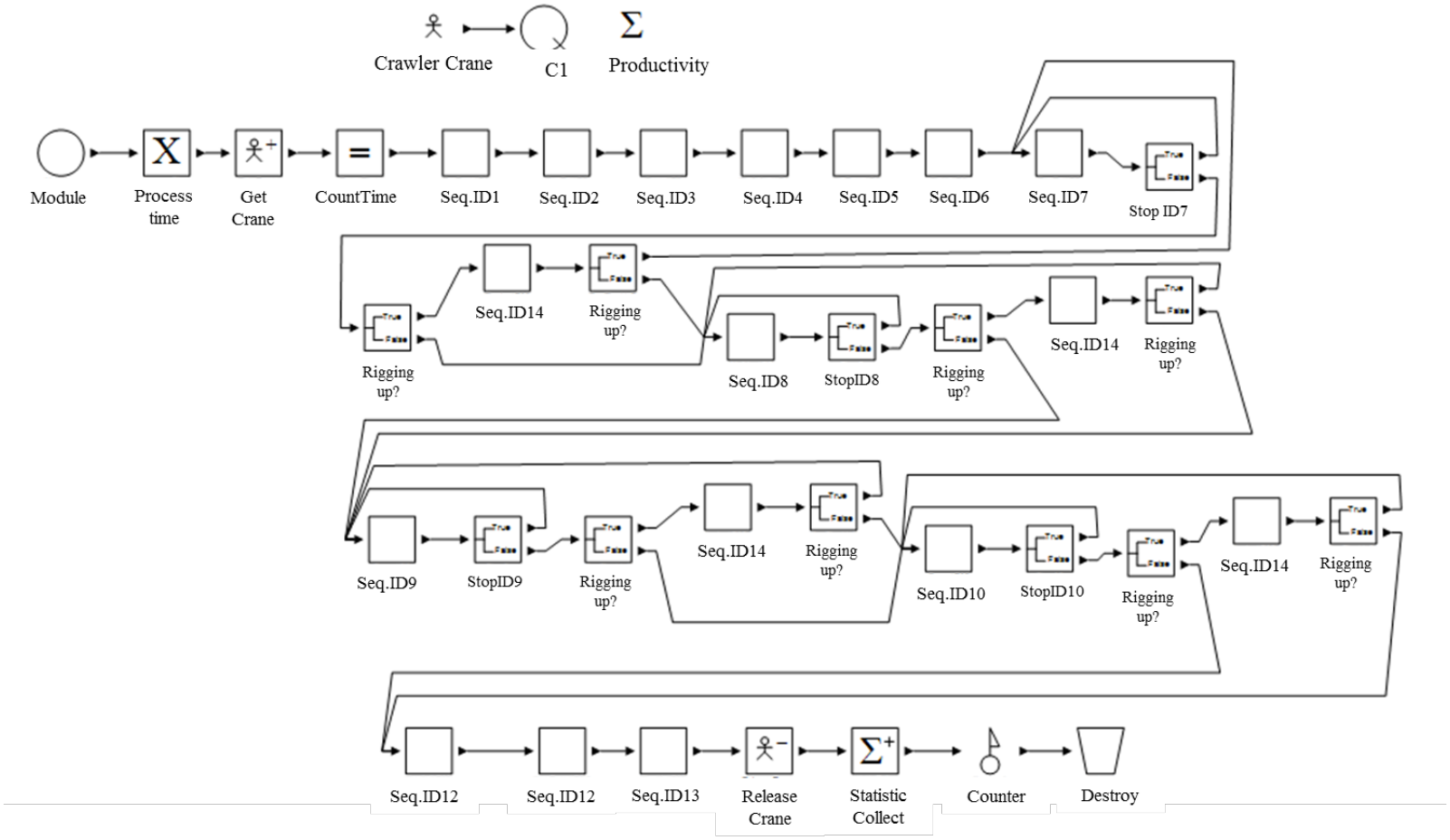

Figure 3.28: A simulation model in Simphony.NET 4.0

3.3.5 BIM-based Crane Information

A high level of collaboration and communication among stakeholders contributes to faster and better management and decision making, which are requisite in completing high quality construction projects successfully and efficiently. To enhance this collaboration and communication, many researchers use building information modelling (BIM), which enhances information sharing among project stakeholders and thus can reduce costs and improve safety, productivity, scheduling, and resource management for projects. Although the definition of BIM varies based on the purpose of its implementation in the given project, previous publications (ISO-29484-1 2010; Nawari, 2012) describe BIM as a shared digital representation of physical and functional information required in the design, construction, and operation of construction facilities. According to this definition, BIM consists mainly of the following information: (1) laws and regulations, (2) material information and specifications, (3) procurement information, (4) facility information, (5) construction information, (6) simulation results, (7) 2D/3D drawings, and (8) visualization/animation models. However, in current practice 3D visualization is the only component of BIM used in lift planning to identify collision errors, even though cranes are the most readily utilized and shared equipment in construction projects. To fully utilize the functionalities of BIM in the crane lift planning, which are efficient information exchange between applications, an automated system and better communication and collaboration among project participants, this research proposes to add digital crane information under construction information in BIM (see Figure

3.29). Crane information includes lift, collision, and productivity information of each lift required in the lift planning process.

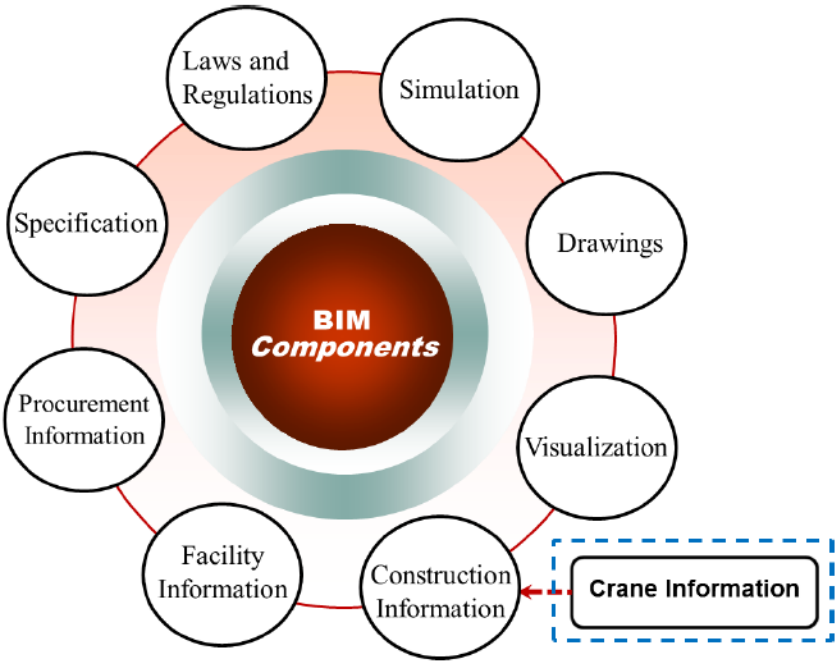

Figure 3.29: Proposed Building Information Modelling

This research proposes a methodology which has the following features: (1) two-way information exchange among simulation, visualization, and customized programs used in lift planning; (2) automated motion planning of mobile crane operation for projects with a large number of lifts; (3) description of 3D visualization of crane operation; (4) representation of lift information, such as how much rotation is required for the crane configuration, and when, where, and to what height the rigging system or hook should be lifted up and down; (5) representation of collision information, such as which, when, and where crane configurations collide; and (6) representation of productivity information. Figure 3.30 illustrates digital crane information with 3D visualization. These features

allow project participants to facilitate motion planning when any information is changed by upstream lift plan users.

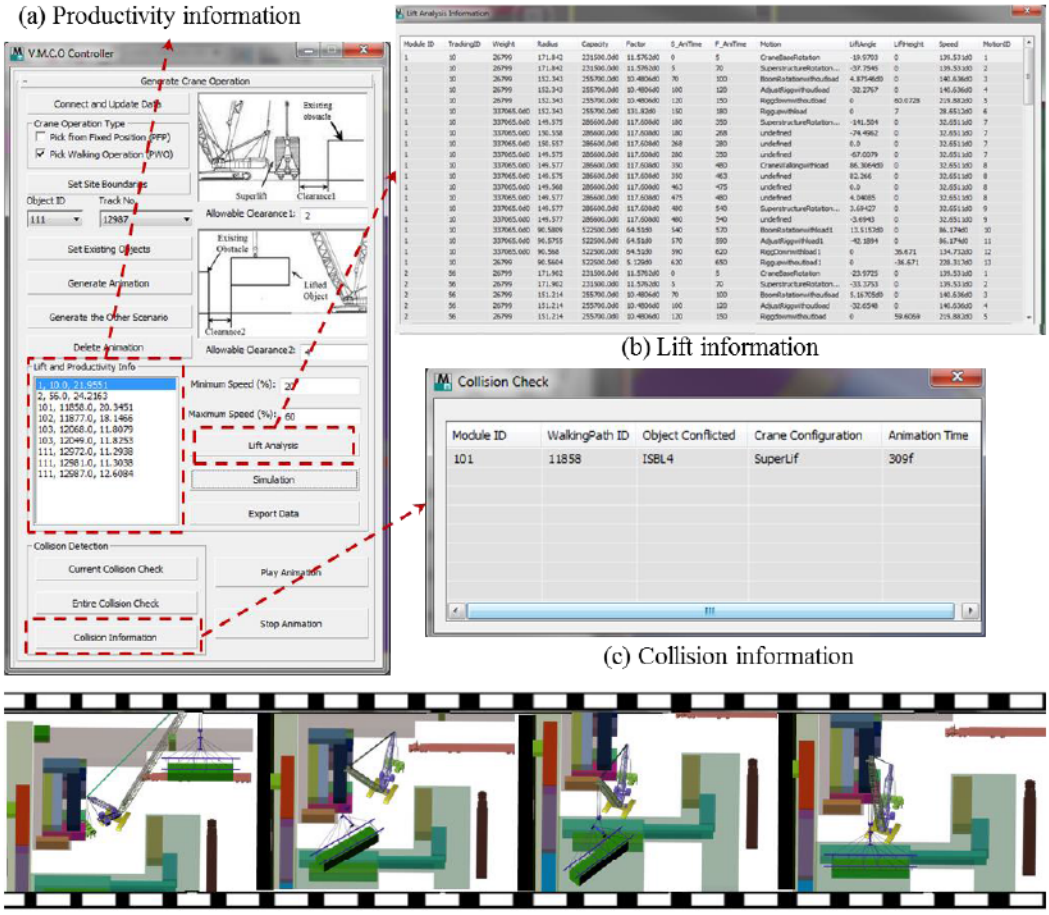

Figure 3.30: BIM-based crane information

For example, as shown in Figure 3.31, two crane operations are designed for a given module based on two alternative module supply positions defined by the user for the same module and set position. From a safety perspective, lift and collision analyses are implemented to ensure 3D visualization of crane operation. Meanwhile, from an efficiency perspective, the post-visualization simulation is executed to determine the cycle time of each lift. To achieve a high level of communication and collaboration among stakeholders, 3D visualization of crane operation with associated crane information is represented on a single computer

screen. As a result, the BIM-based crane information reduces potential errors, time, and cost in order to design motions of crane operations for a large number of lifts when any category of information is subject to frequent changes.

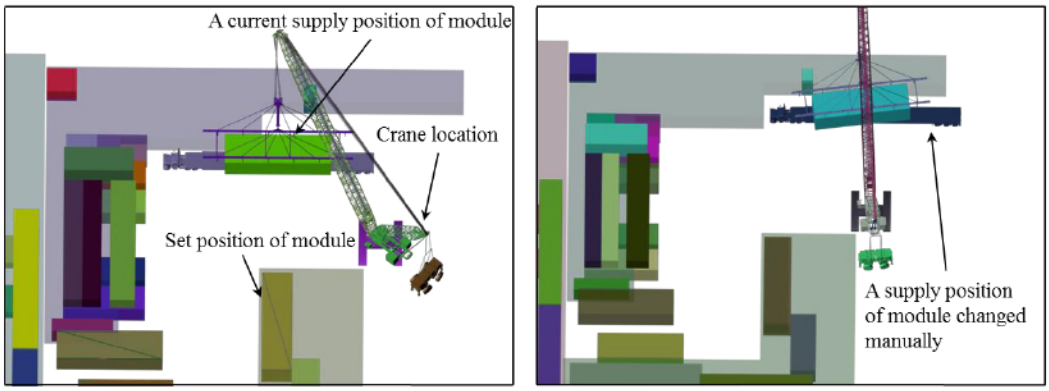

(a) Supply position (b) Changed supply position

Figure 3.31: Motion plans with different module supply positions

3.3.6 Virtual Motion of Crane Operation (VMCO) Controller

To implement the proposed methodology effectively and efficiently, the VMCO controller shown in Figure 3.32 is developed using MAXScript, which is a built-in language tool in 3ds Max. It automatically builds and animates 3D models, including lifted objects, existing obstacles, and site layouts, eliminating the need for manual manipulation. This automated VMCO controller eliminates the need for repetitive tasks such as building various animations and 3D models corresponding to data changes involving lift schedule and site layout changes. The VMCO controller comprises four sections: (1) crane operation generation; (2) lift and productivity information; (3) collision detection; and (4) animation controllers.

The functions involved in generating crane operation consist of the following: (1) “Connect and Update Data”, which reads and imports data from the database in MS Access to 3ds Max; (2) “Crane Operation Types”, which selects the pick from fixed position method or pick and carrying operation method for each lifted object; (3) “Set Site Boundaries”, which draws the 3D site layout, including OSBL and ISBLs; (4) “Object ID”, which uses a drop-down list to display and select a target object that requires either the pick from fixed position or pick and carrying operation; (5) “Track No.”, which provides the identification IDs of mobile crane locations in the selected target object; (6) “Set Existing Objects”, which identifies and builds particular 3D modules as existing obstacles already installed prior to lifting of the target object based on the lift schedule; (7) “Allowance Clearance 1”, which defines the clearance between superlift and existing obstacles; (8) “Allowance Clearance 2”, which defines a distance to be maintained between the lifted object and existing obstacles; (9) “Generate Animation”, which builds animations of the mobile crane operations using rotation and spatial analyses based on scenario 1; (10) “Generate the other scenarios”, which generates animations based on scenario 2; and (11) “Delete Animation”, which deletes the existing animation and all associated 3D models in order to build a new animation for different object IDs and/or Tracking Numbers. It should be noted that the crane operation is redesigned based on scenario 2 without deleting any 3D models or animations when scenario 1 fails to plan collision-free crane operation.

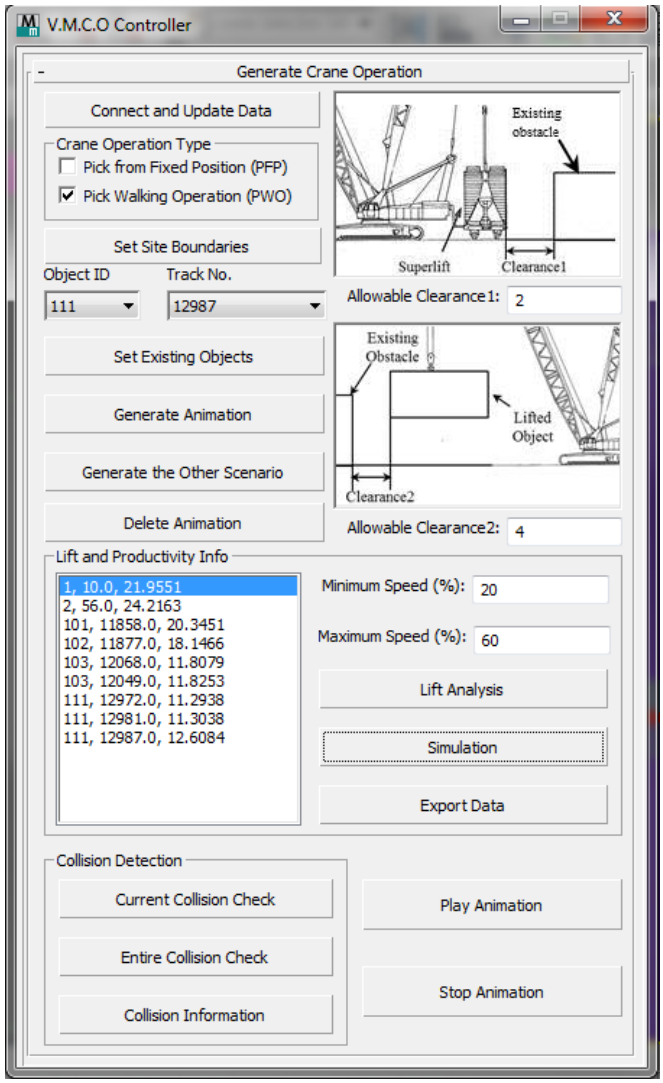

Figure 3.32: Virtual motion of crane operation controller

The lift and productivity information consists of: (1) “Minimum Speed (%)”, which is defined by the minimum percentage of the crane speed by users; (2) “Maximum Speed (%)”, which is the maximum percentage of the user-defined crane speed; (3) “Lift Analysis”, which represents a table including sequences of crane operation and associated crane information such as lifting angles, lifting height, and animation time; (4) “Simulation”, which implements a simulation model in order to determine cycle times of each crane operation based on the crane information generated from the lift analysis; (5) “List box”, which

describes the simulation outputs involving object IDs, tracking numbers, and cycle times of crane operations; and (6) “Export Data”, which stores and/or updates information such as lifting angles and associated crane parts with animation times into the database according to the lifted object IDs. There are three functions of collision detection: (1) “Current Collision Check”, which identifies any collision errors between cranes, existing obstacles, and the lifted object at a specific animation time; (2) “Entire Collision Check”, which continuously checks for spatial conflicts between cranes, existing obstacles, and the lifted object during crane operation; and (3) “Collision Information”, which provides details on any collisions, such as associated crane parts, existing obstacles, and animation times. As animation controllers, “Play” and “Stop” buttons are also developed.

3.4 Summary

This chapter has presented a methodology by which to design motions of mobile crane operation automatically in 3D visualization, considering both crane pick from fixed position and pick and carrying operation methods, for a large number of lifts based on feasible crane location, module supply position, site layout, and lift schedule changes. The significance of the developed motion planning method is that it focuses on improving the safety and efficiency of crane operations. This chapter has also presented a new approach to integrate 3D visualization with a simulation model through a DLL file which allows information to be shared between 3ds Max and Simphony.NET, as well as to execute functionalities of Simphony.NET in 3ds Max without any intermediate step. This system assists in

determining the cycle time of crane operation and facilitating selection of optimal crane operations when more than one crane operation exists for a given lift. This chapter has proposed to extend the domain of construction planning by integrating digital crane information in the BIM structure. This crane information can assist in the construction planning process by improving communication and collaboration among stakeholders, enhancing the accuracy and efficiency of lift design and project scheduling, reducing lifting time and cost without introducing design errors, and increasing the productivity of a project.

Chapter 4: Case Study

4.1 Introduction

This chapter describes a case project involving various site layouts and lift schedules, which demonstrates the effectiveness of the proposed methodology for projects with a large number of modules. To support clear understanding of the case study, this section describes the components of modules. Heavy industrial projects, including oil sands facilities, are constructed with a large number of modules prefabricated in a factory-controlled environment and installed by mobile cranes on site. As shown in Figure 4.1, pipe rack modules comprise steel structures (frames), beams, columns, pipes, and pick points. The pick points are hooked and unhooked by the rigging system of the crane. The volume or weight of each module determines the number of pick points. Since the shape of the module is configured similarly to a box, this research represents modules as 3D box models for the purpose of motion planning in 3D visualization.

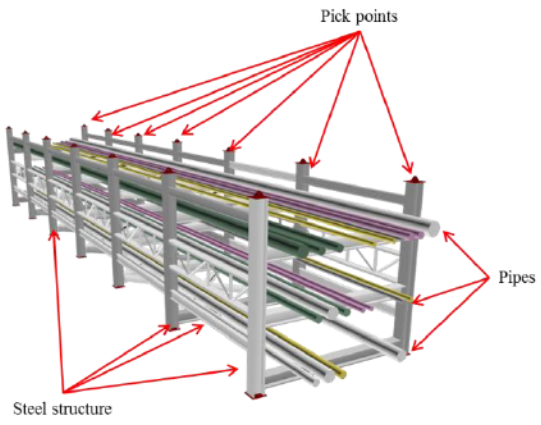

Figure 4.1: Typical pipe rack module

A modular-based construction project by PCL Industrial Management Inc. in Alberta, Canada, shown in Figure 4.2, is selected as a case study. Due to the fact that heavy industrial construction projects such as this one undergo frequent changes to site layout and lift schedule, crane lift planning can identify feasible crane operations accurately and quickly for each module in accordance with site layout and lift schedule changes. The case study involves over 300 modules installed by two types of crane operation, pick from fixed position and pick and carrying operation. The crane path checking and planning developed by Lei et al. (2013) is implemented to determine crane location for crane pick from fixed position operations that use a single mobile crane location. Collision errors are identified for some modules, necessitating crane pick and carrying operations that use two mobile crane locations (start points and finish points of crane walking paths). Although lift engineers in the interest of safety prefer the pick from fixed position method rather than pick and carrying operation, in some congested areas pick and carrying is required in order to deliver the module successfully to its set positions. The mobile crane pick and carrying operation method requires dynamic mobile crane locations, which increases potential collision errors compared with pick from fixed position. To implement the proposed methodology in various scenarios, the case study illustrates two types of crane operation, pick from fixed position and pick and carrying operation.

Figure 4.2: A typical modular site

The crane selected for this case study is the Demag CC 2800 crawler crane with superlift equipment; the capacity of this crane is 660 tons, the boom length is 84 m (276 ft), and the length of the superlift counterweight is 15 m (49 ft). This 3D crane model is built in AutoCAD, and integrated to the bones system in 3ds Max. The VMCO controller developed in 3ds Max is directly connected to a Microsoft Access database as its main input stream. It reads the required information such as module, site layout, and lift schedule from the database, builds the 3D models, designs collision-free motions of mobile crane operation as 3D visualization, represents collision, lift, and productivity information, and writes the user-desired data into the central database. The VMCO controller is thus a primary controller by which to execute the proposed methodology automatically and efficiently. The crane management system provides limited information such as pick areas from which modules can be loaded by the crane, but this information is not sufficient for the proposed methodology since motion planning requires

specific module supply positions (MSPs) in order to design collision-free crane operation. To eliminate these uncertain positions, the VMCO controller uses trucks as module supply positions so that crane operation can be designed whenever the locations of trucks are defined by users. In the case project, lifting cases in the target areas (Areas 1, 2 and 3) total 155 modules. Figure 4.3 presents the following: target areas and site layout; outside site boundary limit (OSBL); inside boundary limit (ISBL); existing obstacles (already installed prior to the target module to be lifted), determined by the lift schedule; module supply positions of lifted objects, described as trucks in target areas; and feasible crane locations. The 3D visualization is thus applied as a design tool to plan detailed motions of mobile crane operation, as well as a validation tool for feasible crane locations for each module.

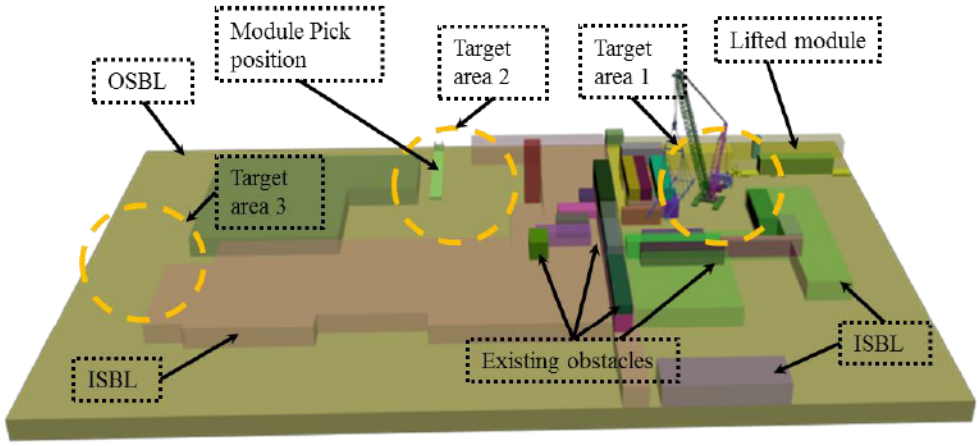

Figure 4.3: Site information

4.2 Pick From Fixed Position

Most modules in this project are installed by pick from fixed position and analyzed by the crane path checking and planning system. This section illustrates

the case of Module 21. This module has a total of 187 tracking numbers, which are the feasible crane locations. Tracking number 2068 at target area 1 is selected in order to describe the sequences of motion planning. The weight of the module is 156.9 tons, and its dimensions are 7.29 m (23.95 ft) × 25.30 m (83 ft) × 7.27 m (23.84 ft). The maximum radius of the mobile crane is 33.52 m (110 ft). The rotation analysis illustrated in Figure 4.4 is implemented as follows: (1) build a 3D visualization of the OSBL and ISBLs to support collision-free lifting plans based on the lift schedule, and move the crane to the pick from fixed position (PFP) specified by tracking number 2068; (2) rotate the superstructure to the supply position of Module 21 by 124.59º (θ_5^{SP}) with a clockwise direction calculated as follows,

$$\cos\left(\theta_5^{SP}\right)=\frac{\overrightarrow{V_5^C}\bullet\overrightarrow{V_5^D}}{\left\|\overrightarrow{V_5^C}\right\|\left\|\overrightarrow{V_5^D}\right\|}=-0.569 \text{ and } \sin\left(\theta_5^{SP}\right)=\frac{\overrightarrow{V_5^C}\times\overrightarrow{V_5^D}}{\left\|\overrightarrow{V_5^C}\right\|\left\|\overrightarrow{V_5^D}\right\|}=0.822$$

$$\theta_5^{SP}=\arctan\left[\frac{\sin(\theta_5^{SP})}{\cos(\theta_5^{SP})}\right]+\left[1-\text{sgn}(\cos(\theta_5^{SP}))\right]\left(\frac{\pi}{2}\right)=124.59°$$

(3) rotate the boom upward by 19.96º (α_{70}^{B}) to coincide with the location of the rigging system and the module supply position; (4) rotate the rigging system by 51.61º (θ_{100}^{RI}) counter-clockwise and lift it up and down; (5) rotate the superstructure by 95.55º (θ_{180}^{SP}) counter-clockwise to the module's set position; (6) rotate the boom downward by 5.94º (α_{400}^{B}) and the rigging system by 5.55º (θ_{450}^{RI}); and (7) lift the rigging system up and down, and check for errors. The

rotations of the crane carrier ($\theta_n^{Carrier}$) and the superstructure (θ_n^{SP}), which is calculated after crane carrying for the pick and carrying position method, are not considered in the pick from fixed position method. (These rotations will be described more clearly in the next section.) It should be noted that the lift height presented in the rotation analysis is used as a general height to avoid potential conflicts between the lifted object and existing obstacles, including the ISBL, as well as to describe the principles of the rotation and spatial analyses clearly. The rotation analysis calculates lifting angles and directions in order to build the motions of mobile crane body configurations. Spatial analysis searches for the material-lifting paths related to lift heights and eliminates potential collision errors during crane operation. Based on the sequences in scenario 1 of the rotation analysis, 3D visualization for motions of crane body configurations is built successfully without any errors in tracking number 2068 of Module 21.

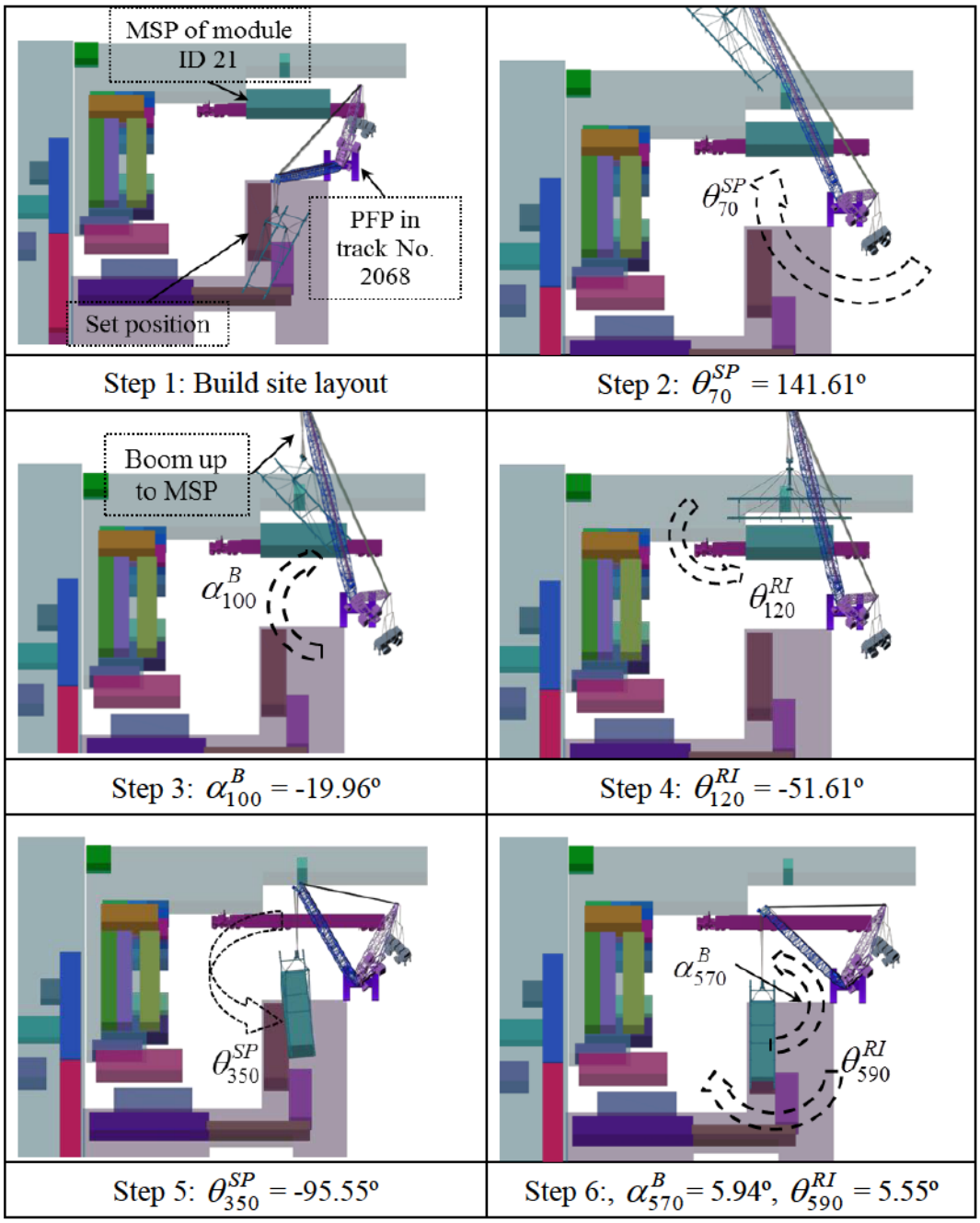

Figure 4.4: Rotation analysis of tracking number 2068 for Module 21

Based on the same rules described above, 3D visualization of the mobile crane configuration for other modules (a total of 10 modules as samples of pick from fixed positions) is developed using rotation analysis. Significant collision errors, referred to as direction errors of lifting angles and depicted in Figure 4.5, are

identified. While the superstructure for loading the lifted modules is rotating to the module supply position, direction errors of lifting angles (e.g., Module 9) are encountered which lead to conflicts between the superlift and one of the ISBLs. To prevent this collision error, the clearance between the superlift and ISBLs is maintained, but the position of the rigging system is not available to load the module supply position. According to the flow of the rotation analysis (see Figure 3.10), 3D visualization of crane operations is developed for Module 9 with the direction change of superstructure rotation through scenario 1. The crane loads the lifted object on the module supply position, and Module 9 is delivered successfully to its set position without any collision errors. As a result, the rotation analysis has some limitations: (1) it does not offer collision detection; (2) it lacks proactive methods to eliminate the conflicts; and (3) does not provide material-lifting path.

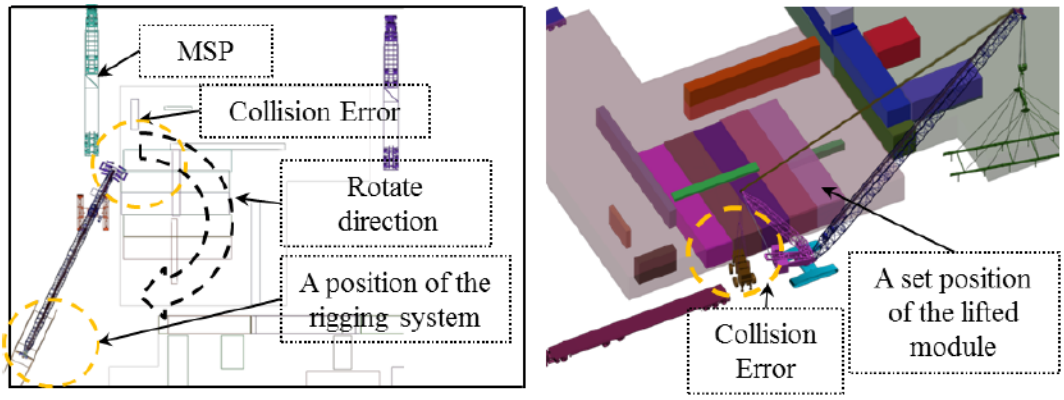

(a) Perspective view (b) Plan view

Figure 4.5: Collision and direction errors in Module 9

To establish successful motion planning by eliminating limitations of the rotation analysis, the spatial analysis is implemented tracking number 410 of Module 9 as a case study as a means of clearly describing the characteristics of

the spatial analysis. To execute each function of the spatial analysis, the clearances for MT-Lift and SubMot are defined as 6 ft and 2 ft, respectively. The sequences of the spatial analysis described in Figure 4.7 are as follows:

(1) Read the current geometric center position of the target object (Module 9) in MT-Lift function, and of the superlift in the SubMot function, represented as $P_n^{TO(module9)}$ and $P_n^{TO(SL)}$, respectively.

(2) Identify target obstacles (TSs) by calculating distances (d_n) from the $P_n^{TO(SL)}$ and $P_n^{TO(module9)}$ to the existing obstacles. It should be noted that SubMot is implemented continuously when the crane body configurations are operating and the ISBL ID 1, defined as the $TS_{ISBL1,}$ is identified as the target obstacle. The MT-Lift is executed after the crane has loaded the lifted object.

(3) Continuously monitor the D_{Actual} from the TO_{SL} to the TS_{ISBL1} in comparison to the clearance (2 ft) during the superstructure rotation. The superstructure rotation is 25.37° in the clockwise direction, thereby maintaining a clearance of (D_{Actual} = 1.98 ft ≤ 2 ft). This is an improvement upon the 176.7° counter-clockwise rotation calculated by the rotation analysis.

(4) Request to change the direction (counter-clockwise) of the superstructure rotation by rotating -183.3°, since the position of the rigging system shown in Step 3 is not located above the supply position of the $TO_{module9}$ for loading. While the superstructure is rotating -183.3°, steps (2) and (3) are repeated. If the position of the

rigging system is still not located above the supply position of the $TO_{module9}$, the associated pick from fixed position fails.

(5) Implement the MT-Lift after loading $TO_{module9}$. The D_{Actual} from the $TO_{module9}$ to $TS_{obstacle66}$, described in Figure 4.6, is 5.93 ft at 208 frames (animation time unit), which is the less than the clearance (6 ft), and the D_{Actual} from the TO_{SL} to TS_{ISBL1} is greater than 2 ft.

(6) Stop the current motion of the mobile crane (superstructure rotation with load) temporarily, lifting the rigging system up by RH (16.5 ft) to reach a 6 ft clearance between the $TO_{module9}$ and $TS_{obstacle66}$ in order to prevent a potential collision error, and restart the superstructure rotation.

Since the TSs were changeable according to the crane operation, Step 2 and 6 were implemented repeatly until the $TO_{module9}$ was delivered to its set position by the crane. After designing the motions of mobile crane operation, visual checking was implemented. As a result, the crane operation for module 9 was acceptable since no errors were identified.

Time	MT-Lift			SubMot		
	Target object	Target obstalce	Distance	Target object	Target obstalce	Distance
196	Module ID 9	Module ID 66	15.58	Superlift	ISBL1	20.07
197	Module ID 9	Module ID 66	14.72	Superlift	ISBL1	20.46
198	Module ID 9	Module ID 66	13.84	Superlift	ISBL1	20.82
199	Module ID 9	Module ID 66	13.04	Superlift	ISBL1	21.17
200	Module ID 9	Module ID 66	12.23	Superlift	ISBL1	21.5
201	Module ID 9	Module ID 66	11.50	Superlift	ISBL1	21.82
202	Module ID 9	Module ID 66	10.78	Superlift	ISBL1	22.13
203	Module ID 9	Module ID 66	10.13	Superlift	ISBL1	22.42
204	Module ID 9	Module ID 66	9.52	Superlift	ISBL1	22.65
205	Module ID 9	Module ID 66	7.12	Superlift	ISBL1	22.89
206	Module ID 9	Module ID 66	6.63	Superlift	ISBL1	23.08
207	Module ID 9	Module ID 66	6.23	Superlift	ISBL1	23.23
208-220	Module ID 9	Module ID 66	5.93	Superlift	ISBL1	23.44
221	Module ID 9	Module ID 66	6.66	Superlift	ISBL1	23.44
222	Module ID 9	Module ID 66	7.45	Superlift	ISBL1	23.47
223	Module ID 9	Module ID 66	8.06	Superlift	ISBL1	23.51
224	Module ID 10	Module ID 144	11.23	Superlift	ISBL1	46.72
225	Module ID 11	Module ID 144	10.02	Superlift	ISBL1	47.24
262	Module ID 12	Module ID 144	8.89	Superlift	ISBL1	47.71
263	Module ID 13	Module ID 144	7.90	Superlift	ISBL1	48.16
264	Module ID 14	Module ID 144	7.06	Superlift	ISBL1	48.53
265	Module ID 15	Module ID 144	6.32	Superlift	ISBL1	48.89
266-278	Module ID 16	Module ID 144	5.71	Superlift	ISBL1	49.19
279	Module ID 17	Module ID 144	6.13	Superlift	ISBL1	49.94
280	Module ID 18	Module ID 144	6.51	Superlift	ISBL1	50.1
281	Module ID 19	Module ID 144	6.87	Superlift	ISBL1	50.37

Less than 6 ft between the lifted object and existing obstacle

Figure 4.6: Monitoring clearances between animation times 196 and 281

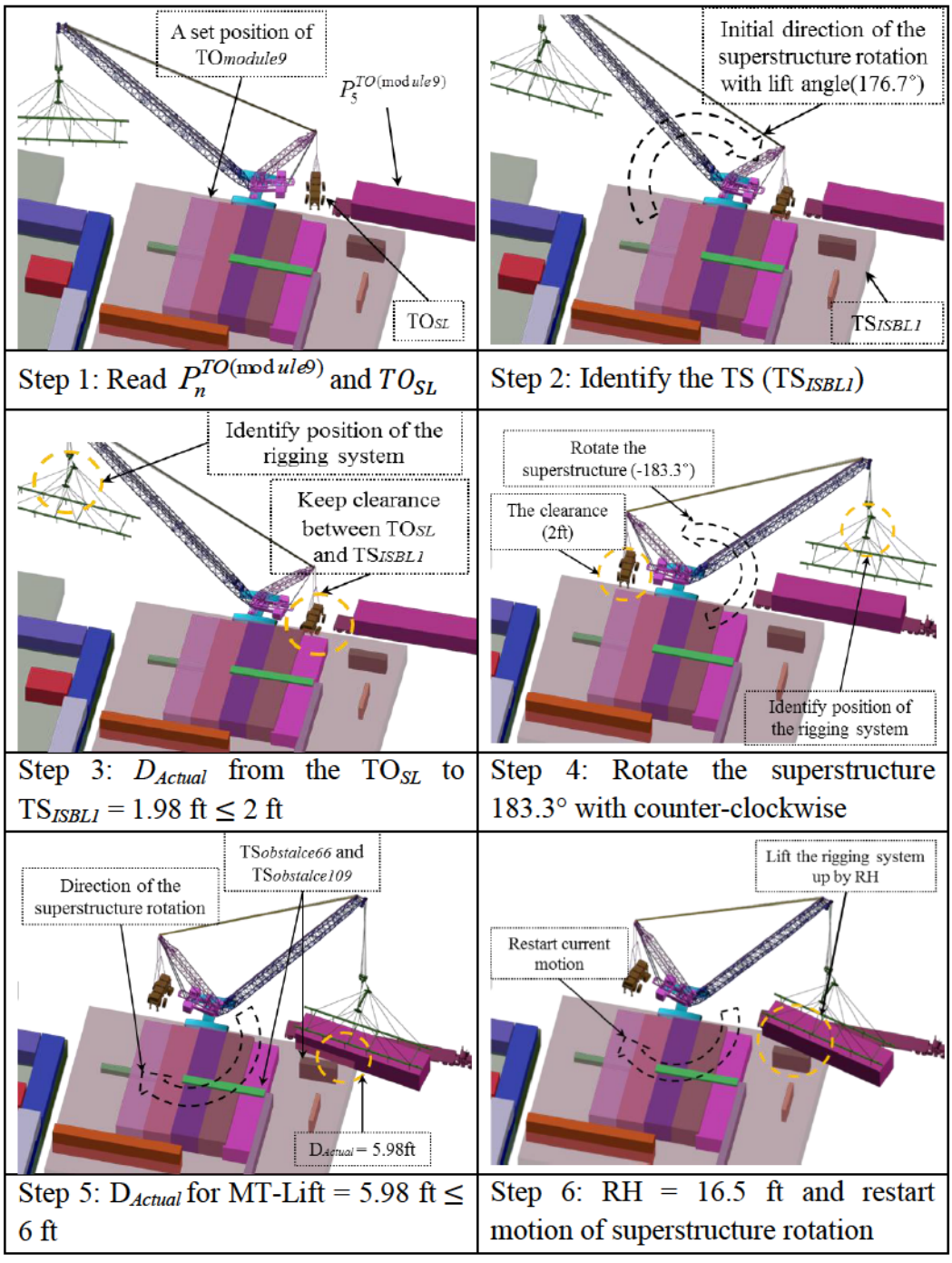

Step 1: Read $P_n^{TO(module9)}$ and TO_{SL}

Step 2: Identify the TS (TS_{ISBL1})

Step 3: D_{Actual} from the TO_{SL} to TS_{ISBL1} = 1.98 ft ≤ 2 ft

Step 4: Rotate the superstructure 183.3° with counter-clockwise

Step 5: D_{Actual} for MT-Lift = 5.98 ft ≤ 6 ft

Step 6: RH = 16.5 ft and restart motion of superstructure rotation

Figure 4.7: Sequences of the spatial analysis for Module 9

For validation purposes, ten cases are selected. As shown in Figure 4.8a and Figure 4.8b, 3D visualizations of mobile crane pick from fixed position are developed for two modules, Modules 21 and 23, according to the

aforementioned principles of the rotation and spatial analyses. Although 3D visualization aids users in analyzing collision errors with sequences of crane operation, users may wish to carefully check workspaces on congested areas in 3D visualization across animation time due to the visual illusion described in Figure 4.8c by which conflicts appear to have been identified between the crane and existing obstacles on site which may or may not exist. These visual illusions can be investigated by zooming-in and rotating the perspective view in order to identify certain workspaces in a closer view on a computer screen. The collision analysis, for convenience, can thus be implemented either at a specific interval or for the entire animation. As a result, the collision-free 3D visualization of crane operation for other modules is successfully developed.

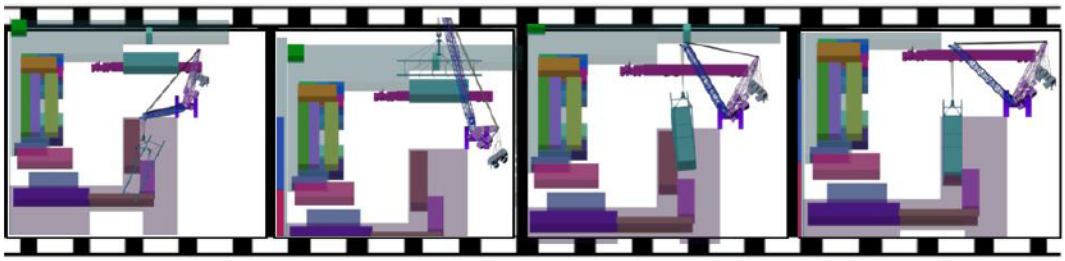

(a) Module 21

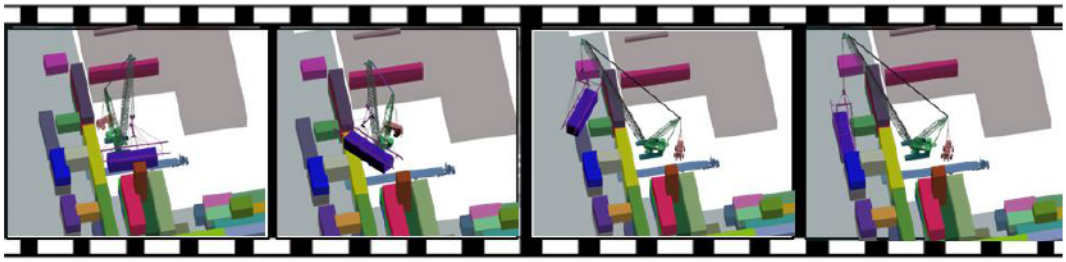

(b) Module 23

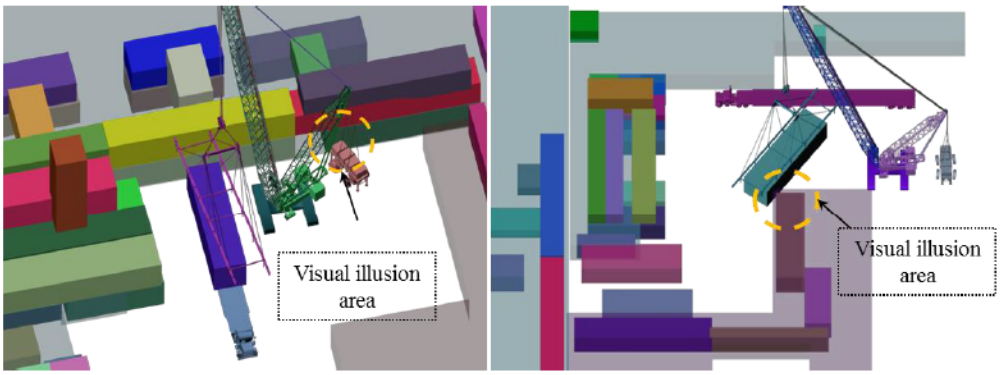

(c) Conflict checking

Figure 4.8: 3D visualization of mobile crane pick from fixed position for Modules 21 and 23

From a safety perspective, one of the most critical criteria in lift planning is crane capacity checking, where the total weights loaded by the crane cannot exceed the crane capacity setting identified by the lifting capacity chart. In this respect, the lift analysis is implemented to ensure the motion of crane operation designed by the proposed methodology is safe, since this case study randomly selects module supply positions based on the swing-free crane pick from fixed position method. As shown in Figure 4.9, the safety factor calculated should be less than or equal to 85%. Otherwise, the module supply position is adjusted and the motion of crane operation is rebuilt to satisfy the requirement of the crane capacity checking.

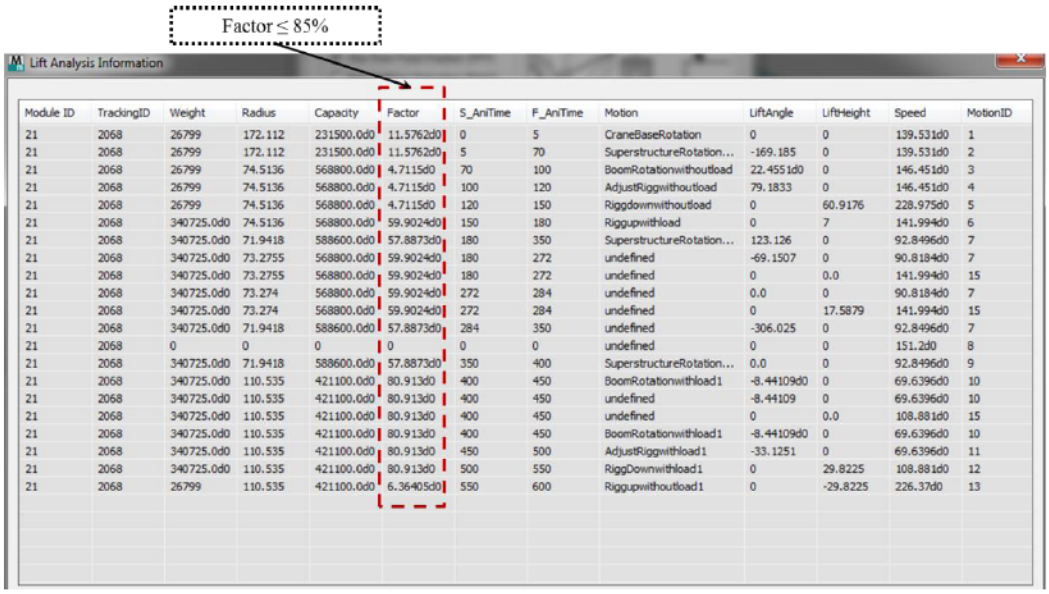

Module ID	TrackingID	Weight	Radius	Capacity	Factor	S_AniTime	F_AniTime	Motion	LiftAngle	LiftHeight	Speed	MotionID
21	2068	26799	172.112	231500.0d0	11.5762d0	0	5	CraneBaseRotation	0	0	139.531d0	1
21	2068	26799	172.112	231500.0d0	11.5762d0	5	70	SuperstructureRotation...	-169.185	0	139.531d0	2
21	2068	26799	74.5136	568800.0d0	4.7115d0	70	100	BoomRotationwithoutload	22.4551d0	0	146.451d0	3
21	2068	26799	74.5136	568800.0d0	4.7115d0	100	120	AdjustRiggwithoutload	79.1833	0	146.451d0	4
21	2068	26799	74.5136	568800.0d0	4.7115d0	120	150	Riggdownwithoutload	0	60.9176	228.975d0	5
21	2068	340725.0d0	74.5136	568800.0d0	59.9024d0	150	180	Riggupwithload	0	7	141.994d0	6
21	2068	340725.0d0	71.9418	588600.0d0	57.8873d0	180	350	SuperstructureRotation...	123.126	0	92.8496d0	7
21	2068	340725.0d0	73.2755	568800.0d0	59.9024d0	180	272	undefined	-69.1507	0	90.8184d0	7
21	2068	340725.0d0	73.2755	568800.0d0	59.9024d0	180	272	undefined	0	0.0	141.994d0	15
21	2068	340725.0d0	73.274	568800.0d0	59.9024d0	272	284	undefined	0.0	0	90.8184d0	7
21	2068	340725.0d0	73.274	568800.0d0	59.9024d0	272	284	undefined	0	17.5879	141.994d0	15
21	2068	340725.0d0	71.9418	588600.0d0	57.8873d0	284	350	undefined	-306.025	0	92.8496d0	7
21	2068	0	0	0	0	0	0	undefined	0	0	151.2d0	8
21	2068	340725.0d0	71.9418	588600.0d0	57.8873d0	350	400	SuperstructureRotation...	0.0	0	92.8496d0	9
21	2068	340725.0d0	110.535	421100.0d0	80.913d0	400	450	BoomRotationwithload1	-8.44109d0	0	69.6396d0	10
21	2068	340725.0d0	110.535	421100.0d0	80.913d0	400	450	undefined	-8.44109	0	69.6396d0	10
21	2068	340725.0d0	110.535	421100.0d0	80.913d0	400	450	undefined	0	0.0	108.881d0	15
21	2068	340725.0d0	110.535	421100.0d0	80.913d0	400	450	BoomRotationwithload1	-8.44109d0	0	69.6396d0	10
21	2068	340725.0d0	110.535	421100.0d0	80.913d0	450	500	AdjustRiggwithload1	-33.1251	0	69.6396d0	11
21	2068	340725.0d0	110.535	421100.0d0	80.913d0	500	550	RiggDownwithload1	0	29.8225	108.881d0	12
21	2068	26799	110.535	421100.0d0	6.36405d0	550	600	Riggupwithoutload1	0	-29.8225	226.37d0	13

Figure 4.9: Lift information for Module 21

Although pick from fixed position operations are validated by designing proposed motion planning, users can have difficulty deciding on the most appropriate location for crane pick from fixed position for each module, due to there being more than one feasible crane location. Another source of difficulty in decision making is uncertainty of the module supply positions, which can increase or decrease process times for each motion. In this respect, a productivity analysis is implemented to aid users in more efficiently selecting locations for crane pick from fixed positions with different module supply positions. Before running a simulation model, process times for each motion of crane operation in 3D visualization are calculated based on lifting angles, lifting height, and hoist and rotation speeds determined by the minimum and maximum percentages of speed (20% and 60% in the case study, respectively). The module ID, its tracking number, and the cycle time of crane operation are then represented in the VMCO. To search for the best location for crane pick from fixed position

with its associated module supply position, motions of crane operation are developed and the productivity analysis is implemented based on various module supply positions and feasible crane locations. As shown in Figure 4.10a, the cycle time of crane operation for Module 21 is 14.4258 minutes for the initial module supply position represented in Figure 4.10b, and the cycle time after changing the module supply position as shown in Figure 4.10c is 10.7903 minutes. The second module supply position is thus the best crane pick from fixed position for Module 21. (It should be noted that the cycle time does not include the installation time of the module on its set position.)

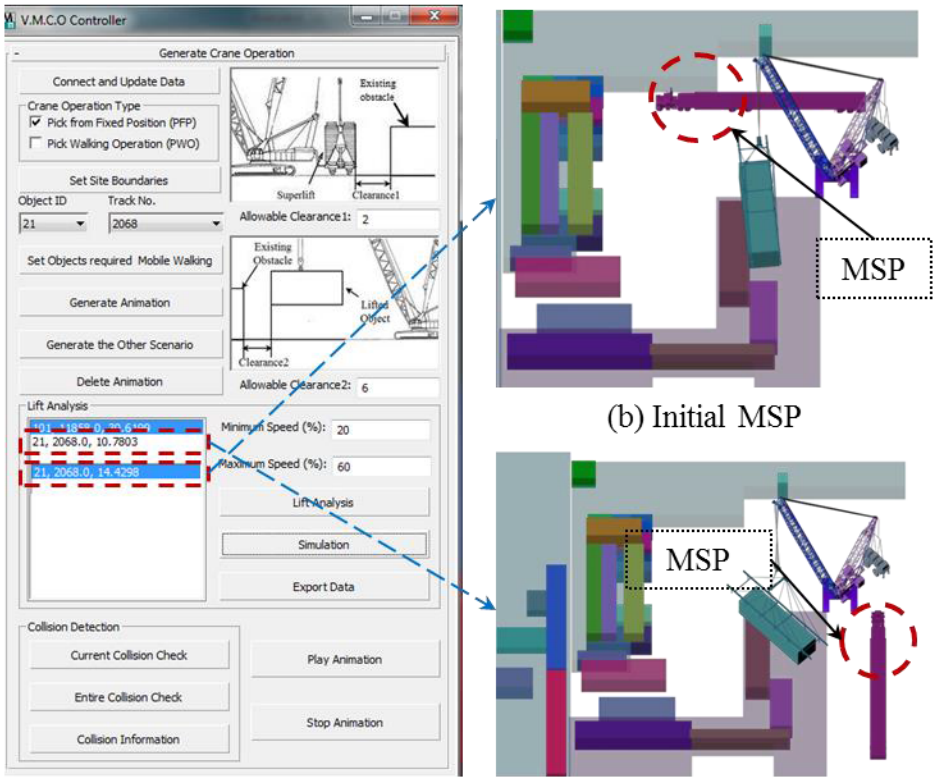

(a) Productivity analysis

(b) Initial MSP

(c) After changing MSP

Figure 4.10: Productivity analysis for Module 21 at different module supply positions

4.3 Pick and Carrying Operation

Although lift engineers and project managers prefer the more efficient pick from fixed position method, in some cases pick and carrying operation is necessary in order to deliver lifted objects to their set positions. In this respect, the case study involves a few modules for which pick from fixed position is not suitable due to area congestion (see Figure 4.11) and constraints imposed by the lift schedule.

Figure 4.11: A typical congested area on-site

Based on mobile crane walking path checking in the crane path checking planning system, 8 modules are identified for installation by mobile crane pick and carrying operations: Modules 1, 2, 12, 85, 101, 102, 103, and 111. A given module may have more than one possible mobile crane-walking path. For example, Module 2 has nine walking paths, denoted in the database by means tracking numbers, while Module 102 has only one walking path. The target walking paths for Module 1, which has a weight of 155.1 tons and dimensions of

5.99 m (19.68 ft) × 29.99 m (98.42 ft) × 6.74 m (22.14 ft), are selected as a primary case for implementation of the proposed methodology. The maximum radius of the mobile crane is 33.52 m (110 ft). Since Module 1 has ten walking paths, given by tracking numbers 1, 5, 10, 16, 27, 32, 37, 42, 46, and 51, the mobile crane is located in the start points of the walking paths at target area 1 of the site. For the walking path corresponding to tracking number 1, the rotation analysis illustrated in Figure 4.12 is implemented as follows:

(1) Build 3D-visualized OSBL and ISBL models as site layout to identify collision-free lifting plans and move the crane to the start point of the walking path specified by tracking number 1.

(2) Rotate the crane-base by 23.97º ($\theta_1^{Carrier}$) at the start point of the walking path.

(3) Rotate the superstructure by -211.8º (θ_{50}^{SP}) to the module supply position of Module 1, and rotate the boom upward by 5.16º (α_{70}^{B}) such that the location of the rigging system coincides with the module supply position.

(4) Rotate the rigging system by 34.22º (θ_{100}^{RI}) and lift it up and down.

(5) Rotate the superstructure by 142.04º (θ_{180}^{SP}) to the finish point of the walking path.

(6) Walk the crane from the start point to the finish point of the walking path (30.39 m).

(7) Rotate the superstructure by -8.43º (θ_{480}^{SP}).

(8) Rotate the boom upward by 15.85º (α_{540}^{B}) and the rigging system by 46.38º (θ_{570}^{RI}).

(9) Lift the rigging system up and down, and check for errors.

Since this rotation analysis only computes the lifting angles to build motions of mobile crane body configurations, the lift heights are used as specific heights, which prevent collision errors between the lifted module and existing obstacles. Based on the sequences in scenario 1 of the rotation analysis, 3D visualization for motions of crane body configurations is built successfully without any errors for tracking number 1 of Module 1.

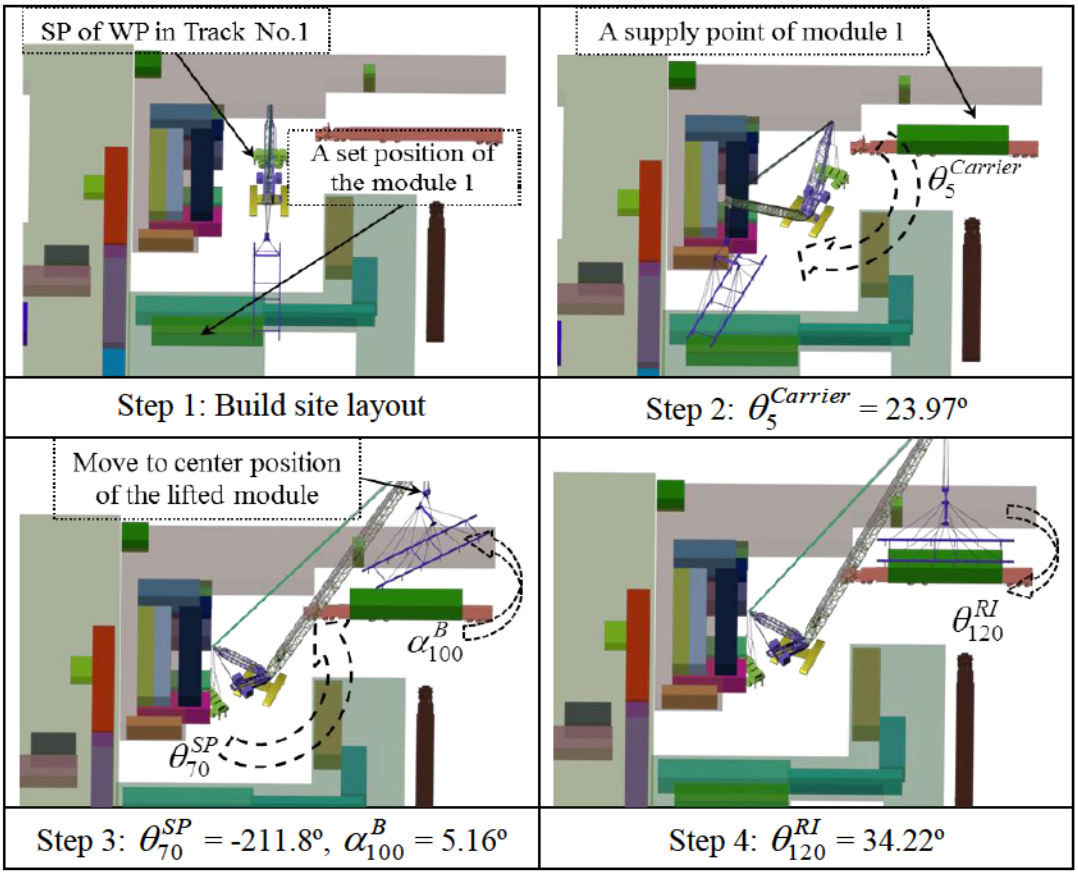

Step 1: Build site layout

Step 2: $\theta_5^{Carrier} = 23.97º$

Step 3: $\theta_{70}^{SP} = -211.8º$, $\alpha_{100}^{B} = 5.16º$

Step 4: $\theta_{120}^{RI} = 34.22º$

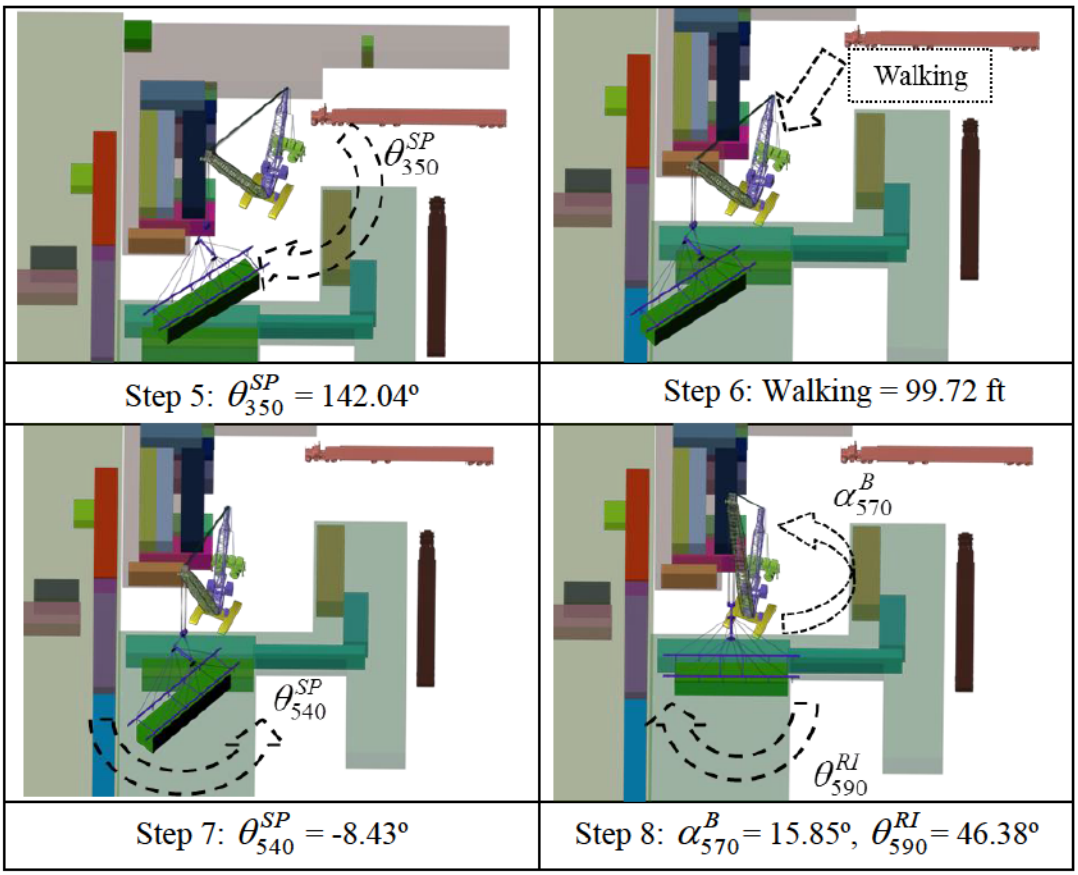

Figure 4.12: Rotation analysis for tracking number 1 of Module 1

According to this procedure, 3D visualization of mobile crane operations for other modules is developed using the rotation analysis. Significant collision errors referred to as lifting angle errors and direction errors of lifting angles—depicted in Figure 4.13a and Figure 4.13b, respectively— are identified in scenario 1. While the superstructure carrying the lifted modules is rotating on the start points and/or finish points of the walking paths, lifting angle errors (Modules 101, 102, and 103) and direction errors of lifting angles (Modules 12 and 92) leading to conflicts between the superlift and one of the ISBLs are encountered. The direction error results in the rigging system failing to be located above the module supply position for loading. According to the flow of the rotation analysis (see Figure 3.10), 3D visualization of crane operations for

Modules 12 and 92 is developed with a direction change (counter-clockwise) of superstructure rotation in order to eliminate direction errors. As a result, Module 92 is delivered successfully to its set position, but the crane operation at the finish point of the walking path for Module 12 still has two collision errors: (1) a collision between the rigging system and the boom when the rigging system is lifted up to avoid the conflict (see Figure 4.13c); and (2) conflicts between the lifted module and the existing obstacle when the rigging system is rotating to accommodate the set position of the module (see Figure 4.13d). These errors result in an existing obstacle leading to a violation of a minimum rope height ($min\text{-}H_{rope}$); the sequences of the crane operation are thus changed from scenario 1 to scenario 2 in order to deliver Module 12 to its set position. Lifting angle errors for Modules 101, 102, and 103 (Figure 4.13a) are generated due to the fact that rotation analysis has not considered surrounding site obstacles, but has focused only on desired positions of each motion of crane operations. In other words, the lifting angle errors have been generated by overcalculating lifting angles from the rotation analysis. To prevent these errors, the superstructure rotation must be stopped immediately when a distance between the superstructure and existing obstacles is the same or less than a clearance defined by a lift engineer.

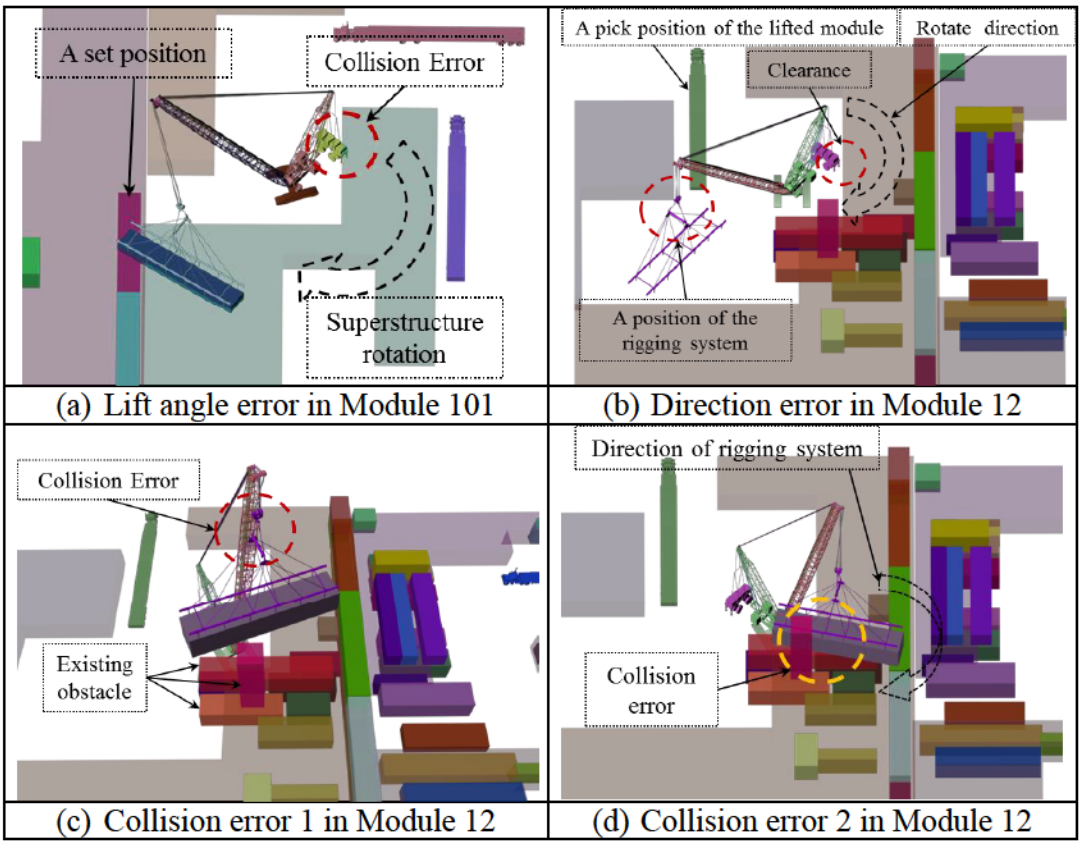

(a) Lift angle error in Module 101 (b) Direction error in Module 12

(c) Collision error 1 in Module 12 (d) Collision error 2 in Module 12

Figure 4.13: Examples of collision errors

To eliminate these limitations of the rotation analysis, spatial analysis is implemented simultaneously to maintain clearances. According to each function of the spatial analysis, these clearances are defined as follows: (1) the MT-Lift ensures 6 ft of clearance between the module as the target object (TO_{module}) and the existing obstacles; and (2) the SubMot ensures 2 ft of clearance between the superlift (TO_{SL}) and ISBLs. To illustrate the spatial analysis, Module 12 ($TO_{module12}$) with walking path ID 761 is selected since it involves all the limitations associated with rotation analysis. The sequences of the spatial analysis described in Figure 4.14 are as follows:

(1) Read the geometric center positions of the $TO_{module12}$ and of the $TO_{Superlift}$, represented as the $P_n^{TO(\mathrm{module12})}$ and $P_n^{TO(SL)}$, respectively.

(2) Identify TSs by calculating distances (*dn*) from the $P_n^{TO(SL)}$ to the existing obstacles. The SubMot is only implemented when the superstructure is rotating and the ISBL ID 3 defined as the TS_{ISBL3} is identified as the TS.

(3) Monitor continuously the D_{Actual} from the TO_{SL} to the TS_{ISBL3} in comparison to the clearance (2 ft) during the superstructure rotation. The superstructure rotation is completed at 75.97° satisfying the clearance (D_{Actual} = 1.93 ft ≤ 2 ft), an improvment upon the 161.1° rotation calculated by the rotation analysis.

(4) Change the direction (counter-clockwise) and lifting angle (198.9°) for the superstructure rotation, since the position of the rigging system shown in Step 3 is not located above the module supply position of the $TO_{module12}$ for loading. While the superstructure is rotating -198.9°, steps (2) to (3) are repeated; if the position of the rigging system is still not located above the module supply position of the $TO_{module12}$ after changing the direction and lifting angle of the superstructure rotation, the associated walking path fails.

(5) Implement the MT-Lift after the crane has loaded $TO_{module12}$. the D_{Actual} from the $TO_{module12}$ to $TS_{obstacle91}$ at 234 frames is 5.78 ft, less than the clearance (6 ft), and the D_{Actual} from the TO_{SL} to TS_{ISBL3} is 5.82 ft, which is greater than 2 ft.

(6) Stop the current motion of the mobile crane (superstructure rotation with load) temporarily at the finish point of the walking path, lifting the rigging system up by RH (42.61 ft) to maintain 6 ft between the $TO_{module12}$ and $TS_{obstacle91}$ in order to prevent a potential collision error, and restart the superstructure rotation.

Since the TSs are changeable according to the crane operation, Steps 5 and 6 are continuously repeated until the $TO_{module12}$ is delivered to its set position. As a result, the crane walking path (ID 761) is deemed acceptable since no errors are identified during 3D visualization of mobile crane operation. It should be noted that the rotation and spatial analyses must be implemented interactively to design successful motion of crane operation for both pick from fixed position and pick and carrying operations.

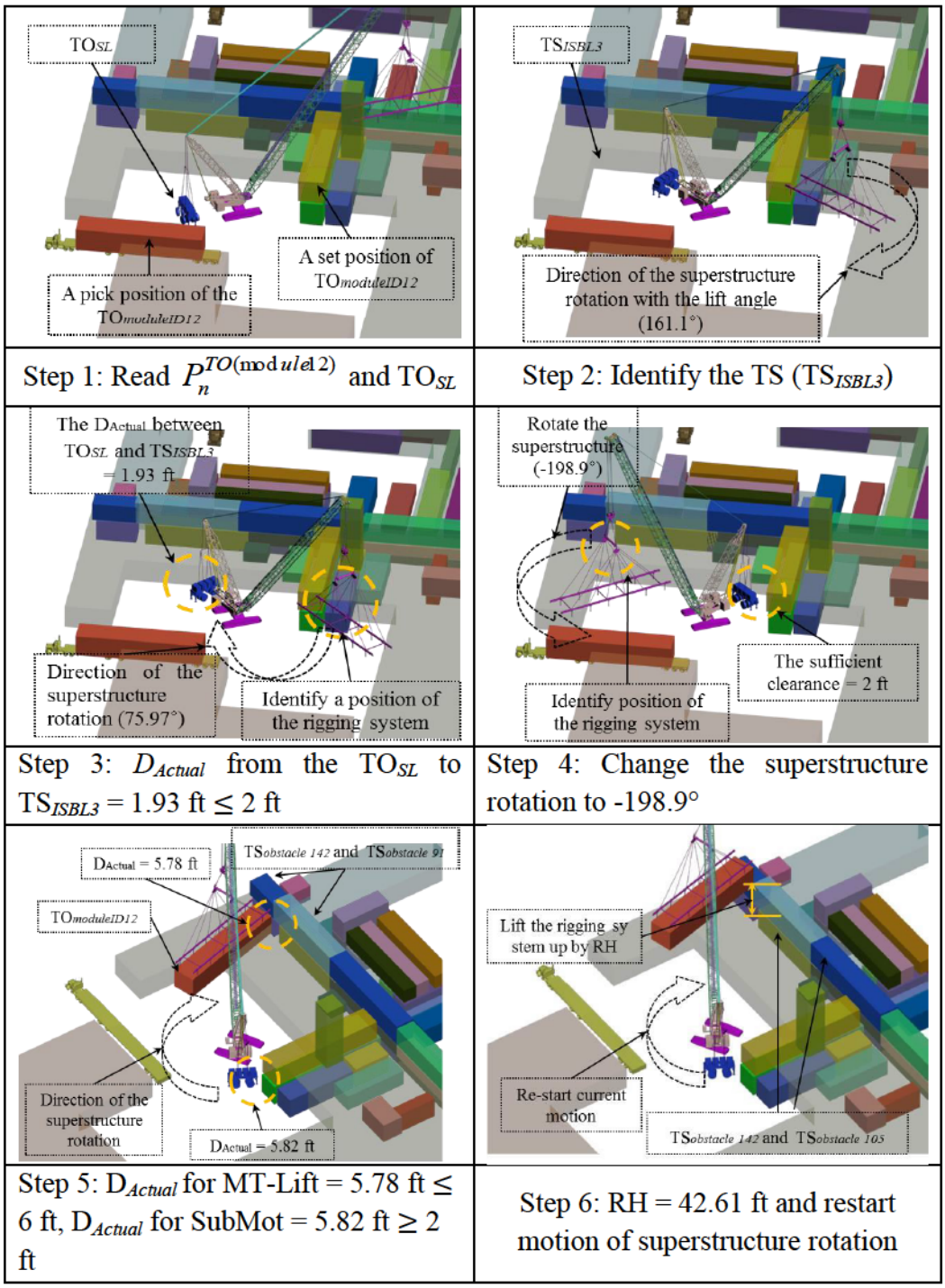

Figure 4.14: Sequences of spatial analysis for Module 12

To validate the spatial analysis in a number of respects, Module 101 ($TO_{module101}$), is selected. The superstructure is rotated 109.53° clockwise with load, rather than

the lifting angle (143.85°) and direction of superstructure rotation (clockwise) being determined by the rotation analysis, since the SubMot identifies that the D_{Actual} between TO_{SL} and TS_{ISBL4} is less than the clearance (2 ft) at 296 frames. In other words, the current superstructure rotation is completed at that time, and then the next motions are subsequently designed. In terms of the MT-Lift function, the D_{Actual} from $TO_{module101}$ to $TS_{obstacle100}$ is less than 6 ft at 401 frames while the mobile crane is walking to the finish point of the walking path. Thus, the current motion is stopped temporarily, the crane lifts the rigging system up by 22.1 ft, and the current motion is re-iterated. Figure 4.15 illustrates motion plans for $TO_{module101}$ with relationship of the spatial and rotation analyses, and 3D timeline.

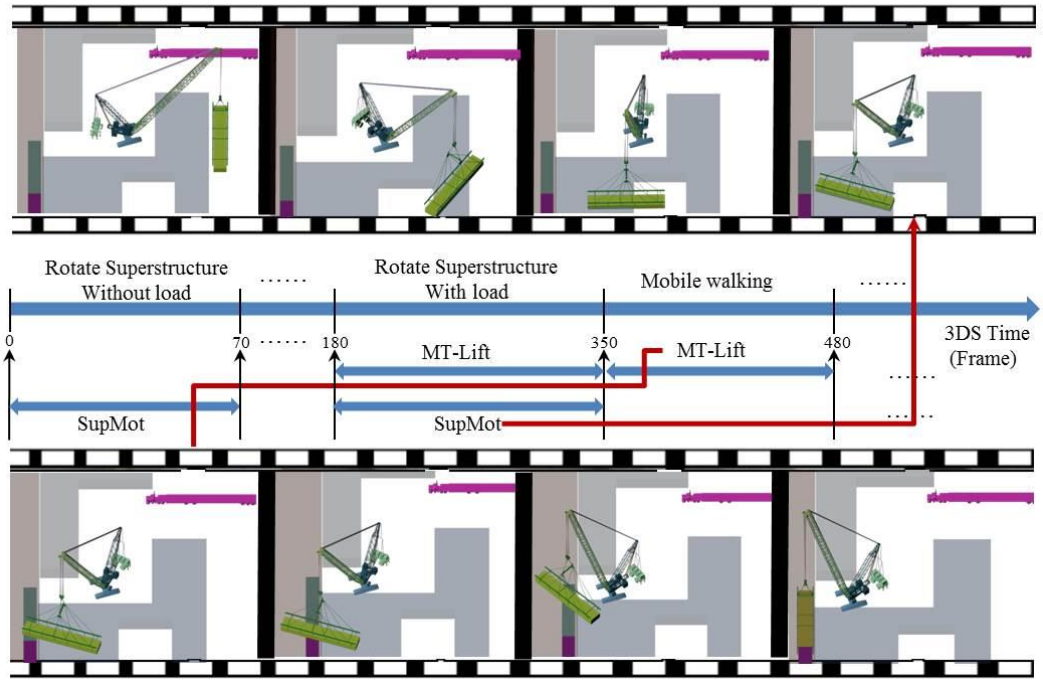

Figure 4.15: Motions of mobile crane operation for Module 101

According to the same methods of rotation and spatial analyses described above, 3D visualization of mobile crane operations for other modules, represented in

Figure 4.16, are built. Most modules use scenario 1 for rotation analysis, but Module 12 uses scenario 2 due to collision errors identified in scenario 1.

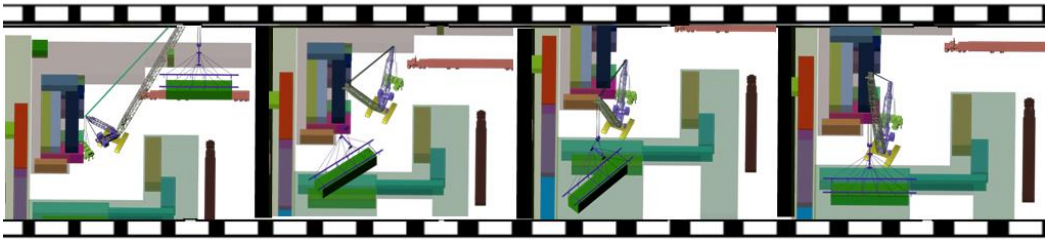

(a) Module 1

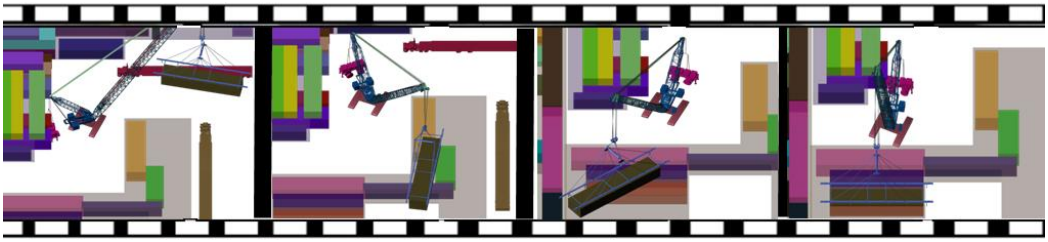

(b) Module 2

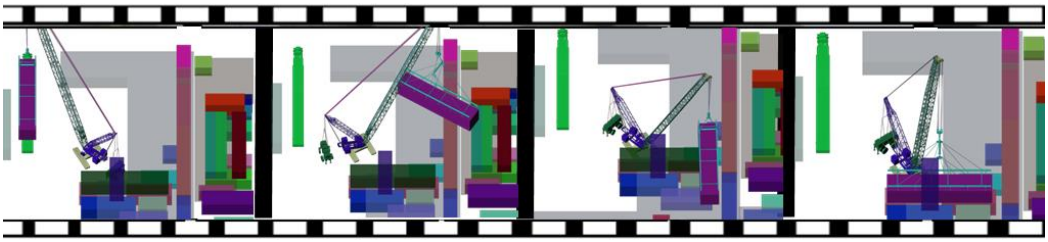

(c) Module 12

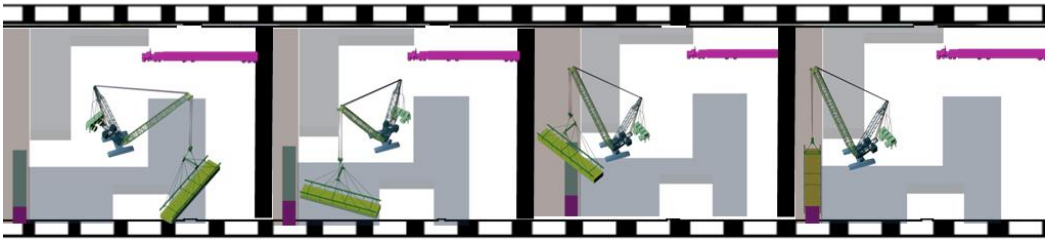

(d) Module 102

Figure 4.16: 3D visualization of mobile crane pick and carrying operation for modules

3D visualization provides an accurate and detailed interpretation of the workspace, including all moving parts of the crane and existing obstacles.

However, users may need to manipulate a display by zooming in and rotating the perspective view, which are repetitive and time-consuming tasks, in order to accurately identify the workspace, especially in congested and complex areas. To remove these unnecessary tasks, collision analysis is implemented. As a result, collision errors, shown in Figure 4.17a, are identified at the start point and finish point of the walking path of Module 85 in the 3D visualization of mobile crane operation, because of the improper crane location analyzed by the mobile crane walking path checking. Regarding these errors, collision information described in Figure 4.17b indicates which existing obstacles and crane configurations are encountered, and at what animation times. Other modules are found to have no collision errors in the 3D visualization.

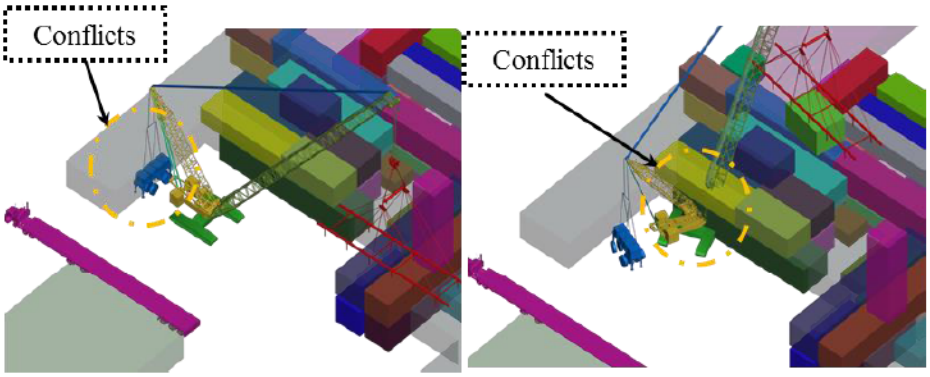

(a) Conflicts on the start point and finish point of the walking path for Module 85

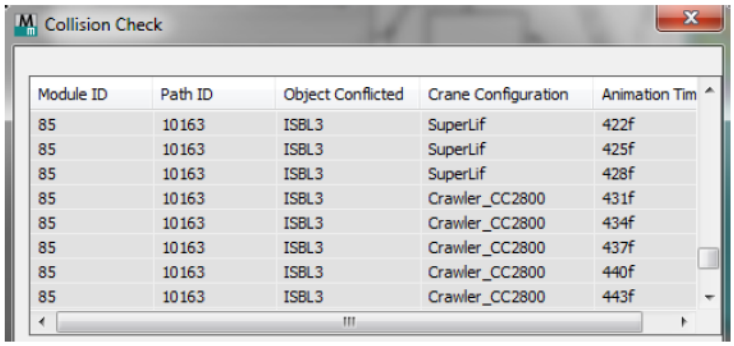

Module ID	Path ID	Object Conflicted	Crane Configuration	Animation Tim
85	10163	ISBL3	SuperLif	422f
85	10163	ISBL3	SuperLif	425f
85	10163	ISBL3	SuperLif	428f
85	10163	ISBL3	Crawler_CC2800	431f
85	10163	ISBL3	Crawler_CC2800	434f
85	10163	ISBL3	Crawler_CC2800	437f
85	10163	ISBL3	Crawler_CC2800	440f
85	10163	ISBL3	Crawler_CC2800	443f

(b) Collision Information

Figure 4.17: Implementation of collision analysis

Although the collision-free motions of mobile crane operations have been established, the module supply positions used in the rotation and spatial analyses are randomly determined on pick areas provided by crane lift binary checking. In the interest of safety, the selected crane type and its configurations must satisfy the required crane capacity and working radius. In this respect, the lift analysis is implemented in order to determine whether or not feasible crane locations and associated module supply positions defined by users are acceptable by satisfying the safety factor calculated as the required crane capacity divided by the crane capacity setting. As shown in Figure 4.18a, the safety factor is found to exceed 95%, meaning that the designed crane operation is not acceptable since the selected module supply position leads to the operation exceeding the maximum crane working radius. To satisfy the safety factor, the motions of crane operation are redesigned after changing the module supply position represented in Figure 4.18b, and lift analysis is then implemented again. For the redesigned crane motions, the safety factor is found to be less than 85%, meaning that is falls within the range of safe crane operation. The lift analysis is implemented for other modules and some module supply positions are changed for pick and carrying operations.

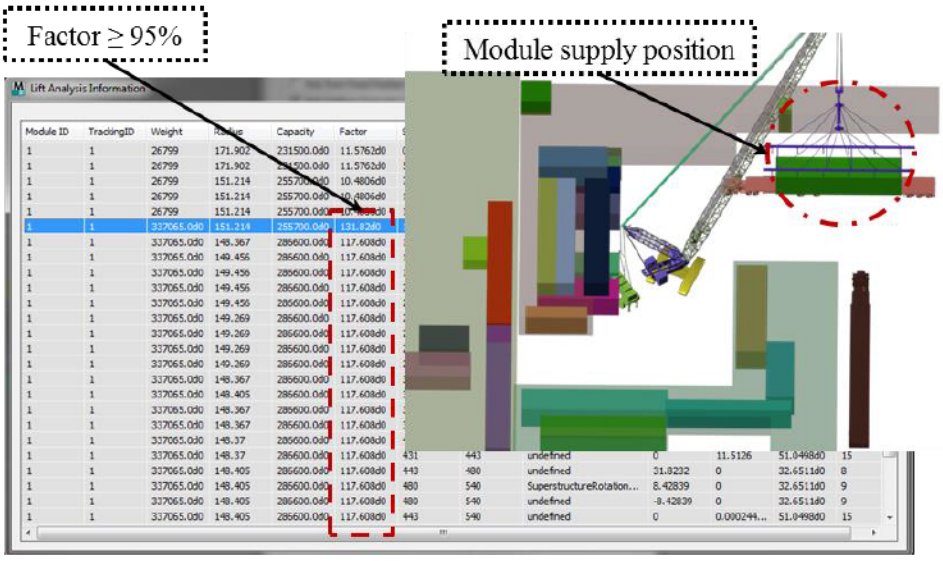

(a) Violation of crane capacity setting for Module 1

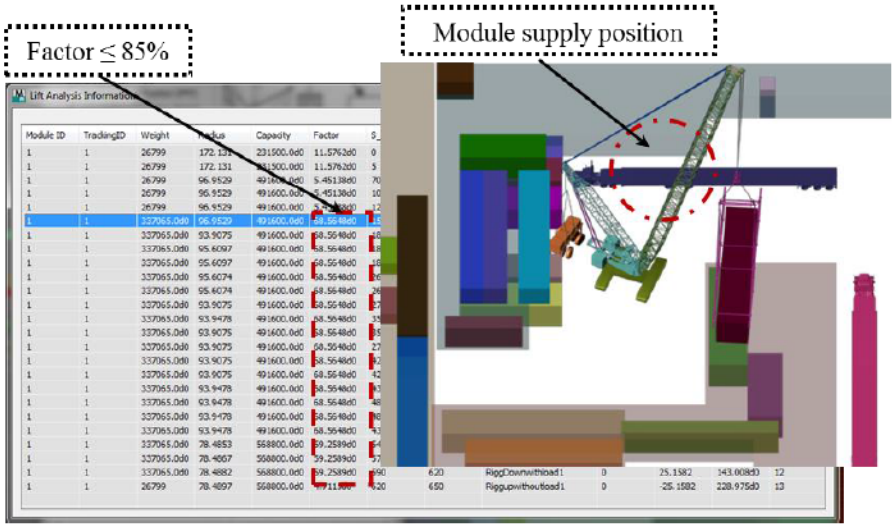

(b) Stable crane capacity

Figure 4.18: Lift information

As describing above, safe crane operation is designed and validated by rotation, spatial, collision, and lift analyses based on walking paths and associated module supply positions on the pick areas. However, these analyses lack decision-making support: (1) when each module has more than one single walking path, lift engineers may have difficulty selecting the best crane operation even though all requirements in the lift analysis are satisfied; and (2) an optimal module

supply position for each walking path of the module cannot be determined even though the safe crane operation is built based on multiple module supply positions. As a solution, the productivity analysis proposed in this research is implemented to determine the cycle time of the crane operation by fully integrating 3D visualization and simulation. This will help lift engineers and project managers to make better decisions more quickly and easily in order to select the best crane operation by comparing cycle times of crane operations. To illustrate productivity analysis, 3D visualization of mobile crane operations for ten walking paths for Module 1 are developed using VMCO. The simulation model reads relevant lift information such as hoist and rotate speeds through the DLL file, and runs in Simphony.NET automatically. To compute the hoist and rotate speeds, the minimum and maximum percentages of speed are defined as 20% and 60%, respectively. As shown in Figure 4.19, the module ID, its tracking number and the cycle time of each crane operation are represented on the VMCO. The optimal crane operation between among walking paths for Module 1 is found to be tracking number 10, which has a cycle time of 25.7653 minutes when the module supply position is the same. It should be noted that this cycle time does not involve the installation time of the module.

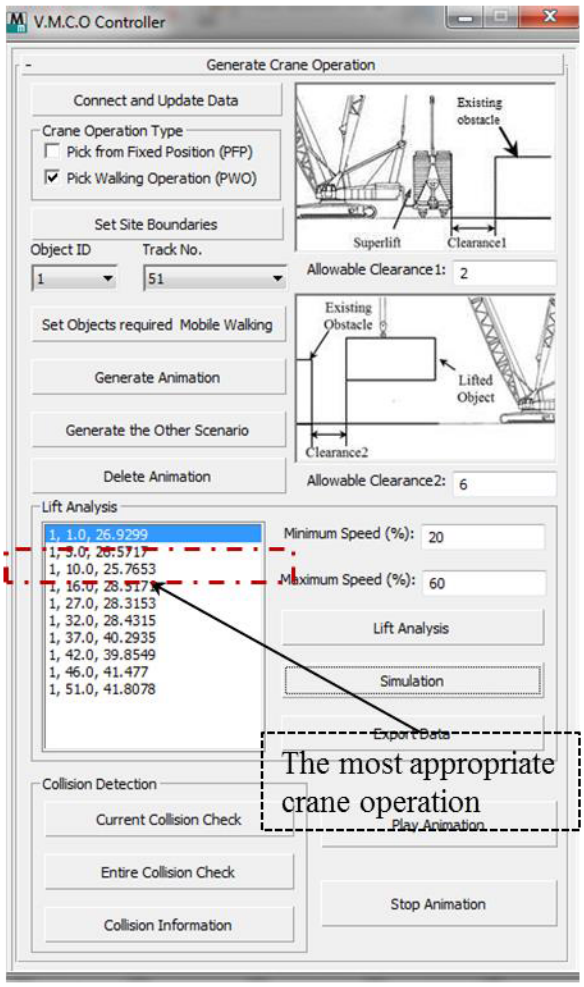

Figure 4.19: Productivity Analysis

Chapter 5: Conclusions

5.1 Research Summary

This research has been motivated by the need for improvement on the current 2D-based lift planning process, which is time-consuming, costly, and error-prone. This thesis has described building information modelling (BIM)-based motion planning for mobile crane operation in heavy industrial off-site projects. It takes into account the dynamic nature of site constraints, such as changes in site layout and lift schedule. The primary focus of the motion planning methodology is to design safe and reliable 3D visualization of crane operation efficiently and accurately, considering crane pick from fixed position and crane pick and carrying operation methods. This research offers the following: (1) better and faster information exchange between the proposed system and the existing crane management system without any synchronization problems; (2) an automated motion planning system which integrates 3D visualization with mathematical algorithms; (3) a decision-making support system integrating 3D visualization with simulation; and (4) an extension of BIM integrating crane information, including 3D visualization and digital numeric information such as lifting angles and heights, lifting radii, and crane capacity.

The characteristics of this research can assist construction planners in the following ways: (1) improve project productivity and safety; (2) reduce crane lift planning time and cost; (3) assist project participants to select the most appropriate crane operation; and (4) improve communication and collaboration

among project participants. In addition, the 3D visualization of crane operation can be used as a guide for crane operators to consult prior to actual construction operations. The proposed BIM-based motion system has been developed using MAXScript, a scripting language in 3ds Max, in order to control all features in this research as well as to provide a user-friendly interface.

5.2 Research Contributions

The current 2D-based lift planning process is error-prone, costly, and time-consuming for complex industrial projects involving numerous lifts. Researching more effective ways to perform motion planning for safe and efficient mobile crane operation leads to the establishment of better practices within the construction industry. BIM-based motion planning of mobile crane operation can enhance the efficiency of lift planning in terms of time and cost. The specific contributions of this research to current construction practice are summarized below:

- *Automated motion planning*: This research has described an approach which integrates 3D visualization with mathematical models based on scenarios of crane operation. The automated motion planning is a general system which includes two types of mobile crane operation, pick from fixed position and pick and carrying operation. Based on project and crane information, this system efficiently builds 3D site layouts, 3D existing obstacle models, and 3D visualization of crane operation. The proposed motion planning approach can reduce the time and cost requirements of lift planning for large-scale modular-based projects that

involve a large number of lifts and unexpected design changes. This system takes approximately thirty (30) minutes to design the motion of mobile crane operation for twenty-seven (27) case study lifts. This is to be contrasted with the current manual-based planning which requires approximately two weeks.

- *Post-Visualization Simulation*: This research develops a framework, called post-visualization simulation, which integrates 3D visualization with simulation in order to enhance the decision-making process by calculating the cycle time of crane operations. The most appropriate crane operation, including crane location and an associated modular supply positions, can thus be determined when a module has more than one feasible crane location with uncertain modular supply positions.
- *BIM-based system:* This research presents a BIM-based system which offers the following advantages: (1) reduced redundancy and human error by enabling efficient information exchange between 3ds Max and digital spreadsheet-based information; and (2) improved communication and collaboration by representing pertinent crane information such as collision, lift, and productivity information. This system also contributes to the establishment of a comprehensive automated crane management system comprising crane location selection, crane type selection, support system design, motion planning, and lift scheduling. It also serves to extend the domain of BIM by fully integrating crane planning within the construction domain.

- *Insight of Planning Crane Operation*: 3D visualization of mobile crane operations, shared with the crane operator, lifting crews, and lift engineers, assists in providing an overview of crane operation, including any potential risk of collision between the crane and existing objects, prior to the beginning of actual construction operations. 3D visualization can be used as a guide to enhance the safety and reduce the process time of crane operations in practice.

5.3 Research Limitations

This research involves a number of limitations, as outlined below:

1. Since the motion planning in this research uses the central database developed by PCL Industrial Management Inc. in Alberta, Canada, this work can be used by other companies provided they develop a similar database which contains project and crane information in order to use the motion planning algorithms.
2. The best crane operation is determined by various factors including time, cost, safety, and energy consumption. However, the scope of the decision support system in this resesearch considers only the cycle time of crane operation in assisting with selection of the appropriate crane operation.
3. The motions of crane operation are designed according to the preferred sequence of the industrial partner, i.e. PCL Industrial Management Inc. As a result, the lifting paths generated by the motion planning in this research does not address their optimization, e.g. shortest path, energy

utilization and effect of wind speeds. The main purpose of this research is to identify efficiently the technical feasibility of crane operations based on potential crane fixed positions and crane walking paths.

4. The methodology described in this research focuses on designing single-crane operations for a given case based on feasible crane pick from fixed positions and pick and carrying operation methods. It does not support the design of multi-crane operations even though oil sands projects generally utilize mobile cranes in multi-crane operations to facilitate module installation. In multi-crane operations, the motions of crane operation may be different since the operations of each crane can affect those of the others working in cooperation.
5. To implement the proposed methodology in this research successfully, a full-scale 3D crane model is essential. A 3D crane model built by AutoCAD can be imported to 3ds Max, and then manually mapped with bones into each crane configuration in order to achieve identical performances between the 3D crane model and the actual crane. At this point, one limitation with mapping bones into 3D crane models is the time-consuming and repetitive nature of the mapping when different crane models are applied.
6. The other limitation of this research is that the simulation model used to determine the cycle time of crane operation is not based on a probabilistic model, which would predict the expected crane productivity

more accurately than the deterministic model used in this research, due to the lack of process time information for each mobile crane motion.

5.4 Recommendations for Future Work

While this research has explored the prospect of improving crane operation and collaboration among participants through a BIM-based motion planning system incorporating rotation, spatial, collision, lift, and productivity analyses, there are areas that may require further research:

- Development of an algorithm by means of which to establish a central database including all information required by the proposed system in order to achieve fully the utilization of motion planning procedures.
- Development of a methodology to design collision-free multi-crane operations for heavy industrial construction.
- Development of a methodology to optimize lift scheduling based on the identification of any schedule errors from the motion planning proposed in this research.
- Development of a methodology that accounts for wind speeds to plan more realistic and safe motions of crane operations, accounting for such phenomena as sway of the rigging system.
- Development of a methodology to improve the decision-making system for crane operation selection proposed in this research, by considering not only cycle time, but cost, safety and energy consumption.

- Development of a methodology to extend the proposed research to other mobile crane types (boom truck, mobile hydraulic, rough terrain, and tower crawler) and configurations (jib).
- Development of a CAD-based system to build 3D crane models and to map bones into each crane configuration automatically in order to enhance the proposed methodology in this research based on parametric information of each crane configuration.

REFERENCES

Autodesk (2011). "3D Studio MAXScript Help." <http://docs.autodesk.com/3DSMAX/14/ENU/MAXScript%20Help%202012/> (Aug. 4, 2014).

AbouRizk, S. (2010). "Role of Simulation in Construction Engineering and Management." *Journal of Construction Engineering and Management*, 136(10), 1140–1153.

Abudayyeh, O. and Al-Battaineh, H. T. (2003). "As-Built Information Model for Bridge Maintenance." *Journal of Computing in Civil Engineering*, 17(2), 105–112.

Albahnassi, H. and Hammad, A. (2012). "Near Real-Time Motion Planning and Simulation of Cranes in Construction : Framework and System Architecture." *Journal of Computing in Civil Engineering*, 26(1), 54–63.

Al-Hussein, M., Alkass, S., and Moselhi, O. (2000). "D-CRANE : a database system for utilization of cranes." *Canadian Journal of Civil Engineering*, 27, 1130–1138.

Al-Hussein, M., Alkass, S., and Moselhi, O. (2001). "An algorithm for mobile crane selection and location on construction sites." *Construction Innovation Journal*, 4175(2), 91–105.

Al-Hussein, M., Alkass, S., and Moselhi, O. (2005). "Optimization Algorithm for Selection and on Site Location of Mobile Cranes." *Journal of Construction Engineering and Management*, 131(5), 579–590.

Al-Hussein, M., Athar Niaz, M., Yu, H., and Kim, H. (2006). "Integrating 3D visualization and simulation for tower crane operations on construction sites." *Automation in Construction*, 15(5), 554–562.

Ali, M. S. A. D., Babu, N. R., and Varghese, K. (2005). "Collision Free Path Planning of Cooperative Crane Manipulators Using Genetic Algorithm." *Journal of Computing in Civil Engineering*, 19(2), 182–193.

Beavers, J. E., Moore, J. R., Rinehart, R., and Schriver, W. R. (2006). "Crane-Related Fatalities in the Construction Industry." *Journal of Construction Engineering and Management*, 132(9), 901–910.

Behm, M. (2005). "Linking construction fatalities to the design for construction safety concept." *Safety Science*, 43(8), 589–611.

Van Den Bergen, G. (1997). "Efficient collision detection of complex deformable models using AABB trees efficient collision detection of complex deformable models using AABB trees." *Journal of Graphics Tools*, 2(4), 37–41.

Bynum, P., Issa, R. R. A., and Olbina, S. (2013). "Building information modeling in support of sustainable design and construction." *Journal of Construction Engineering and Management*, 139(1), 24–34.

Chang, Y.-C., Hung, W.-H., and Kang, S.-C. (2012). "A fast path planning method for single and dual crane erections." *Automation in Construction*, Elsevier B.V., 22, 468–480.

Chi, H.-L. and Kang, S.-C. (2010). "A physics-based simulation approach for cooperative erection activities." *Automation in Construction*, Elsevier B.V., 19(6), 750–761.

Ernst and Young. (2012). "Exploring the top 10 opportunities and risks in Canada's oil sands." Ernst and Young LLP, 1-40.

Eastman, C., Teicholz, P., Rafael, S., and Liston, K. (2011). *A Guide to Building Information Modeling for Owners, Managers, Designers, Engineers, and Contractors*. John Wiley & Sons, Inc.

EPA (2005). "Emission facts: Average carbon dioxide emissions resulting from gasoline and diesel fuel." <<http://www.epa.gov/OTAQ/climate/420f05001.htm>>.

Everett, J. G. and Slocum, A. H. (1993). "CRANIUM: Device for improving crane productivity and safety." *Journal of Construction Engineering and Management*, 119(1), 23–39.

Fazio, P., He, H. S., Hammad, A., and Horvat, M. (2007). "IFC-Based Framework for Evaluating Total Performance." *Journal of Architectural Engineering*, 13(1), 44–53.

Giel, B. K. and Issa, R. R. A. (2013). "Return on Investment Analysis of Using Building Information Modeling in Construction." *Journal of Computing in Civil Engineering*, 27(5), 511–521.

Goedert, J. D. and Meadati, P. (2008). "Integrating construction process documentation into building information modeling." *Journal of Construction Engineering and Management*, 134(7), 509–516.

Gökçe, K. U., Gökçe, H. U., and Katranuschkov, P. (2013). "IFC-Based Product Catalog Formalization for Software Interoperability in the Construction Management Domain." *Journal of Computing in Civil Engineering*, 27(1), 36–50.

Hajjar, D. and AbouRizk, S. M. (1999). "Simphony: An environment for building special purpose construction simulation tools." *Proc. of the 31st Conf. on Winter Simulation, IEEE, New York*, 998–1006.

Halfawy, M. M. R. and Froese, T. M. (2007). "Component-Based Framework for Implementing Integrated Architectural / Engineering / Construction Project Systems 1." *Journal of Computing in Civil Engineering*, 21(6), 441–452.

Halpin, D. and Riggs, L. (1992). “Construction management.” *2nd Edition, Wiley, New York*.

Han, S. H., Al-Hussein, M., Al-Jibouri, S., and Yu, H. (2012). “Automated post-simulation visualization of modular building production assembly line.” *Automation in Construction*, Elsevier B.V., 21, 229–236.

Han, S. H., Hasan, S., Bouferguene, A., Al-Hussein, M., and Kosa, J. (2014). “Utilization of 3D visualization of mobile crane operations for modular construction on-site assembly.” *Accepted to Journal of Management in Engineering*.

Han, S. H., Hasan, S., Lei, Z., Altaf, M. S., and Al-Hussein, M. (2012). “A framework for crane selection in large-scale industrial construction projects.” *30th International Symposium on Automation and Robotics in Construction and Mining*, Montréal, QC, Canada.

Hanna, A. S. and Lotfallah, W. B. (1999). “A fuzzy logic approach to the selection of cranes.” *Automation in Construction*, 8(5), 597–608.

Hasan, S., Al-Hussein, M., Hermann, U. H., and Safouhi, H. (2010). “Interactive and Dynamic Integrated Module for Mobile Cranes Supporting System Design.” *Journal of Construction Engineering and Management*, 136(2), 179–186.

Hasan, S., Bouferguene, A., Al-Hussein, M., Gillis, P., and Telyas, A. (2013). "Productivity and CO_2 emission analysis for tower crane utilization on high-rise building projects." *Automation in Construction*, 31, 255–264.

Hasan, S., Zaman, H., Han, S. H., Al-Hussein, M., and Su, Y. (2012). "Integrated building information model to identify possible crane instability caused by strong winds." *Construction Research Congress 2012*, Indiana, USA, 1–10.

Hendrickson, C. and Horvath, A. (2000). "Resource use and environmental emissions of U.S. construction sectors." *Journal of Construction Engineering and Management*, 126(1), 38–44.

Hermann, U. (Rick), Hendi, A., Olearczyk, J., and Al-Hussein, M. (2010). "An Integrated System to Select, Position, and Simulate Mobile Cranes for Complex Industrial Projects." *Construction Research Congress 2010*, American Society of Civil Engineers, Reston, VA, 267–276.

Hermann, U. H., Hasan, S., Al-Hussein, M., and Bouferguene, A. (2011). "Innovative System for Off-the-Ground Rotation of Long Objects Using Mobile Cranes." *Journal of Construction Engineering and Management*, 137(7), 478–485.

Huang, C., Wong, C. K., and Tam, C. M. (2011). "Optimization of tower crane and material supply locations in a high-rise building site by mixed-integer

linear programming." *Automation in Construction*, Elsevier B.V., 20, 571–580.

ISO-29484-1. (2010). "Building Information Modeling - Information Delivery Manual - Part1: Methodology and Format." *ISO TC59 SC 13*.

Jerman, B. (2006). "An Enhanced Mathematical Model for Investigating the Dynamic Loading of a Slewing Crane." *Proceedings of the Institution of Mechanical Engineers, Part C: Journal of Mechanical Engineering Science*, 220(4), 421–433.

Kang, S., Chi, H., and Miranda, E. (2009). "Three-Dimensional Simulation and Visualization of Crane Assisted Construction Erection Processes." *Journal of Construction Engineering and Management*, 23(6), 363–371.

Kang, S. and Miranda, E. (2006). "Planning and visualization for automated robotic crane erection processes in construction." *Automation in Construction*, 15, 398–414.

Kang, S. and Miranda, E. (2008). "Computational Methods for Coordinating Multiple Construction Cranes." *Journal of Computing in Civil Engineering*, 22(4), 252–263.

Kam, C. and Fischer, M. (2002). "Product model & 4D CAD – Final report." *Technical Report Nr. 143, Center of Integrated Facility Engineering*, Stanford University, CA, USA.

Kim, H. and Anderson, K. (2013). "Energy Modeling System Using Building Information Modeling Open Standards." *Journal of Computing in Civil Engineering*, 27(3), 203–211.

Kim, S.-K., Kim, J.-Y., Lee, D.-H., and Ryu, S.-Y. (2011). "Automatic optimal design algorithm for the foundation of tower cranes." *Automation in Construction*, Elsevier B.V., 20(1), 56–65.

Kłosiński, J. (2005). "Swing-free stop control of the slewing motion of a mobile crane." *Control Engineering Practice*, 13(4), 451–460.

Lai, K.-C. and Kang, S.-C. (2009). "Collision detection strategies for virtual construction simulation." *Automation in Construction*, Elsevier B.V., 18(6), 724–736.

Lee, G., Cho, J., Ham, S., Lee, T., Lee, G., Yun, S.-H., and Yang, H.-J. (2012). "A BIM- and sensor-based tower crane navigation system for blind lifts." *Automation in Construction*, Elsevier B.V., 26, 1–10.

Lee, G., Ph, D., Won, J., Ham, S., and Shin, Y. (2011). "Metrics for Quantifying the Similarities and Differences between IFC Files." *Journal of Computing in Civil Engineering*, 25(2), 172–181.

Lee, U. K., Kang, K. I., Kim, G. H., and Cho, H. H. (2006). "Improving tower crane productivity using wireless technology." *Computer-Aided Civil and Infrastructure Engineering*, 21(8), 594–604.

Lei, Z., Han, S., Bouferguene, A., Taghaddos, H., Hermann, U. (Rick), and Al-Hussein, M. (2014). “An algorithm for mobile crane walking path planning in congested industrial plants.” *Accepted to Journal of Construction Engineering and Management*.

Lei, Z., Taghaddos, H., Hermann, U., and Al-Hussein, M. (2013). “A methodology for mobile crane lift path checking in heavy industrial projects.” *Automation in Construction*, Elsevier B.V., 31, 41–53.

Lei, Z., Taghaddos, H., Olearczyk, J., Al-Hussein, M., and Hermann, U. (2013). “Automated Method for Checking Crane Paths for Heavy Lifts in Industrial Projects.” *Journal of Construction Engineering and Management*, 5(2003), 1–9.

Lin, K. and Haas, C. T. (1996). “Multiple heavy lifts optimization.” *Journal of Construction Engineering and Management*, 122(4), 354–362.

Lin, M. C. and Canny, J. F. (1991). “A fast algorithm for incremental distance calculation.pdf.” *Proceedings of the 1991 IEEE International Conference on Robotics and Automation Sacramento, California*, 1008–1014.

Lin, Y., Wu, D., Wang, X., Wang, X., and Gao, S. (2012). “Statics-Based Simulation Approach for Two-Crane Lift.” *Journal of Construction Engineering and Management*, 138(10), 1139–1149.

Moghadam, M. (2014). “Lean-MOD: An Approach to Modular Construction Manufacturing Production Efficiency Improvement.” Doctor of Philosophy (PhD), University of Alberta, Canada.

Mohamed, Y. and AbouRizk, S. M. (2005). “Framework for Building Intelligent Simulation Models of Construction Operations.” *Journal of Computing in Civil Engineering*, 19(3), 277–291.

Nawari, N. O. (2012). “BIM Standard in Off-Site Construction.” *Journal of Architectural Engineering*, 18(2), 107–113.

Neeley, D. (2010). “The Speed of Change.” *2010SMARTBIM*, <www.smartbim.com>.

Neitzel R. L., Seixas, N. S., and Ren, K. K. (2001). “A review of crane safety in the construction industry.” *Applied Occupational Environmental Hygiene*, 16(12), 1106–1117.

Olearczyk, J. (2010). “Crane Lifting Operation Planning and Lifted Object Spatial Trajectory Analysis.” University of Alberta.

Park, T., Kim, M. K., Kim, C., and Kim, H. (2009). “Interactive 3D CAD for Effective Derrick Crane Operation in a Cable-Stayed Bridge Construction.” *Journal of Construction Engineering and Management*, 135(11), 1261–1270.

Porwal, A. and Hewage, K. N. (2012). "Building Information Modeling – Based Analysis to Minimize Waste Rate of Structural Reinforcement." *Journal of Construction Engineering and Management*, 138(8), 943–954.

Reddy, H. R. and Varghese, K. (2002). "Automated path planning for mobile crane lifts." *Computer-Aided Civil and Infrastructure Engineering*, 17(6), 439–448.

Rodriguez-ramos, W. E. and Francis, R. L. (1984). "Single crane location optimization." *Journal of Construction Engineering and Management*, 109(4), 387–397.

Russell, A., Staub-French, S., Tran, N., and Wong, W. (2009). "Visualizing high-rise building construction strategies using linear scheduling and 4D CAD." *Automation in Construction*, Elsevier B.V., 18(2), 219–236.

Safouhi, H., Mouattamid, M., Hermann, U., and Hendi, a. (2011). "An algorithm for the calculation of feasible mobile crane position areas." *Automation in Construction*, Elsevier B.V., 20(4), 360–367.

Sawhney, A. and Mund, A. (2002). "Adaptive Probabilistic Neural Network-based Crane Type Selection System." *Journal of Construction Engineering and Management*, 128(3), 265–273.

Shapira, A., Lucko, G., and Schexnayder, C. J. (2007). “Cranes for Building Construction Projects.” *Journal of Construction Engineering and Management*, 133(9), 690–700.

Shapira, A., Rosenfeld, Y., and Mizrahi, I. (2008). “Vision System for Tower Cranes.” *Journal of Construction Engineering and Management*, 134(5), 320–332.

Sierra Systems (2011). “Unlocking the Prize: Metal Fabrication Procurement for Development and Operation of Alberta’s Oil Sands; Alberta Oil Sands Supply Chain Opportunity Analysis.” Alberta Finance and Enterprise, 1-42.

Sivakumar, P. L., Varghese, K., and Babu, N. R. (2003). “Automated Path Planning of Cooperative Crane Lifts Using Heuristic Search.” *Journal of Computing in Civil Engineering*, 17(3), 197–207.

Sochacki, W. Ã. (2007). “The dynamic stability of a laboratory model of a truck crane.” *Thin-Walled Structures*, 45, 927–930.

Song, L. and AbouRizk, S. M. (2006). “Virtual Shop Model for Experimental Planning of Steel Fabrication Projects.” *Journal of Computing in Civil Engineering*, 20(5), 308–316.

Suraji, A., Duff, A. R., and Peckitt, S. J. (2001). “Development of Causal Model of Construction Accident Causation.” *Journal of Construction Engineering and Management*, 127(4), 337–344.

Taghaddos, H., AbouRizk, S., Mohamed, Y., and Hermann, U. (2010). "Simulation-based multiple heavy lift planning in industrial construction." *Construction Research Congress 2010*, 349–358.

Taghaddos, H., AbouRizk, S., Mohamed, Y., and Hermann, U. (2012). "Simulation-Based Auction Protocol for Resource Scheduling Problems." *Journal of Construction Engineering and Management*, 138(1), 31–42.

Taghaddos, H., Hermann, U., AbouRizk, S., and Mohamed, Y. (2014). "Simulation-Based Multiagent Approach for Scheduling Modular Construction." *Journal of Computing in Civil Engineering*, 28(2), 263–274.

Tam, C. M., Tong, C. M., Thomas, K. L., and Chan, W. K. W. (2002). "Genetic Algorithm for optimizing supply locations around tower crane." *Journal of Construction Engineering and Management*, 127(4), 315–321.

Tamate, S., Suemasa, N., and Katada, T. (2005). "Analyses of Instability in Mobile Cranes due to Ground Penetration by Outriggers." *Journal of Construction Engineering and Management*, 131(6), 689–704.

Tantisevi, K. and Akinci, B. (2007). "Automated generation of workspace requirements of mobile crane operations to support conflict detection." *Automation in Construction*, 16(3), 262–276.

Tantisevi, K. and Akinci, B. (2008). "Simulation-Based Identification of Possible Locations for Mobile Cranes on Construction Sites." *Journal of Computing in Civil Engineering*, 22(1), 21–30.

Tantisevi, K. and Akinci, B. (2009). "Transformation of a 4D product and process model to generate motion of mobile cranes." *Automation in Construction*, Elsevier B.V., 18(4), 458–468.

Thomas, H. R. and Yiakoumis, I. (1988). "Factor model of construction productivity." *Journal of Construction Engineering and Management*, 113(4), 623–639.

Wang, P., Mohamed, Y., AbouRizk, S. M., and Rawa, A. R. T. (2009). "Flow Production of Pipe Spool Fabrication : Simulation to Support Implementation of Lean Technique." *Journal of Construction Engineering and Management*, 135(10), 1027–1038.

US Bureau of Labor Statistics (2008). "Crane-related occupational fatalities." <http://www.bls.gov/iif/oshwc/osh/os/osh_crane_2006.pdf> (Sep. 26, 2013).

Wu, D., Lin, Y., Wang, X., and Gao, S. (2011). "Algorithm of Crane Selection for Heavy Lifts." *Journal of Computing in Civil Engineering*, 25(1), 57–65.

Yan, W., Culp, C., and Graf, R. (2011). "Integrating BIM and gaming for real-time interactive architectural visualization." *Automation in Construction*, Elsevier B.V., 20(4), 446–458.

Zayed, T. M. and Halpin, D. W. (2004). "Simulation as a Tool for Pile Productivity Assessment." *Journal of Construction Engineering and Management*, 130(3), 394–404.

Zhang, C. and Hammad, A. (2012). "Improving lifting motion planning and re-planning of cranes with consideration for safety and efficiency." *Advanced Engineering Informatics*, Elsevier Ltd, 26(2), 396–410.

Zhang, P., Harris, F. C., Olomolaiye, P. O., Holt, G. D. (1999). "Location optimization for a group of tower cranes." *Journal of Construction Engineering and Management*, 125(2), 115–122.